UNIVERSITY OF AMSTERDAM

UvA-DARE (Digital Academic Repository)

Growth and functioning of the microbial plankton community: effects of temperature, nutrients and light

Brauer, V.S.

Publication date
2015

Document Version
Final published version

Link to publication

Citation for published version (APA):
Brauer, V. S. (2015). *Growth and functioning of the microbial plankton community: effects of temperature, nutrients and light*.

General rights
It is not permitted to download or to forward/distribute the text or part of it without the consent of the author(s) and/or copyright holder(s), other than for strictly personal, individual use, unless the work is under an open content license (like Creative Commons).

Disclaimer/Complaints regulations
If you believe that digital publication of certain material infringes any of your rights or (privacy) interests, please let the Library know, stating your reasons. In case of a legitimate complaint, the Library will make the material inaccessible and/or remove it from the website. Please Ask the Library: https://uba.uva.nl/en/contact, or a letter to: Library of the University of Amsterdam, Secretariat, Singel 425, 1012 WP Amsterdam, The Netherlands. You will be contacted as soon as possible.

UvA-DARE is a service provided by the library of the University of Amsterdam (https://dare.uva.nl)

Download date:10 Nov 2022

Growth and Functioning of the Microbial Plankton Community

Verena Brauer

Growth and Functioning of the Microbial Plankton Community:

Effects of Temperature, Nutrients and Light

Verena Brauer

Growth and functioning of the microbial plankton community:

effects of temperature, nutrients and light

Verena S. Brauer

Brauer VS, 2014. Growth and functioning of the microbial plankton community: effects of temperature, nutrients, and light

PhD thesis, University of Amsterdam, The Netherlands

This research was supported by the Earth and Life Sciences Foundation (ALW), which is subsidized by the Netherlands Organization for Scientific Research (NWO)

Growth and functioning of the microbial plankton community:

effects of temperature, nutrients and light

ACADEMISCH PROEFSCHRIFT

ter verkrijging van de graad van doctor
aan de Universiteit van Amsterdam
op gezag van de Rector Magnificus
prof. dr. D.C. van den Boom
ten overstaan van een door het college voor promoties
ingestelde commissie,
in the openbaar te verdedigen in de Agnietenkapel
op donderdag 9 april 2015, te 10:00 uur

door

Verena Sibylle Brauer
geboren te Freiburg im Breisgau, Duitsland

PROMOTIECOMMISSIE

Promotoren:	**Prof. dr. J. Huisman**
	Prof. dr. L.J. Stal
Copromotoren:	**Dr. M. Stomp**
	Prof. dr. F.J. Weissing
Overige leden:	**Prof. dr. C.P.D. Brussaard**
	Dr. J.M. Gasol
	Prof. dr. H. Hillebrand
	Prof. dr. W.M. Mooij
	Prof. dr. G. Muyzer
	Prof. dr. E. van Donk

Faculteit der Natuurwetenschappen, Wiskunde en Informatica

Content

Summary

Microbial plankton form the basis of the food web in aquatic habitats. Due to their vast abundances they influence the cycling of elements and the Earth's climate at a global scale. Planktonic microorganisms are highly diverse and form complex networks of interactions. The growth and functioning of microbial plankton communities is strongly influenced by environmental factors, in particular by temperature and the availability of nutrients and light. This thesis aims at a better understanding of how these factors affect microbial plankton communities, which is highly relevant in the context of global climate change and anthropogenic changes in nutrient cycling.

As a first step this thesis focuses on a single species, the marine N_2-fixing cyanobacterium *Cyanothece*. A series of batch culture experiments revealed interactive effects of temperature, light and nitrogen source on the physiology and growth of *Cyanothece*. The rates of N_2 fixation and growth generally increased with light intensity until they levelled off at high light. Addition of nitrate suppressed N_2 fixation and slightly stimulated the growth rate, which increased with temperature across the entire experimental range from 14 to 38 °C. However, when grown on N_2 only, temperature increased the rates of N_2 fixation and growth only in the range from 18 to 30 °C. Above 30 °C, N_2 fixation became limited by the rate at which oxygen diffused into the cell, which prevented a further increase of N_2 fixation and growth with temperature. Interestingly, temperatures below 21 °C also limited N_2 fixation and induced nitrogen deficiency in *Cyanothece* because of two reasons: low temperature (i) delayed the timing of N_2 fixation until late in the night, and (ii) sharply increased the respiratory cost of N_2 fixation. These results offer a physiological explanation for why free-living N_2-fixing cyanobacteria in the open ocean are generally restricted to the warm waters of the (sub)tropical oceans.

In a second step this thesis advances towards a plankton community consisting of the N_2-fixing *Cyanothece* and its associated free-living chemotrophic bacteria. A series of chemostat experiments revealed that temperature and nutrients had interactive effects on plankton community structure. At steady state, higher temperatures strongly increased the abundance of *Cyanothece* but only mildly influenced the abundance of chemotrophic bacteria, which led to a higher proportion of *Cyanothece* at higher temperatures. Conversely, a higher supply of nitrogen and organic carbon had minor effects on *Cyanothece* but large effects on the abundance and species composition of the chemotrophic community. *Cyanothece* appeared to influence the composition of its associated bacterial community through a combination of competition for nutrients and facilitation due to the release of fixed nitrogen and carbon. These results suggest that the composition of free-living bacteria associated with N_2-fixing cyanobacteria is mainly driven by ecological niche differentiation rather than by tight evolutionary relationships with the N_2-fixing 'host'.

In a third step this thesis turns its focus on phytoplankton communities. I present a theoretical model for the competition between multiple phytoplankton species for two nutrients and light. The model results are summarized by the nutrient-load hypothesis, which states the following. In oligotrophic ecosystems phytoplankton species compete for nutrients and the species composition of the community depends on the ratio at which the growth-limiting nutrients are supplied to the system, as predicted by the well-established resource-ratio hypothesis. In eutrophic ecosystems, however, phytoplankton species compete for light, because the high nutrient loads generate high biomasses that induce self-shading. In this situation the species composition of phytoplankton communities does not depend on nutrient ratios but is determined by the absolute nutrient loads and often dominated by a single species. The nutrient-load hypothesis predicts that highest phytoplankton diversity is found at intermediate nutrient loads, where phytoplankton species compete for both nutrients and light. The nutrient-load hypothesis offers a solution for several discrepancies between classical resource-ratio theory and field observations, explains why eutrophication often leads to diversity loss, and thereby provides a new conceptual framework for patterns of biodiversity and community structure observed in nature.

In a fourth step this thesis focuses on a natural plankton community that was sampled from the Dutch Wadden Sea. A series of batch culture experiments revealed that, in the absence of nutrient and light limitation, temperature increased the maximum specific growth rate of the entire plankton community in accordance with the Arrhenius equation. This supports the prediction of the Metabolic Theory of Ecology that metabolic processes provide the foundation for a universal temperature response of ecological processes.

The insights obtained from this thesis show that temperature, nutrients and light have interactive effects on the growth and functioning of microbial plankton communities. Under ideal growth conditions temperature strongly increases plankton growth rates, suggesting that global warming will have a strong direct effect on the growth and species composition of plankton communities in eutrophic systems. However, low nutrient concentrations and low light availability dampen the effect of temperature, suggesting that oligotrophic ecosystems are generally more constrained by nutrient limitation than by temperature. Furthermore, the temperature response varies among species depending on their physiological traits. In particular, our results suggest that global warming will favor marine N_2-fixing cyanobacteria more than other phytoplankton species.

Samenvatting

Plankton vormt de basis van de voedselketens in meren, zeeën en oceanen. Omdat 70 % van het aardoppervlak is bedekt met water, speelt het plankton een cruciale rol in de wereldwijde kringloop van onder meer koolstof en stikstof. Plankton gemeenschappen vertonen een grote diversiteit aan soorten die onderling complexe netwerken van interacties vormen. Het plankton staat continue bloot aan veranderingen in omgevingsfactoren, zoals temperatuur en de beschikbaarheid van licht en nutriënten. Het doel van dit proefschrift is om beter te begrijpen hoe deze veranderingen in temperatuur, licht en nutriënten de groei en soortensamenstelling van plankton gemeenschappen beïnvloeden, wat met name met het oog op klimaatsverandering en eutrofiëring van het oppervlaktewater van groot belang is.

Als eerste stap onderzoekt dit proefschrift de effecten van temperatuur, licht en stikstof op de mariene stikstof-fixerende cyanobacterie *Cyanothece*. Deze eencellige soort fixeert stikstof (N_2) gedurende de nacht, waarbij eerst de zuurstof afkomstig van fotosynthese gerespireerd moet worden om het zuurstofgevoelige enzym nitrogenase te beschermen. De experimenten laten zien dat toename van de lichtintensiteit leidt tot een toename in stikstoffixatie en groei, totdat verzadiging optreedt bij hogere lichtintensiteiten. Als er voldoende nitraat aanwezig is, dan fixeert *Cyanothece* geen stikstof en bereikt het hogere groeisnelheden. In aanwezigheid van nitraat neemt de groeisnelheid toe over de range van 14 tot 38 °C. Zonder nitraat nemen stikstoffixatie en groei toe over een nauwere range van 18 tot 30 °C. De waarschijnlijke verklaring is dat bij hogere temperatuur ook de diffusie van zuurstof de cel in toeneemt, wat een verdere toename van de stikstoffixatie boven 30 °C verhinderd. Temperaturen kouder dan 21 °C hebben tot gevolg dat de stikstoffixatie pas laat in de nacht op gang komt, terwijl de kosten gemoeid met het zuurstofvrij houden van de cel drastisch toenemen. Deze temperatuurgevoeligheid biedt een eenvoudige fysiologische verklaring voor de biogeografische verspreiding van eencellige stikstof-fixerende cyanobacteriën, die voornamelijk voorkomen in het warme water van tropische en subtropische oceanen.

Als tweede stap bestudeert dit proefschrift een plankton gemeenschap bestaande uit de stikstof-fixerende *Cyanothece* en de bijbehorende gemeenschap van chemotrofe bacteriën. Chemostaat experimenten laten zien dat hogere temperaturen leiden tot een sterke toename in de abundantie van *Cyanothece*, terwijl het effect op de chemotrofe bacteriën marginaal is. Vice versa is *Cyanothece* weinig gevoelig voor de toevoeging van stikstof en organisch koolstof, terwijl dit grote effecten heeft voor de abundantie en soortensamenstelling van de chemotrofe bacteriën. *Cyanothece* lijkt de samenstelling van de bacteriële gemeenschap te beïnvloeden door een combinatie van competitie om nutriënten en facilitatie door uitscheiding van gefixeerd stikstof en koolstof. Deze resultaten laten zien dat de soortensamenstelling van chemotrofe bacteriën die geassocieerd zijn met N_2-fixerende cyanobacteriën meer door ecologische niche

differentiatie wordt gedreven dan door een nauwe evolutionaire relatie met de stikstof-fixerende 'gastheer'.

Als derde stap richt dit proefschrift zich op de soortensamenstelling van het fytoplankton, waarbij ik een theoretisch model heb ontwikkeld dat de competitie om nutriënten en licht tussen soorten beschrijft. De klassieke "resource-ratio hypothese" voorspelt dat de relatieve verhouding waarin nutriënten worden aangevoerd de soortensamenstelling van het fytoplankton bepaalt. De reden hiervoor is dat soorten onderling verschillen in hun nutriëntenbehoeften, waardoor verschuivingen in het nutriëntenaanbod leiden tot veranderingen in de competitieve balans tussen soorten. Echter, Mijn model laat zien dat deze theorie alleen opgaat voor voedselarme ecosystemen. In voedselrijke ecosystemen zijn vaak zoveel nutriënten beschikbaar dat het nutriëntenaanbod niet meer werkt als selecterende factor. Hierdoor kan de aanwas van fytoplankton dusdanig hoog worden dat door beschaduwing licht limiterend wordt. In deze 'groene soep' hangt de soortensamenstelling van het fytoplankton niet af van de relatieve verhouding van de nutriënten maar van de absolute hoeveelheid nutriënten, waarbij er vaak een enkele soort domineert die het meest profiteert van de lage lichtbeschikbaarheid. Deze verschuiving naar lichtlimitatie is dan ook een verklaring waarom eutrofiëring vaak leidt tot verlies van biodiversiteit. Deze voorspellingen worden samengevat in de "nutriënten-vracht hypothese", dat een nieuw conceptueel kader biedt waarmee veranderingen in de biodiversiteit en soortensamenstelling van ecosystemen voorspeld en verklaard kunnen worden.

Als vierde stap onderzoekt dit proefschrift het effect van temperatuur op een natuurlijke plankton gemeenschap geïsoleerd uit de Nederlandse Waddenzee. Batchcultuur experimenten laten zien dat bij een overvloed aan nutriënten en licht de groeisnelheid van de totale plankton gemeenschap toeneemt met temperatuur volgens de klassieke Arrhenius vergelijking. De Arrhenius vergelijking die oorspronkelijk het effect van temperatuur op biochemische reacties beschrijft, blijkt dus ook van toepassing op gehele fytoplankton gemeenschappen. Dit is in overeenstemming met de Metabole Theorie van de Ecologie, die stelt dat metabolisme de grondslag vormt voor een universele temperatuur-afhankelijkheid van ecologische processen.

De inzichten van dit proefschrift laten zien dat de groei en het functioneren van microbiële plankton gemeenschappen sterk gestuurd worden door zowel temperatuur, nutriënten als licht, waarbij de meest limiterende factor vaak doorslaggevend is. Als nutriënten en licht voldoende voorradig zijn, dan heeft temperatuur een groot effect op de soortensamenstelling en groeisnelheid van het plankton. Onder voedselarme condities is de invloed van temperatuur echter veel beperkter, en is de nutriënten-beschikbaarheid bepalend. Dit zou betekenen dat plankton gemeenschappen in met

name voedselrijk water gevoelig zijn voor global warming, terwijl voedselarme wateren gevoeliger zijn voor eutrofiëring. Bovendien laten onze resultaten zien dat de gevoeligheid voor temperatuur sterk afhangt van de fysiologische processen die in verschillende soorten een rol spelen, en dat met name mariene stikstof-fixerende cyanobacteriën sterker zullen profiteren van het opwarmen van de aarde dan vele andere plankton soorten.

Acknowledgement

I am indebted to many people that have supported me during the different stages of my PhD. First and foremost, I thank my supervisors for giving me the opportunity to carry out my thesis in their groups, and for their professional guidance of my work. I am grateful to my promotor Jef Huisman for great advices on theoretical and experimental issues whenever needed, and for his diligent work on our manuscripts. He was the most influential person of my work and shaped my way of thinking about research. I enjoyed our scientific cooperation every day. I am also grateful to my promotor Lucas Stal for his helpful advices particularly on N_2 fixation, for his liberalness, and for the many times he travelled all the way from Yerseke to Amsterdam to discuss my project. I very much regret that the circumstances did not allow a closer collaboration at his lab in Yerseke. My co-promotor and daily supervisor Maayke Stomp is thanked for her many constructive comments, ideas and initiatives that continuously improved my research and kept it going. I am glad of having learned from these highly scientific minds.

My PhD at Amsterdam would not have started and probably would not have ended without the support of Franjo Weissing from the University of Groningen, to whom I am much obliged. I am glad that eventually he became a co-promotor of my thesis. I also thank Victor de Jonge and Anita Buma for their help and supervision during my former time in Groningen.

During my time at the University of Amsterdam I very much enjoyed the cooperative atmosphere of the Aquatic Microbiology Group. Elisa Benincà and Michael Kehoe are thanked for their help in programming and for stimulating scientific discussions. A warm thank goes to Elisa for taking care of my daughter during evening shifts in the lab. During the experimental phase of my thesis I profited from the expertise of Hans Matthijs, Jolanda Verspagen, Petra Visser, Amanda Burson, Dina Stanic, Susanne Wilken, Giovanni Sandrini and Dedmer van de Waal. I am thankful to Pieter Slot, Corrien Sigon, Bas van Beusekom and Barabara Emmerich for valuable lab support. A special thank goes to Bas van Beusekom for fruitful collaboration on the *Cyanothece*-project, which resulted in the development of a computer-controlled set-up for online-measurements of respiration and the highest quality data I have ever produced! I also thank my master-student Camillo Rosso for his dedication in the lab. I would not have been able to measure N_2 fixation by gas chromatography without the generous technical help of Joke Westerveld and Frans van der Wielen from the Earth Surface Science Group. I also thank Chiara Cherli for her readiness to help others in the lab.

From the Aquatic Microbiology Group I am particular thankful to Hans Matthijs for this helpfulness. He was willing to deal with all scientific and practical lab problems

and managed the movement of the lab to the new university building. He would also share his encyclopedic knowledge and enthusiasm on microbial physiology at any time Moreover, thanks to his considerateness I was able to find my first accommodation in Amsterdam and to establish my contact to the ECOSYM-group in Montpellier.

At a certain point a further pursuing of my PhD required the union of my family and a relocation to Montpellier. I am therefore deeply grateful to my French colleagues for welcoming me as an unknown, foreign PhD-student in their laboratories despite the bureaucratic difficulties, which they must have feared beforehand. In particular I thank Thierry Bouvier for his openness and for hosting me in his group. He would help me out whenever necessary. I also thank Eric Fouilland and Christophe Leboulanger for their collaboration and facilitation of my research. The three of them made me aware that "there is more in the water than only phytoplankton" and it is thanks to them that my thesis now also carries a chapter on marine bacteria. Once more I very much regret that we did not have the opportunity to work together more closely. I further thank Marc Troussellier and Marc Bouvy as the heads of the group for welcoming me at ECOSYM and Nicolas Mouquet (ISEM) for placing me at the right institute. It was not easy to build up and run chemostat experiments in a foreign lab in a one-person operation. I am therefore thankful to the many people that lend their equipment or lab space, helped me out with consumables or shared their experience, most notably: Sylvain Gandon and Thomas Berngruber (CEFE), Nico Nouwen (LSTM), and Corinne Bouvier, Rutger de Wit, Patrice Got, Claire Carré, Beatrice Bec, Ives Collos, Séverine Boyer, Daniel Grzebyk, Mohamed Laabir, Estelle Masseret, Cécile Roques and Alain Hervé (all ECOSYM). A warm thank goes to Ivan Bettarel and Judith Klein for welcoming me in their appartment for one week. I would still be living in France, if I had the choice.

In my final writing period I was lucky to enjoy a great though laborious 2-weeks stay in the molecular labs of Lucas Stal at Yerseke. I thank Veronique Confurius-Guns and Lilian van der Linde for teaching me how to construct clone libraries and I thank Henk Bolhuis for introducing me to sequence analysis.

Last but not least I am deeply thankful to my parents Dorothee and Wolfgang Brauer for their everlasting support. In those years where I had to fulfill being a "single mother" and PhD-student at the same time, my parents would regularly come up all the long way to Amsterdam to lend me a hand. I thank Thomas, Lisa Marie, and Dominique for sharing my life with me.

Chapter 1

Introduction

Microbial plankton - tiny but prominent

Microbes are tiny and cannot be seen with the naked eye. In the 17th century, the Dutch salesman Antonie van Leeuwenhoek was the first to see and to describe microorganisms using the microscopes that he made. He discovered that a droplet of water was teeming with little organisms – the microbial plankton. Leeuwenhoek already identified various microorganisms in the water, and provided his fellow scientists with a first glimpse of microbial diversity: some organisms were moving in spirals, some had oval shapes, and some were green and formed chains.

Today we know that planktonic microbes encompass many different taxa with a large genetic diversity (Pedrós-Alió, 2006). They can be assigned to different functional groups (Azam, 1998; Fig. 1.1). Eukaryotic microalgae and cyanobacteria represent the primary producers, which convert sunlight into chemical energy and fix CO_2 for biosynthesis. They form the basis of the pelagic food web. Cyanobacteria are a special group of bacteria that possess chlorophyll a and perform oxygenic photosynthesis. Some cyanobacteria are also able to fix atmospheric N_2 and therefore represent an important source of new nitrogen for the planktonic community (Mulholland, 2007). Other members of the bacteria and archaea are important decomposers of dissolved organic matter (DOM) and mineralizers of organic nutrients, thereby making inorganic nutrients available to primary producers and preventing the loss of nutrients into the deep ocean. A considerable number of microbes can also act as mixotrophs by combining phototrophic and heterotrophic processes. For instance, some strains of the ubiquitous marine cyanobacteria *Prochlorococcus* and *Synechococcus* can also use simple organic substrates, and the widely abundant proteobacteria SAR11 and Roseobacter also gain energy by harvesting light with the help of photopigments (Eiler, 2006).

Bacteria and small phytoplankton are preyed upon by protists such as ciliates, heterotrophic flagellates or amoeboids. Protists and the larger bacteria and phytoplankton are consumed by organisms at higher trophic levels, e.g. by zooplankton. All microorganisms can in principle become infected by viruses, which occur either as free particles or as proviruses integrated into the host genome. Viruses are highly abundant and are known to have a strong impact on populations of aquatic bacteria and phytoplankton (Bratbak *et al.*, 1994; Fuhrman, 1999; Bouvy *et al.*, 2011; Mojica and Brussaard, 2014).

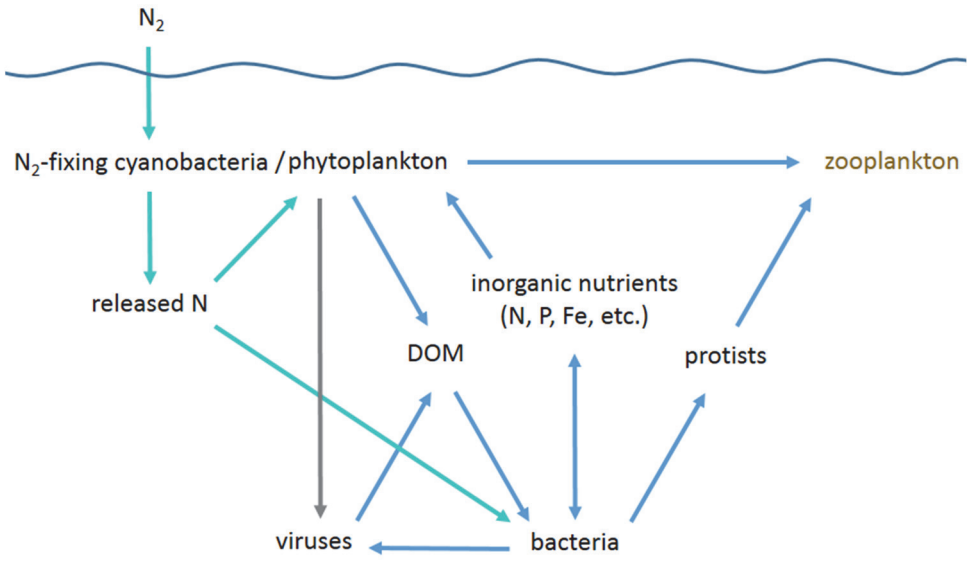

Figure 1.1: Major pathways of carbon and nutrient fluxes in an oceanic microbial plankton community, with special emphasis on N_2 fixation by cyanobacteria, which are part of the phytoplankton. Blue arrows represent the microbial food web as drawn in Azam (1998), green arrows show fluxes of released fixed nitrogen (N) as discussed in Mulholland (2007).

Aquatic microbes are highly abundant (Whitman *et al.*, 1998) and influence oceanic nutrient budgets, global biochemical cycles and the world's climate. For instance, bacteria, including cyanobacteria, are the major drivers of the global cycling of nitrogen (Falkowski *et al.*, 2008). Furthermore, the planktonic microbes of the ocean are responsible for a considerable part of global sulfur emission to the atmosphere by producing the gas dimethyl sulfide (Simó, 2001). This gas acts as an important condensation nucleus for the formation of clouds and therefore has a strong influence on the global climate. Last but not least, the phytoplankton of the ocean, i.e. mostly cyanobacteria and diatoms, account for approximately 50 % of the global primary production, thereby sequestering large amounts of the greenhouse gas CO_2 (Falkowski *et al.*, 2008; Field *et al.*, 2010).

The aim of this thesis is to obtain a better understanding of the factors and mechanisms that control the growth and functioning of the microbial plankton community, with special focus on the roles of temperature, nutrients, and light. Although a lot is known about how these factors influence single species, their impact on more complex communities is less clear. This thesis addresses open questions in the

community ecology of microbial plankton that range from rather detailed questions on the physiology and growth of marine N_2-fixing cyanobacteria to more general questions on the mechanisms controlling the species composition and functioning of entire communities. The thesis proceeds by gradually increasing system complexity using theoretical models and controlled experiments. The insights obtained in this thesis contribute to our understanding of natural microbial plankton communities, whose composition and functioning is currently undergoing major shifts due to global climate change (Karl *et al.*, 2001; Hays *et al.*, 2005; Paerl and Huisman, 2009; Sarmento *et al.*, 2010).

The first part of this thesis investigates the effects of temperature and light on the physiology of a unicellular N_2-fixing cyanobacterium (chapter 2) and the effects of temperature and nutrients on the interaction between a unicellular N_2-fixing cyanobacterium and its associated bacterial community (chapter 3). The second part of this thesis investigates the influence of temperature and resources on microbial plankton communities in a more general way. This is achieved with a mechanistic model on the competition between multiple phytoplankton species for two nutrients and light (chapter 4) and an experimental test of the 'universal temperature dependence' predicted by the metabolic theory of ecology (chapter 5).

A special group: N_2-fixing cyanobacteria

Chapters 2 and 3 of this thesis pay special attention to N_2-fixing cyanobacteria. N_2 fixation is the biological reduction of atmospheric N_2 to NH_3, and is carried out exclusively by certain bacteria and archaea. Organisms capable of fixing N_2 are called diazotrophs (= feeding on dinitrogen). N_2 fixation represents a crucial link in the global nitrogen cycle, as it is the only process that counteracts the loss of nitrogen as N_2 into the atmosphere by other microbial processes such as denitrification or anaerobic ammonium oxidation (Gruber and Sarmiento, 1997; Arrigo, 2005).

Diazotrophs fix N_2 with the help of the enzyme nitrogenase, which catalyzes the reduction of a single molecule of N_2 to 2 molecules of NH_3 and one molecule of H_2. Because N_2 is highly inert, the organism needs to invest 16 ATP and 8 reducing equivalents to fix one molecule of N_2 (Fig. 1.2).

Oxygen leads to the irreversible inactivation of the nitrogenase and, hence, makes N_2 fixation impossible (Fay, 1992). Many diazotrophs therefore live under (nearly) anoxic

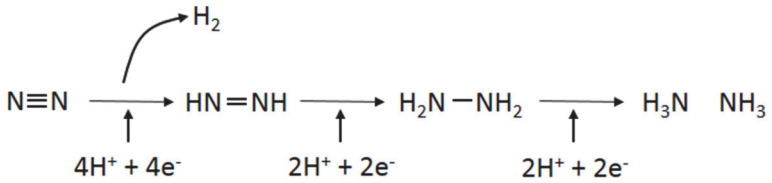

Figure 1.2: Biological nitrogen fixation: reduction of dinitrogen (N_2) to ammonia (NH_3). The production of H_2 is an obligate byproduct of the reaction.

conditions. Yet, diazotrophic cyanobacteria are aerobic organisms that face the dilemma that they require oxygen for respiration and even produce oxygen as a product of photosynthesis. In order to protect nitrogenase from oxygen, these organisms have evolved special adaptations. In brackish and freshwater systems diazotrophic cyanobacteria are filamentous and separate oxygenic photosynthesis and N_2 fixation spatially by differentiating heterocysts, which are special cells for N_2 fixation that lack the oxygen-evolving photosystem II and that possess a thick cell wall acting as a gas diffusion barrier that also limits the diffusion of oxygen. In marine habitats, however, diazotrophic cyanobacteria are non-heterocystous. The abundant filamentous *Trichodesmium* forms a kind of equivalent of the heterocyst, the diazocyte, and its strategy seems to be a combination of a spatial and temporal separation of photosynthesis and N_2 fixation (Berman-Frank *et al.*, 2001). The free-living unicellular diazotrophic cyanobacteria (groups UCYN-B and UCYN-C) separate the two processes temporally by confining N_2 fixation to the night (Gallon, 1992). The recently discovered group of unicellular diazotrophic cyanobacteria (UCYN-A) has evolved a symbiotic relationship with a prymnesiophyte alga, which enables a spatial separation of the two processes (Zehr *et al.*, 2008; Thompson *et al.*, 2012).

Diazotrophic cyanobacteria account for approximately 50 % of the global N_2 fixation and for virtually all N_2 fixation in the ocean (Gruber and Sarmiento, 1997). Probably, they are ecologically successful because they use light as the source of energy and water as the source of electrons, and thus have access to the two most important requirements for fixing N_2. Moreover, the ability to fix N_2 renders diazotrophic cyanobacteria independent of combined nitrogen, and therefore gives them a strong competitive advantage in the generally nitrogen-limited waters of the ocean (Vitousek and Howarth, 1991; Agawin *et al.*, 2007). By introducing new nitrogen into the pelagic realm, they alleviate nitrogen limitation and stimulate the productivity of the whole planktonic community (LaRoche and Breitbarth, 2005; Mulholland, 2007).

Yet, despite the fact that nitrogen limitation is widespread in the open ocean, N_2-fixing cyanobacteria are largely restricted to the warmer waters in the tropics and subtropics (Staal *et al.*, 2003; Stal, 2009). Chapter 2 of this thesis addresses the question whether the distribution of N_2-fixing cyanobacteria in the open ocean is limited by temperature. To investigate this question the effects of temperature, light, and nitrogen source on the growth and N_2-fixation rate of the unicellular diazotrophic cyanobacterium *Cyanothece* are studied in a series of batch cultures. Chapter 3 presents a follow-up study that investigates the effects of temperature and nutrients on the interactions between *Cyanothece* and its associated microbiome in a series of chemostat experiments.

Resource competition and community structure

The growth of microbes is influenced by the availability of growth-limiting resources and by physical factors. Physical factors such as temperature, pH, or salinity influence microbial growth but they are not consumed. In contrast, resources such as nutrients and light stimulate growth and their availability is decreased through consumption and shading, respectively (Tilman, 1982).

Resource competition theory provides a framework for understanding how growth-limiting resources determine the structure of microbial plankton communities, i.e. the species composition and the interaction network (Tilman, 1982; Grover, 1997). In a well-mixed monoculture where cells and nutrients are homogeneously distributed, a species grows and increases in abundance whereby it decreases the concentration of nutrients. At a certain point, the nutrient concentrations become so low that the species' per capita growth rate is strongly decreased and eventually equals its loss rate. The critical nutrient concentration, at which the net growth rate is zero, is called the R^*-value. The R^*-value reflects the physiology of the organism rather than environmental characteristics and is therefore species-specific. Resource competition theory predicts that when several species are competing for a single growth-limiting nutrient, competition is won by the species with the lowest R^*-value for that nutrient *i*n monoculture (principle of competitive exclusion; Grover, 1997). Figure 1.3 illustrates the R^*-rule in a chemostat experiment where the freshwater cyanobacterium *Synechocystis* sp. and the green alga Chlorella vulgaris compete for phosphorus (Passarge *et al.*, 2006). In monoculture, each species grows until it reaches a phosphorus-limited steady state, where *Synechocystis* exploits the phosphate concentrations to a lower level (0.03 µmol/L) than Chlorella (0.059 µmol/L; Fig.

1.3A, B). Consequently, *Synechocystis* is the superior competitor for phosphate and displaces Chlorella when grown in a mixed culture (Fig. 1.3C).

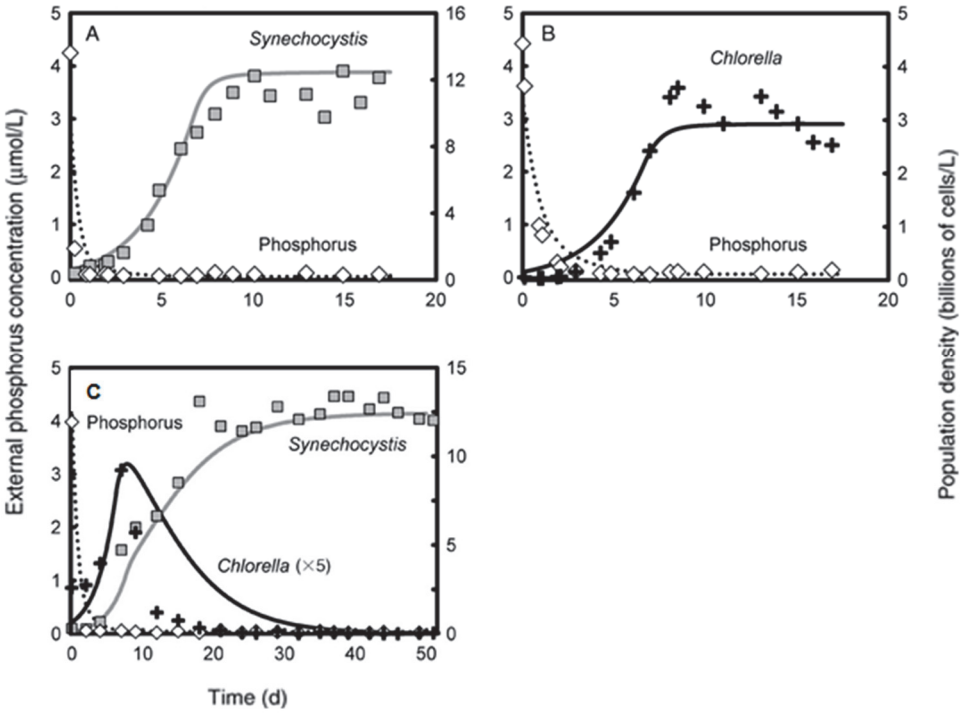

Figure 1.3: Growth and competition of two phytoplankton species in phosphorus-limited chemostats. A, monoculture time series of Synechocystis sp. density and phosphorus concentration. B, monoculture time series of Chlorella vulgaris density and phosphorus concentration. C, Competition for phosphorus between Synechocystis and Chlorella. Figures taken from Passarge et al. (2006).

Phototrophic species may also become limited by light. Competition for light is more complex than competition for nutrients because the underwater light intensity always exhibits a vertical gradient from the surface to the bottom of the water column. In a well-mixed water column a phototrophic species grows and increases in abundance, whereby it decreases the availability of light under water due to self-shading. The minimum light requirement of a species is characterized by a light gradient where the net species growth rate, integrated over the whole depth of the water column, equals zero (Huisman and Weissing, 1994). For a fixed incident light intensity, water column

depth and background turbidity, the minimum light requirement of a species can be defined by the light intensity at the bottom of the water column, I_{out}^*. Resource competition theory predicts that when several species compete for light, competition is won by the species with the lowest I_{out}^*-value in monoculture (Huisman and Weissing, 1994; 1995).

Phytoplankton communities in natural marine and freshwater systems are often co-limited by two or more nutrients at the same time, especially by nitrogen and phosphorus (Elser *et al.*, 2007). Resource competition theory predicts that when several species compete for two limiting nutrients, two species might stably coexist, or a single species outcompetes all other species. Figure 1.4 illustrates competition of two species for nitrogen (N) and phosphorus (P) using a graphical-mechanistic approach (Tilman, 1982; 1985). The solid lines represent the species' zero-net-growth isoclines, which are given by the R^*-values of each species for the two nutrients. In Figure 1.4, species 1 is the superior competitor for phosphorus because it has the lower R^*-value for that nutrient, and species 2 is the superior competitor for nitrogen. The dashed lines show the consumption vectors of the two species, i.e. the ratio at which each species consumes both nutrients. The resource-ratio hypothesis (Tilman, 1982; 1985) predicts that the outcome of competition of two species for two nutrients depends on the ratio of nitrogen to phosphorus, at which the nutrients are supplied to a system. The critical N:P supply ratios are defined by the consumption vectors of the two species, which divide Figure 1.4 into three regions of different nutrient supply ratios leading to one of three different outcomes at steady state: i) relatively high N:P supply ratios in the upper left region of the graph lead to limitation by nutrient 1 and the exclusive dominance of species 1, ii) relatively low N:P supply ratios in the lower right region of the graph lead to limitation by nutrient 2 and the exclusive dominance of species 2, iii) intermediate N:P supply ratios in the middle part of the graphs lead to co-limitation by both nutrients. In this example, the consumption vectors are chosen in a way that each species consumes relatively more of the nutrient, for which it is the inferior competitor, which results in stable coexistence of the two species at intermediate supply ratios. The resource-ratio hypothesis can be applied to the competition between two species but also to the competition between groups of species. For instance, (toxic) freshwater cyanobacteria, which are typically strong competitors for nitrogen and weak competitors for phosphorus, tend to develop blooms in lakes that exhibit a low ratio of total N: total P, whereas other

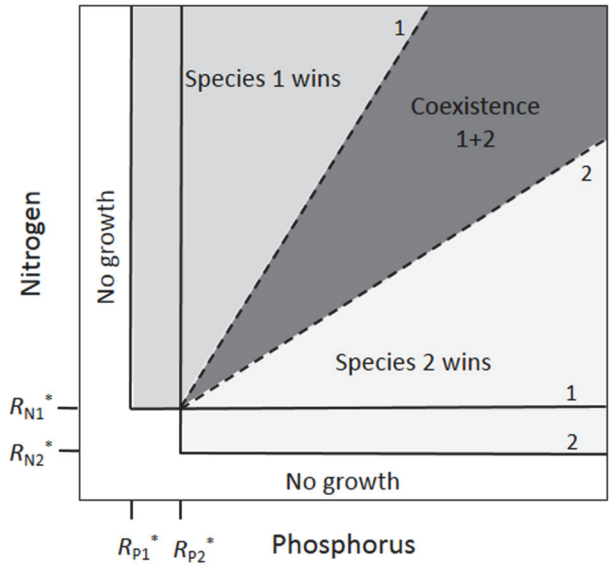

Figure 1.4: Graphical-mechanistic approach to the competition of two species for two nutrients after Tilman (1982). Solid lines show zero-net-growth isoclines of species 1 and 2, dashed lines show their nutrient consumption vectors. Shaded areas show different regions of nutrient supply ratios leading to different outcomes of competition.

phytoplankton species dominate in lakes with a high ratio of total N:total P (Smith, 1983).

When more than two nutrients are limiting the microbial community can be more diverse (Huisman and Weissing, 1999; 2001; Revilla and Weissing 2008) and its composition changes along multidimensional gradients of different nutrient supply ratios. Highest species diversity is expected at the intermediate supply ratios (Tilman, 1982; Sommer, 1993). Yet, eutrophication research has pointed at the fact that the composition of phytoplankton and plant communities also changes when absolute nutrient concentrations increase, and that very high nutrient loads lead to a decrease in species diversity, probably because the system shifts from competition for nutrients to competition for light (e.g. Downing *et al.*, 2001; Hautier *et al.*, 2009). Changes in the outcome of competition along a productivity gradient cannot be predicted by changes in the light: nutrient supply ratios in a simple way (Huisman and Weissing 1995). Therefore, in chapter 4 of this thesis new theory is presented, which aims at disentangling how nutrient supply ratios and absolute nutrient loads affect phytoplankton community structure. This is achieved by combining a classical model

for the competition for two nutrients with a model for the competition for light, and by analyzing the outcome of competition along the productivity gradient.

Temperature dependence of biological processes

Temperature is a fundamental factor that influences life because it determines the rate of biochemical (enzymatic) reactions (Precht, 1973). Organisms are adapted to live within a certain temperature range, where increasing temperature typically raises the rates of metabolism and growth until an optimum temperature is reached, beyond which these rates often drop dramatically (Angilletta *et al.*, 2003). In the face of global warming it is of major importance to better understand the effects of temperature on microbial growth and the functioning of microbes within aquatic communities.

For biochemical reactions the effect of temperature on the reaction rate, r, is often described by the Arrhenius function:

$$r(T) = Ae^{-Ea/kT}, \qquad (1.1)$$

where A is a constant, E_a is the activation energy, k is Boltzmann's constant ($k = 8.62 * 10^{-5}$ eV), and T is absolute temperature in Kelvin. Equation (1.1) describes the increase of the reaction rate with increasing temperature. It does not describe the deceleration and decrease of the reaction rate at high temperatures at which the enzyme loses its activity. The Arrhenius-function is a widely used temperature function in biology. Although it was originally developed for (bio)chemical reactions, it often provides a good phenomenological description of the effect of temperature on very different kinds of biological rates such as per capita growth rate, nutrient uptake rate, or respiration rate of individuals, populations or communities (e.g. Gillooly *et al.*, 2001; Enquist *et al.*, 2003; López-Urrutia *et al.*, 2006; Dell *et al.*, 2011).

Temperature plays a central role in the Metabolic Theory of Ecology (MTE), which argues that the metabolic rate of organisms is the fundamental biological rate that governs most observed patterns in ecology (Brown *et al.*, 2004). MTE can be considered as an energy-based theory that, in its essence, describes the effect of temperature and body size on the metabolic rate of organisms. MTE assumes that the Arrhenius-equation describes the temperature dependence of metabolic processes, provided that they are corrected for the effect of body size. Heterotrophic processes are predicted to show a stronger temperature-dependence than photoautotrophic processes, exhibiting a mean activation energy of 0.65 eV and 0.32 eV, respectively (Gillooly *et al.*, 2001; Allen *et al.*, 2005; Wilken *et al.*, 2013), although there is

considerable variation around these values (e.g. Dell *et al.*, 2011). According to MTE, the metabolic rate of an individual determines all other rates of that individual.

MTE further implies that the Arrhenius-equation can be scaled up to the levels of whole communities and ecosystems (Brown *et al.*, 2004). The idea that the fundamental temperature-dependence of biochemical reaction rates (equation 1) is quantitatively reflected in virtually all biological processes is denominated 'universal temperature dependence'. Chapter 5 provides one of the first experimental tests of this universal temperature dependence at the community level, by using natural microbial plankton assemblages from the Dutch Wadden Sea. The communities are grown in the lab in enriched seawater medium and at high light intensities for eight days, and the rates of biomass increase are assessed at five different temperatures between 6 °C and 20 °C. To critically test whether the universal temperature dependence applies to the growth rate of entire communities, chapter 5 compares the model fits of four different temperature functions that are frequently used in biology.

Thesis outline

This thesis combines experimental and theoretical approaches to investigate the effects of temperature, nutrients, and light on the growth of specific microbes and the functioning of whole microbial plankton communities. Chapters 2 and 3 investigate the specific case of marine nitrogen-fixing cyanobacteria, whereas chapters 4 and 5 deal with general theories of ecological communities and their predictions for microbial plankton communities in particular.

In chapter 2 I ask the question why marine nitrogen-fixing cyanobacteria in the open ocean are restricted to the tropics and subtropics, and whether this global distribution reflects the physiological feasible temperature range of nitrogen fixation in oceanic diazotrophic cyanobacteria. To investigate this question I measure the effects of temperature and light on the rates of growth, nitrogen fixation, and respiration as well as on the cellular carbon and nitrogen content of the unicellular diazotrophic cyanobacterium *Cyanothece* sp. Miami BG043511 in batch cultures. Moreover, the experiments are performed in nitrogen-fixing cultures as well as in non-nitrogen fixing (i.e. nitrate assimilating) cultures, to specify the physiological consequences of N_2 fixation for this organism.

In chapter 3 I explore the interactions between the nitrogen-fixing cyanobacterium *Cyanothece* sp. Miami BG043511 and its accompanying community of chemotrophic

bacteria in chemostats. To this aim the consortium of *Cyanothece* and associated bacteria are cultured under different concentrations of nitrate and glucose and at different temperatures. During the course of the experiments I follow the dynamics of the population densities and the concentrations of glucose, nitrate, and phosphate. Furthermore, the consortium at steady state is analyzed in terms of species composition and elemental composition. The results are discussed with regard to the role of diazotrophic cyanobacteria in shaping the community composition of microbial plankton.

In chapter 4 I formulate a model of multiple phytoplankton species competing for two inorganic nutrients and light in a well-mixed water column. The study explores the dynamics of competition between phytoplankton species that differ in their resource requirements. The model makes predictions about resource limitation, community composition and biodiversity of phytoplankton and plant communities along a nutrient enrichment gradient. The study aims at reconciling discrepancies between the predictions of the well-established resource ratio theory and field observations, by tackling the question whether resource ratios or absolute nutrients loads determine the structure of natural phytoplankton and plant communities. It also offers a solution to a central debate in eutrophication research, which questions whether the ratio of total nitrogen:total phosphorus or the absolute loads of these nutrients are better predictors for the occurrence of harmful cyanobacteria blooms in freshwater lakes.

In chapter 5 I switch to the metabolic theory of ecology. I specifically focus on the concept of the universal temperature dependence, which states that the Arrhenius-relationship that describes the effect of temperature on the reaction rate of enzymes can be scaled up to many different biological rates at all levels of organization. The study uses controlled experiments to test whether the Arrhenius-relationship can describe the effect of temperature on the growth rate of a whole plankton community. It provides one of the first and very few controlled community experiments that have been specifically designed to test predictions of the metabolic theory of ecology.

In chapter 6 I provide an overview over the main results and discuss new questions that arise from the results presented in this thesis.

Chapter 2

Low temperature delays timing and enhances respiratory cost of nitrogen fixation in the unicellular cyanobacterium *Cyanothece* sp.

Verena S. Brauer, Maayke Stomp, Camillo Rosso, Sebastiaan A. M. van Beusekom, Barbara Emmerich, Lucas J. Stal, Jef Huisman

The ISME Journal 7, 2105-2115, 2013

ABSTRACT

Marine nitrogen-fixing cyanobacteria are largely confined to the tropical and subtropical ocean. It has been argued that their global biogeographical distribution reflects the physiologically feasible temperature range at which they can perform nitrogen fixation. In this study we refine this line of argumentation for the globally important group of unicellular diazotrophic cyanobacteria, and pose the following two hypotheses: (i) nitrogen fixation is limited by nitrogenase activity at low temperature and by oxygen diffusion at high temperature, which is manifested by a shift from strong to weak temperature dependence of nitrogenase activity, and (ii) high respiration rates are required to maintain very low levels of oxygen for nitrogenase, which results in enhanced respiratory cost per molecule of fixed nitrogen at low temperature. We tested these hypotheses in laboratory experiments with the unicellular cyanobacterium *Cyanothece* sp. BG043511. In line with the first hypothesis, the specific growth rate increased strongly with temperature from 18 to 30 °C, but leveled off at higher temperature under nitrogen-fixing conditions. As predicted by the second hypothesis, the respiratory cost of nitrogen fixation and also the cellular C:N ratio rose sharply at temperatures below 21 °C. In addition, we found that low temperature caused a strong delay in the onset of the nocturnal nitrogenase activity, which shortened the remaining nighttime available for nitrogen fixation. Together, these results point at a lower temperature limit for unicellular nitrogen-fixing cyanobacteria, which offers an explanation for their (sub)tropical distribution and suggests expansion of their biogeographical range by global warming.

INTRODUCTION

The global distribution of dinitrogen (N_2)-fixing cyanobacteria across the world's ocean exhibits a striking relationship with temperature. Marine N_2-fixing cyanobacteria occur in high numbers only in the tropics and subtropics, at water temperatures above 20 °C, while they are virtually absent from temperate and polar regions (Staal *et al.*, 2003; Stal, 2009). This temperature-related geographic pattern seems to hold for different phylogenetic groups of oceanic N_2-fixing cyanobacteria, such as the filamentous *Trichodesmium* (Capone *et al.*, 1997; Lugomela *et al.*, 2002; Chen *et al.*, 2003; Langlois *et al.*, 2005, 2008), unicellular cyanobacteria (UCYN) of the groups B and C (Mazard *et al.*, 2004; Staal *et al.*, 2007; Church *et al.*, 2008; Langlois *et al.*, 2008; Moisander *et al.*, 2010), and the heterocystous symbionts of diatoms (Foster *et al.*, 2007; Dore *et al.*, 2008; Fong *et al.*, 2008). Representatives of the uncultured, symbiotic UCYN-A show peak abundances in subtropical waters, but it appears that their temperature range is somewhat broader (Needoba *et al.*, 2007; Church *et al.*, 2008; Langlois *et al.*, 2008; Moisander *et al.*, 2010).

The effect of temperature on the global distribution pattern of N_2-fixing cyanobacteria might be direct or indirect. Indirect temperature effects may operate for instance through negative correlations of temperature with the availability of nitrate and ammonium, which may favor the dominance of N_2-fixers in warm combined nitrogen-poor waters (Monteiro *et al.*, 2011). Furthermore, high surface temperature causes water column stratification, which may favor the dominance of floating N_2-fixing species such as *Trichodesmium* (Sonntag and Hense, 2011). The temperature response of N_2-fixation may explain the ecological success of N_2-fixers. For instance, Breitbarth *et al.* (2007) showed that the temperature range for growth and N_2-fixation of *Trichodesmium* IMS-101 in laboratory experiments matched the biogeographical distribution of *Trichodesmium* in the ocean. Similar experiments revealed that also N_2-fixing UCYN have their temperature niche above 20 °C (Falcón *et al.*, 2005; Webb *et al.*, 2009)

A possible physiological mechanism explaining the thermal properties of N_2-fixing cyanobacteria was proposed by Staal *et al.* (2003) and Stal (2009). These authors hypothesized that N_2-fixing cyanobacteria are restricted to warm waters because at low temperature the organism is unable to maintain sufficiently low levels of oxygen in the N_2-fixing cell to avoid the inactivation of nitrogenase. Here, we refine this hypothesis for UCYN-B and -C, which contribute substantially to the global oceanic nitrogen budget (Zehr, 2011; Großkopf *et al.*, 2012). Representatives of the UCYN groups B and C exhibit a strong diurnal pattern in N_2-fixation, respiration, and photosynthesis

(Peschek *et al.*, 1991; Schneegurt *et al.*, 1994b; Colón-López *et al.*, 1997; Červený and Nedbal, 2009). In order to protect nitrogenase from high oxygen concentrations produced during photosynthesis, these organisms fix nitrogen typically during the night. Their nocturnal N_2-fixation is fueled by respiration of the glycogen pool that has been built up by photosynthesis during daytime (Schneegurt *et al.*, 1994a; Dron *et al.*, 2012a).

As pointed out by Staal *et al.* (2003) and Stal (2009), respiration of glycogen requires oxygen, and UCYN therefore face an important trade-off. Oxygen levels in the cell should be sufficiently low to prevent inactivation of nitrogenase, yet the influx of oxygen should be sufficiently high to enable respiration for N_2-fixation. Oxygen diffusion into cells shows only a weak temperature dependence (Fig. 2.1A). In contrast, respiration and N_2-fixation are enzymatic processes that, in potential, will increase faster with temperature than oxygen diffusion. Hence, at high temperature, the actual N_2-fixation activity may become limited by the oxygen influx (Fig. 2.1A). Conversely, at low temperature, nitrogenase activity will be the rate-limiting step for N_2-fixation. However, the respiration rate needs to be high enough to protect nitrogenase against the diffusive influx of oxygen. A low nitrogenase activity in combination with sustained high levels of respiration results in high respiration costs per molecule of N_2 fixed at low temperature (Fig. 2.1B). We thus derived two testable hypotheses: (1) N_2-fixation rates of UCYN will increase more strongly with temperature at low temperature than at high temperature (Fig. 2.1A), and (2) low temperature enhances the respiratory cost of N_2-fixation (Fig. 2.1B).

In this study, we test these hypotheses by investigating N_2-fixation and respiration rates of the unicellular cyanobacterium *Cyanothece* sp. BG043511 at different temperatures. To infer the respiratory cost of N_2-fixation, we compared the respiration rates of *Cyanothece* under diazotrophic versus non-diazotrophic growth conditions. In addition, we measured the light response of the N_2-fixation and growth rates of *Cyanothece* at different temperatures. Our results show strong effects of temperature on the respiratory cost as well as the timing of N_2-fixation in *Cyanothece*, which offers a mechanistic explanation for the temperature dependence of the global biogeographical distribution of other N_2-fixing UCYN.

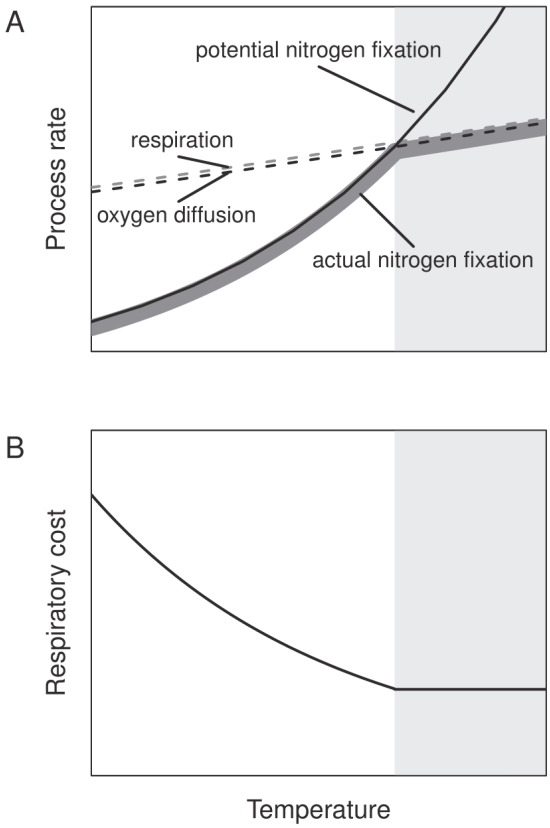

Figure 2.1: Conceptual visualization of the two hypotheses explaining temperature dependence of N_2-fixation in unicellular cyanobacteria. (A) Rates of oxygen diffusion (black dashed line) and potential N_2-fixation (black solid line) as function of temperature. The actual N_2-fixation rate (thick grey line) equals the potential N_2-fixation rate at low temperature, but is limited by the oxygen diffusion rate at high temperature. The respiration rate (grey dashed line) matches the rate of oxygen diffusion into the cells in order to maintain a low-oxygen environment for nitrogenase. (B) Comparison of the respiration rate with the actual N_2-fixation rate, in panel a, shows that the respiratory cost of N_2-fixation (i.e., the oxygen respired per molecule of N_2 fixed) will increase strongly at low temperature. Background shading indicates temperature regions where nitrogen fixation is controlled by the reaction rate of nitrogenase (white background) or the rate of oxygen diffusion (dark background).

MATERIALS AND METHODS

Experimental design

The strain *Cyanothece* sp. Miami BG043511 was grown in batch cultures with a volume of 50 mL in 250 mL-Erlenmeyer flasks on artificial sea water medium enriched with nutrients (Mitsui and Cao, 1988). The mineral medium was provided either with 1.5 mM nitrate (non-diazotrophic condition) or without combined nitrogen (diazotrophic condition). The cultures were grown under an alternating 12:12 h light:dark cycle. A shaking cryostat bath controlled the temperature and guaranteed continuous mixing of the cultures. The effects on growth of *Cyanothece* of seven different temperatures from 14 °C to 38 °C and nine light intensities from 3 to 133 µmol photons m^{-2} s^{-1}, as well as the growth with or without nitrate, were investigated. Prior to the experiment, *Cyanothece* was acclimated to the applied

temperature and nitrogen source at an intermediate light intensity of approximately 30 μmol photons m^{-2} s^{-1} for at least one week.

Growth rates

The specific growth rate of each population was determined during the exponential growth phase. Cells were counted in triplicate almost every day using an automatic cell counter (Casy Cell Coulter, Schaerfe System GmbH, Reutlingen, Germany). Specific growth rates were calculated as the slope of the regression line of the natural logarithm of population density versus time.

One growth experiment was carried out for each temperature, nitrogen source and light intensity. At each experimental temperature, the light response of the specific growth rate, $\mu(I)$, was described by the Monod equation (Monod, 1950; Huisman, 1999):

$$\mu(I) = \frac{\mu_{\max} I}{(\mu_{\max} / \alpha) + I} \tag{2.1}$$

where I is light intensity, μ_{max} is the maximum specific growth rate, and α is the initial slope of the $\mu(I)$-function. Equation (2.1) was fitted to the measured growth rates using nonlinear regression with minimization of the residual sum of squares (R version 2.13.1).

Subsequently, the temperature dependence of the maximum specific growth rate was described by the Arrhenius equation (Gillooly *et al.*, 2001):

$$\mu_{\max}(T) = c\, e^{\frac{-E}{kT}} \tag{2.2}$$

where c is a normalization constant, E is the activation energy, k is Boltzmann's constant (8.62 x 10^{-5} eV K^{-1}) and T is the absolute temperature in Kelvin. The activation energy quantifies the temperature dependence, and was calculated as the slope of the linear regression of $\ln(\mu_{max})$ plotted against the inverse of temperature, $1/kT$. Activation energy was converted to Q_{10}-values according to Vasseur and McCann (2005).

Nitrogen fixation rates

N_2-fixation rate was determined during the exponential growth phase using the acetylene reduction assay (Hardy *et al.*, 1968). Whole-night N_2-fixation was measured in duplicate incubations of 12 hours. In addition, we used six consecutive incubations of 2 hours each to follow the temporal pattern of nocturnal N_2 fixation. Whole-night incubations were done in 5-mL crimp-top vials (Chrompack, Middelburg) using 1 mL of *Cyanothece* culture and a headspace acetylene concentration of 20 %. For the 2-hours incubations 3 mL of culture and 11 % acetylene was used. After incubation, gas samples of 300 µL were withdrawn from the headspace with a disposable syringe and injected into a gas chromatograph (GC14A, Shimadzu) equipped with a flame ionization detector (FID) to measure the concentrations of ethylene and acetylene. The temperatures of oven, injector, and detector were set to 60 °C, 100 °C, and 150 °C, respectively. N_2-fixation was expressed as acetylene reduction, and was calculated according to Stal (1988) using acetylene as internal standard.

Analogous to the specific growth rates, the light response of N_2-fixation was fitted to the Monod equation (Equation 2.1) by expressing the whole-night N_2-fixation as function of the light intensity provided during the preceding daytime. Subsequently, the maximum whole-night N_2-fixation obtained from the Monod equation (n_{max}) was fitted to the Arrhenius equation (Equation 2.2) to quantify its temperature dependence.

Cost of nitrogen fixation

We used two measures to quantify the respiratory cost of N_2-fixation. First, we calculated the gross cost of N_2-fixation (C_{gross}), which we defined as the whole-night respiration of N_2-fixing cultures divided by the whole-night N_2-fixation:

$$C_{gross} = \frac{\int_0^{12h} r_{N2}(t)dt}{\int_0^{12h} Nf(t)dt} \tag{3.3}$$

where $r_{N2}(t)$ is the respiration rate of the N_2-fixing culture as function of time, and $Nf(t)$ is its N_2-fixation rate. Accordingly, the gross cost of N_2-fixation includes respiration associated directly with N_2-fixation as well as respiration required for the maintenance of other cellular processes.

Second, we calculated the net cost of N_2-fixation (C_{net}), defined as the difference between the whole-night respiration of N_2-fixing and non-N_2-fixing cultures divided by the whole-night N_2-fixation:

$$C_{net} = \frac{\int_0^{12h} [r_{N2}(t) - r_{NO_3}(t)]dt}{\int_0^{12h} Nf(t)dt} \quad (3.4)$$

where $r_{NO3}(t)$ is the respiration rate of the non-N_2-fixing culture as function of time. Hence, the net cost of N_2-fixation excludes the maintenance cost associated with other metabolic processes. For both measures, a conversion factor of 4 was used to calculate N_2-fixation from acetylene reduction (e.g. Stal, 1988).

Respiration rates

Respiration was monitored during the 12-hours dark period using automated recording of oxygen consumption. *Cyanothece* was grown in Erlenmeyer flasks under high-light conditions (130 µmol photons m^{-2} s^{-1}) and a 12:12 h light:dark cycle, at 5 different temperatures (from 18 °C to 30 °C) under both N_2-fixing and non- N_2-fixing conditions. The cultures were continuously mixed with magnetic stirrers. Each Erlenmeyer flask was connected to a temperature-controlled flow-through cuvette with a chamber volume of approximately 5 mL. Every 30 min a peristaltic pump (Watson Marlow 101U, Falmouth, UK) connected to a computer-controlled USB-time relay (H-TRONIC, Hirschau, Germany) flushed the flow-through cuvette during 7 min with a new air-saturated sample taken from the Erlenmeyer flask. Subsequently, the pump was stopped and the decline in oxygen concentration was measured on-line during 10 min using optical oxygen sensors connected to a fiber optic oxygen transmitter (Oxy-4-mini, PreSens, Regensburg, Germany). The respiration rate was calculated as the slope of the regression line of oxygen concentration versus time.

Cellular carbon and nitrogen

At the end of a 12 hours night, 5 to 10 mL of the high-light cultures were filtrated on pre-combusted glass fiber filters (GF/F, Watson). The filters were rinsed with demineralized water, and stored at -20 °C. Amounts of organic carbon and nitrogen

on each filter were determined with an element analyzer (NA-2500, Thermo Scientific, Whaltham (MA), USA) to determine cellular carbon and nitrogen contents.

RESULTS

Growth and nitrogen fixation

The specific growth rate of *Cyanothece* increased with light intensity and became saturated at higher light intensities except those of the cultures grown at the expense of nitrate at 34 and 38 °C, which did not saturate at the highest light intensity tested (Fig. 2.2). The exact response to light, however, depended on temperature and nitrogen source. Likewise, whole-night nitrogen fixation was a saturating function of the light intensity received during the preceding daytime, and varied with temperature (Fig. 2.3). The light responses could be well described by the Monod equation (black lines in Fig. 2.2 and 2.3), and the parameter values obtained from these Monod fits are plotted as function of temperature in Figure 2.4.

Nitrogenase activity (acetylene reduction) was not detectable in cultures grown under non- N_2-fixing conditions (with NO_3^-) (results not shown). At 14 °C, *Cyanothece* showed only marginal growth under non-N_2-fixing conditions, while we were unable to grow *Cyanothece* diazotrophically at this temperature (Fig. 2.2A, 2.4A). From 18 to 30 °C, the maximum specific growth rate of the N_2-fixing and non- N_2-fixing cultures increased with temperature in a similar manner (Fig. 2.4A), with activation energies of 0.81 eV (95% CI: 0.76 - 0.85 eV, $df = 3$, $p < 0.001$; $Q_{10} = 2.89$) and 0.90 eV (95% CI: 0.70 - 1.11 eV, $df = 3$, $p = 0.0134$; $Q_{10} = 3.28$) under N_2-fixing and non-N_2-fixing conditions, respectively. The maximum specific growth rate continued to increase with temperature up to 34 °C under non- N_2-fixing conditions, whereas it leveled off above 30 °C under N_2-fixing conditions. Hence, at high temperature, *Cyanothece* reached much higher specific growth rates under non-N_2-fixing than under N_2-fixing conditions.

Maximum whole-night N_2-fixation showed a unimodal response to temperature (Fig. 2.4B). At 14 and 18 °C, whole-night N_2-fixation did not exceed the detection limit in most cases (see Fig. 2.3B). Maximum whole-night N_2-fixation increased strongly with temperature from 22 to 30 °C, with an activation energy of 1.27 eV (95% CI: 0.05 - 2.5 eV, $df = 2$, $p = 0.29$; $Q_{10} = 5.2$). Above 30 °C, however, maximum N_2-fixation decreased with temperature (Fig. 2.4B).

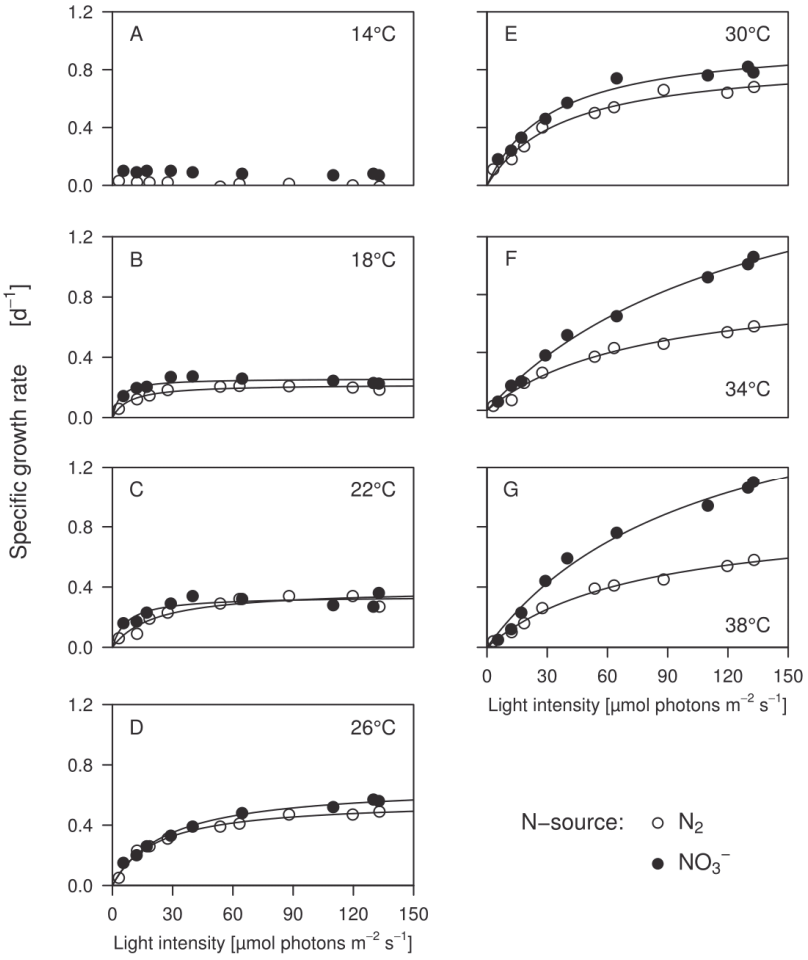

Figure 2.2: Light-response curves of the specific growth rate at different temperatures. Each panel compares the light response of N_2-fixing cultures (open circles) versus cultures grown on nitrate (closed circles). Each data point is from a unique growth experiment. Solid lines show light-response curves fitted by the Monod equation.

At 18 and 22 °C, the initial slope of the light-dependent growth rate (α_μ) was higher for non-N_2-fixing cultures than for N_2-fixing cultures (Fig. 2.4C). Above 22 °C, the initial slope of the light-dependent growth rate seemed largely temperature independent, and was essentially similar under both N_2-fixing and non- N_2-fixing conditions. The initial slope of the light-dependent whole-night N_2-fixation (α_n) showed considerable variation, but seemed also largely independent of temperature (Fig. 2.4D). The low value of α_n at 18 °C might be an outlier due to the technical

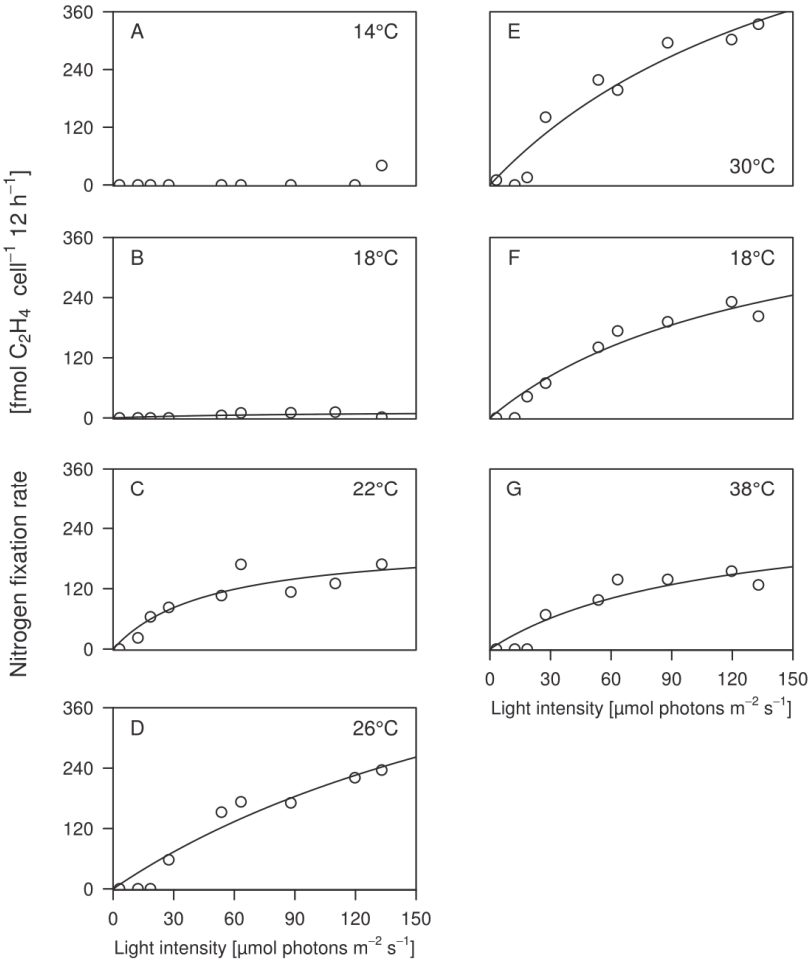

Figure 2.3: Light-response curves of whole-night N_2-fixation at different temperatures. N_2-fixation is expressed as acetylene reduction, integrated over the entire 12 hours-night. Light intensities were measured during the preceding daytime. Each data point is from a unique experiment. Solid lines show light-response curves fitted by the Monod equation.

difficulty to obtain an accurate light-response curve from the low N_2-fixation rates measured at this temperature (cf. Fig. 2.3B).

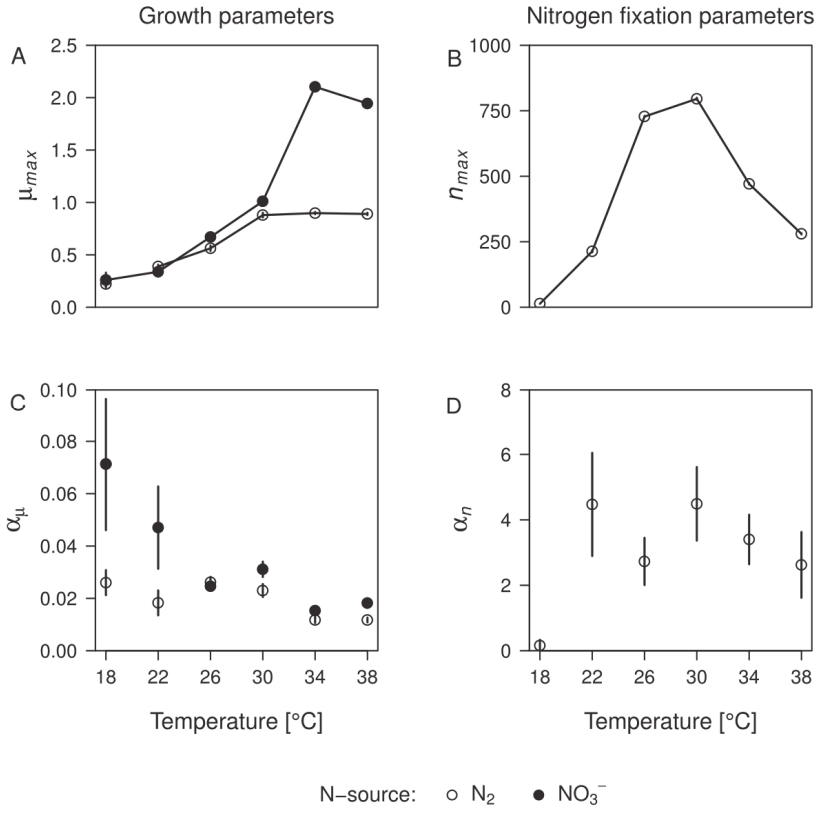

Figure 2.4: Monod parameters for the light response of the specific growth rate and of the whole-night N_2-fixation, plotted as function of temperature. (A) Maximum specific growth rate, μ_{max}; (B) maximum whole-night N_2-fixation, n_{max}; (C) initial slope, α_μ, of the light-response curves of the specific growth rates, (D) initial slope, α_n, of the light-response curves of whole-night N_2-fixation. Open circles represent N_2-fixing cultures; closed circles represent cultures grown on nitrate. Vertical lines show standard errors of the estimate. The parameter estimates are based on the Monod fits shown in Figures 2.2 and 2.3.

Nocturnal patterns of nitrogen fixation and respiration

As a next step, we investigated how temperature affects temporal patterns of N_2-fixation (acetylene reduction) and respiration (oxygen consumption) during the 12 h dark period. This revealed that N_2-fixation and respiration exhibited very similar nocturnal patterns (Fig. 2.5). In most cases, N_2-fixation started after the onset of

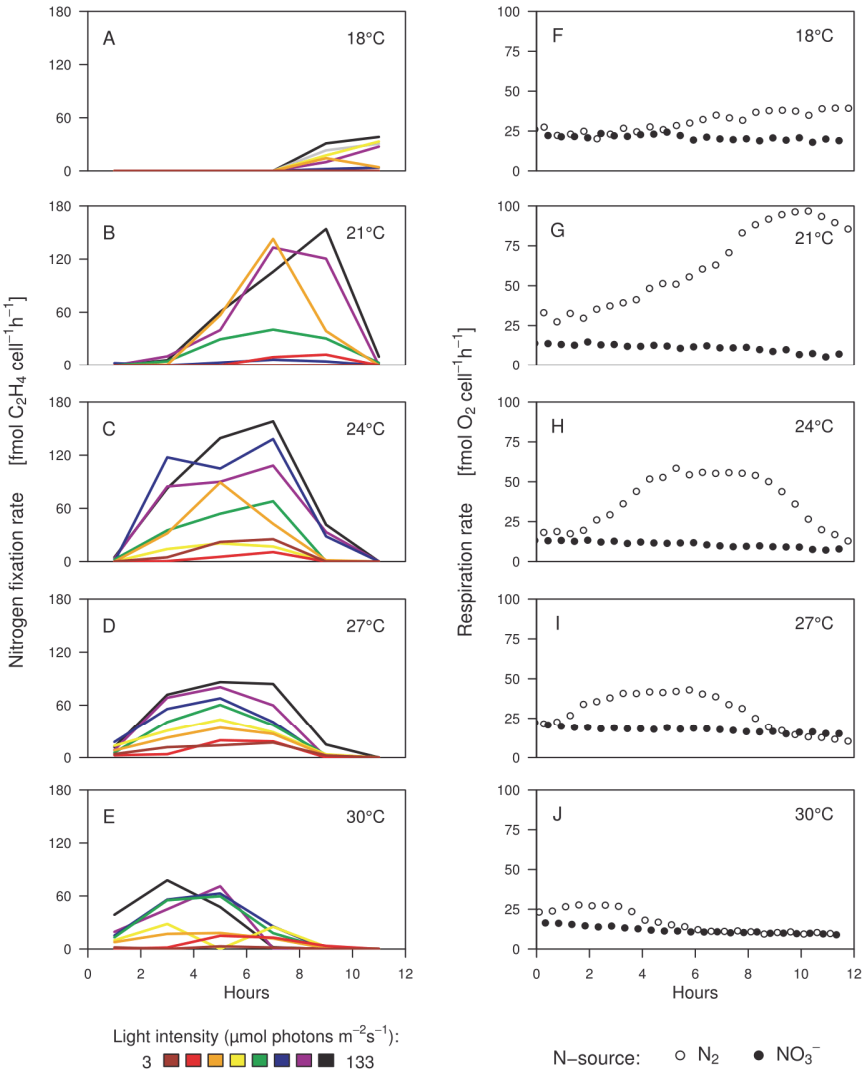

Figure 2.5: Nocturnal patterns of N_2-fixation (acetylene reduction) and respiration (oxygen consumption) at different temperatures. (A-E) The N_2-fixation rate was measured during six consecutive intervals of two hours each, covering the entire 12 h dark period. The different light intensities provided during daytime are indicated by different colors. (F-J) Respiration rate of N_2-fixing cultures (open circles) and non-N_2-fixing cultures (closed circles) during the 12 h dark period, after exposure to a daytime light intensity of 130 µmol photons m^{-2} s^{-1}. N_2-fixation and respiration rates were measured in separate cultures.

darkness and ceased before daybreak. However, the precise timing of the N_2-fixation activity was strongly determined by temperature. The N_2-fixation peak shifted from

the end of the dark period at 18 °C to the beginning of the dark period at 30 °C (Fig. 2.5A-E). N_2-fixation reached the highest rate at intermediate temperatures from 21 to 27 °C (Fig. 2.5B-D). At each temperature, N_2-fixation rates in the night increased with the light intensity provided during the preceding daytime, but light intensity did not affect the temporal pattern of N_2-fixation (Fig. 2.5A-E).

The temporal pattern of respiration reflected that of N_2-fixation (Fig. 2.5F-J). Respiration rates of N_2-fixing cultures reached a maximum during the night, and the timing of this maximum shifted from the end of the dark period at low temperature to the beginning of the dark period at high temperature (open circles in Fig. 2.5F-J). The highest respiration rates were found at intermediate temperatures (Fig. 2.5G-I). In contrast, respiration rates of non-N_2-fixing cultures remained low and were basically constant during the dark period (closed circles in Fig. 2.5F-J).

Cost of nitrogen fixation

We introduced two measures of the respiratory cost per molecule of N_2 fixed. The gross cost of N_2-fixation considers the whole-night respiration of the N_2-fixing culture (i.e., the area underneath the open circles in Figures 2.5F-J integrated over the 12 h-dark period), while the net cost considers the difference in whole-night respiration between the N_2-fixing and non-N_2-fixing culture (i.e., the area between the open and closed circles in Fig. 2.5F-J integrated over the 12 h-dark period). Both measures strongly increased with decreasing temperature (Fig. 2.6A). At 18 °C, the gross cost of N_2-fixation was about five times higher than at 30 °C, while the net cost of N_2-fixation was about four times higher. Likewise, the C:N-ratio of the cells determined at the end of the 12 h-dark period increased at low temperature, particularly for the N_2-fixing cultures at 14 °C and 18 °C (Fig. 2.6B).

DISCUSSION

Mechanisms controlling temperature dependence

The results show that temperature has major effects on growth, N_2-fixation and respiration of the unicellular N_2-fixing cyanobacterium *Cyanothece*. In agreement with the first hypothesis, displayed in Figure 2.1A, the maximum specific growth rate of *Cyanothece* grown under N_2-fixing conditions showed a strong temperature dependence at low temperature but a weak temperature dependence at high

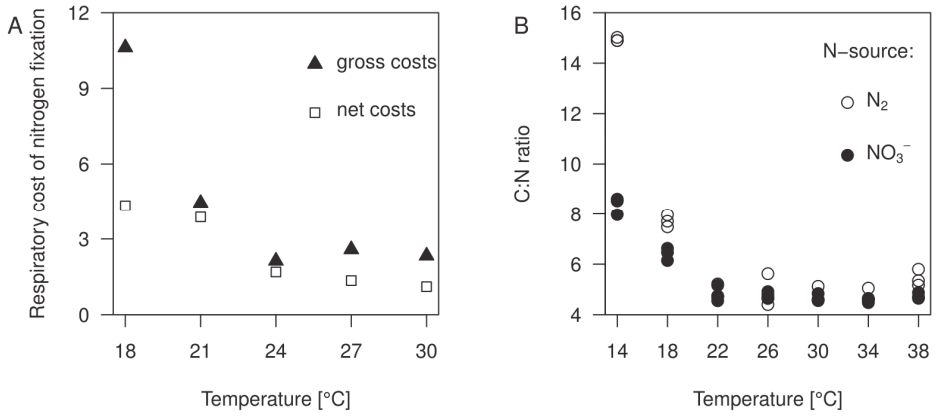

Figure 2.6: Respiratory cost of N_2-fixation. (A) Gross respiratory cost (closed triangles) and net respiratory cost (open squares) of N_2-fixation as function of temperature. Gross respiratory cost represents the ratio of whole-night respiration over whole-night N_2-fixation, net respiratory cost represents the same ratio but corrected for respiration not associated with N_2-fixation. (B) Cellular C:N ratio of N_2-fixing (open circles) and non-N_2-fixing cultures (closed circles). The C:N ratios were measured at the end of the 12 h dark period in cultures exposed to 80-130 µmol photons m^{-2} s^{-1} during daytime.

temperature (Fig. 2.4A). The switch from strong to weak temperature dependence occurred at 30 °C, suggesting that the diffusive influx of oxygen (and possibly N_2) limited a further increase of the diazotrophic growth rate at higher temperatures. In contrast, the specific growth rate under non-N_2-fixing conditions still increased steeply with temperature at this temperature range, demonstrating that cells were capable of a much higher growth rate if they were not limited by the N_2-fixation process (Fig. 2.4A).

While the specific growth rate leveled off above 30 °C, the maximum whole-night N_2-fixation declined above this temperature. Gallon *et al.* (1993) observed a similar decline of the N_2-fixation rate in the cyanobacteria *Anabaena* cylindrica and Gloeothece. Their results indicate that the decline is probably not caused by thermal inactivation of nitrogenase, because in vitro studies showed that thermal inactivation of nitrogenase required much higher temperatures. Instead, Gallon *et al.* (1993) attributed the decreased N_2-fixation rate to an enhanced sensitivity of nitrogenase to oxygen inhibition at elevated temperature. Another possible explanation is that the observed decrease of the acetylene reduction rate above 30 °C does not represent the actual N_2-fixation rate. This latter explanation would be compatible with the

observation that the growth rate did not decline (Fig. 2.4A) and cellular C:N ratio remained low (Fig. 2.6B) above 30 °C.

Respiratory cost of nitrogen fixation

Our findings support the hypothesis, in Figure 2.1B, that the respiratory cost of N_2-fixation increases at low temperature (Fig. 2.6A). It is well known that N_2-fixing cyanobacteria often have elevated respiration rates compared to non-N_2-fixing organisms (e.g. Wastyn *et al.*, 1988; Peschek *et al.*, 1991). This is typically ascribed to the high energy demand of nitrogenase (Bergman *et al.*, 1997). However, the observed increase in respiratory cost at low temperature suggests that part of the respiratory oxygen consumption is independent of the energy demand of N_2-fixation, and is used to maintain low intracellular oxygen levels. Großkopf and LaRoche (2012) estimated that the N_2-fixing UCYN *Crocosphaera watsonii* invested only 40 % of the energy obtained from respiration directly into N_2-fixation and maintenance metabolism, while up to 60 % of the respiratory cost represented an indirect cost for removal of intracellular oxygen or reversal of oxidative damage e.g. by *de novo* nitrogenase synthesis. Our results show that this indirect cost varies with temperature. More specifically, the fourfold rise in net respiratory cost above the baseline value (Fig. 2.6A) suggests that, at low temperature, the indirect cost associated with oxygen removal may constitute up to 80 % of the total cost of N_2-fixation.

We currently do not know which oxygen-scavenging mechanisms are present in *Cyanothece* sp. BG043511. One possible strategy is 'respiratory protection', where organisms possess a branched electron transport chain with multiple terminal oxidases, as has been shown for a number of bacteria and the unicellular N_2-fixing cyanobacterium Gloeothece (Maryan *et al.*, 1986; Gallon, 1992). An alternative strategy is 'autoprotection', where the nitrogenase enzyme protects itself by reducing oxygen to H_2O and H_2O_2 (Gallon, 1992; Bergman *et al.*, 1997).

High respiratory cost of N_2-fixation at low temperature have also been found in diazotrophic symbionts of terrestrial plants. Using Frankia-infected root nodules of alder, Winship and Tjepkema (1985) showed that nitrogenase activity decreased faster with temperature than the respiration rate. As a consequence, the respiratory cost per molecule of fixed N_2 rose sharply at low temperature, similar to our findings. This indicates that the high respiratory cost of N_2-fixation at low temperature, required to maintain low intracellular oxygen concentrations, might be a common challenge for N_2-fixing organisms in both aquatic and terrestrial habitats.

The cultures were lightly contaminated by other bacteria but their contribution to the measured rates of respiration, if at all, would not affect our conclusions. It is reasonable to assume that the background respiration would be constant and would in worst case give a small and constant error in the actual respiration rate. The fact that respiration in nitrate-grown cultures decline slightly is in agreement with the depletion of the internal storage carbohydrate of *Cyanothece*. Respiration in the N_2-fixing cultures is very much higher than in the nitrate-grown cultures and also always and strictly follows the pattern of nitrogenase activity. One would not expect this difference in respiration nor this pattern when respiration originated from contaminating heterotrophic bacteria. Moreover, since we rely on the difference between respiration in N_2-fixing and nitrate-grown cultures our data are not affected by respiration by contaminating bacteria. Then, the four-fold increase in respiration cost with decreasing temperature in N_2-fixing cultures is associated with *Cyanothece* and could not be explained by heterotrophic activity. The growth medium that we used is a fully mineral medium designed exclusively for photoautotrophic organisms. Hence, it does not contain any substrate to respire for chemotrophic bacteria. Our results therefore supports unequivocally the hypotheses that respiratory cost increases with decreasing temperature, as predicted by theory and reported for another UCYN, *Crocosphaera watsonii* (Großkopf and LaRoche, 2012).

Timing of dinitrogen fixation

In addition to the predicted results, we found that temperature has also a remarkable effect on the timing of N_2-fixation. The timing of N_2-fixation and many other processes involved in the nitrogen and carbon metabolism of the genus *Cyanothece* is under the tight control of a circadian clock. N_2-fixation and respiration show a distinct 24 h-periodicity, and photosynthesis peaks about 12 h out of phase (Peschek *et al.*, 1991; Schneegurt *et al.*, 1994b; Colón-López *et al.*, 1997; Červený and Nedbal, 2009). The circadian oscillations of N_2-fixation and other processes are expressed independently of external triggers, under continuous light (Colón-López *et al.*, 1997; Toepel *et al.*, 2008; Červený and Nedbal, 2009), under continuous darkness (Schneegurt *et al.*, 1994), and under various day-night cycles (Červený and Nedbal, 2009; Toepel *et al.*, 2009). Studies on the phosphorylation cycle of the cyanobacterial clock protein KaiC demonstrated that the period of oscillations is independent of nutrient status and temperature (Nakajima *et al.*, 2005; Tomita *et al.*, 2005). In addition, our study shows that differences in light intensity during the daytime did not affect the timing of N_2-fixation during the night. However, decreasing the

temperature strongly delayed the onset of N_2-fixation (Fig. 2.5). A possible explanation might be that the synthesis of nitrogenase proceeds at a lower rate at low temperature. In N_2-fixing UCYN nitrogenase is inactivated by oxygen during the day and has to be resynthesized *de novo* every night (Mullineaux *et al.*, 1981; Huang *et al.*, 1988; Gallon, 1992; Bergman *et al.*, 1997). Thus, even if the circadian clock is temperature-compensated and always initiates the synthesis of nitrogenase at exactly the same time, there might be a temperature-dependent delay in the delivery of the functional enzyme. This may cause a decrease in N_2-fixation capacity if low temperature would delay the synthesis of active nitrogenase to such an extent that the remaining nighttime becomes insufficient to cover the nitrogen demands of the cell. The observed delay in the timing of N_2-fixation may thus contribute to the steep decline of the whole-night N_2-fixation activity (Fig. 2.4B) and to the high cellular C:N ratio (Fig. 2.6B) at low temperature.

Biogeographical distribution

Although many environmental factors may influence the distribution of N_2-fixing cyanobacteria, such as the availability of dissolved nitrogen, iron and phosphorus (e.g Sañudo-Wilhelmy *et al.*, 2001; Mills *et al.*, 2004; Monteiro *et al.*, 2011), there is ample evidence that temperature plays also an important role (Stal, 2009). According to our laboratory results, *Cyanothece* grows well over a temperature range from 18 to at least 38 °C. This is in good agreement with the observation that N_2-fixing UCYN-B and -C occur only in natural waters above 20 °C (Mazard *et al.*, 2004; Langlois *et al.*, 2005; Staal *et al.*, 2007; Church *et al.*, 2008; Langlois *et al.*, 2008; Moisander *et al.*, 2010). The global biogeographical distribution might thus reflect the direct effect of temperature on the physiology and growth of these organisms (see also Breitbarth, 2007). In nature, competitive interactions with other species may further restrict the temperature range of N_2-fixing UCYN, particularly below 21 °C when the respiratory cost of N_2-fixation becomes high. Our experiments thus support the idea that the lower temperature limit is related to the high respiratory cost of N_2-fixation. Moreover, we also found that low temperature might incur additional costs by delaying the timing of N_2-fixation.

Together, these results provide novel experimental evidence supporting the general hypothesis that the temperature sensitivity of N_2-fixation is a key determinant of the biogeographical distribution of N_2-fixing UCYN across the world's ocean. An

important implication of these findings is that global warming is likely to facilitate the expansion of N_2-fixing UCYN to higher latitudes.

Acknowledgements
We thank Joke Westerveld and Frans van der Wielen for technical assistance in gas chromatography, Hans Matthijs for his interest and scientific discussions, and Franjo Weissing for facilitating the research. The research of V.S.B, M.S., and J.H. was supported by the Earth and Life Sciences Foundation (ALW), which is subsidized by the Netherlands Organization for Scientific Research (NWO).

Chapter 3

Competition and facilitation between a marine nitrogen-fixing cyanobacterium and its associated bacterial community

Verena S. Brauer, Maayke Stomp, Thierry Bouvier, Eric Fouilland, Christophe Leboulanger, Veronique Confurius-Guns, Franz J. Weissing, Lucas J. Stal, Jef Huisman

Frontiers in Microbiology 5, 795, 2015

ABSTRACT

N_2-fixing cyanobacteria represent a major source of new nitrogen and carbon for marine microbial communities, but little is known about their ecological interactions with associated microbiota. In this study we investigated the interactions between the unicellular N_2-fixing cyanobacterium *Cyanothece* sp. Miami BG043511 and its associated free-living chemotrophic bacteria at different concentrations of nitrate and dissolved organic carbon (DOC) and different temperatures. High temperature strongly stimulated the growth of *Cyanothece*, but had less effect on the growth and community composition of the chemotrophic bacteria. Conversely, nitrate and carbon addition did not significantly increase the abundance of *Cyanothece*, but strongly affected the abundance and species composition of the associated chemotrophic bacteria. In nitrate-free medium the associated bacterial community was co-dominated by the putative diazotroph *Mesorhizobium* and the putative aerobic anoxygenic phototroph *Erythrobacter* and after addition of organic carbon also by the Flavobacterium *Muricauda*. Addition of nitrate shifted the composition toward co-dominance by *Erythrobacter* and the Gammaproteobacterium *Marinobacter*. Our results indicate that *Cyanothece* modified the species composition of its associated bacteria through a combination of competition and facilitation. Furthermore, within the bacterial community, niche differentiation appeared to play an important role, contributing to the coexistence of a variety of different functional groups. An important implication of these findings is that changes in nitrogen and carbon availability due to, e.g., eutrophication and climate change are likely to have a major impact on the species composition of the bacterial community associated with N_2-fixing cyanobacteria.

INTRODUCTION

Nitrogen is one of the key elements limiting the primary productivity of large parts of the oceans (Vitousek and Howarth, 1991; Moore *et al.*, 2013). Hence, the input of new nitrogen by dinitrogen (N_2)-fixing cyanobacteria will not only benefit the diazotrophs themselves but may also affect other members of the oceanic plankton community. For example, in a laboratory study, Agawin *et al.* (2007) demonstrated that the unicellular diazotroph *Cyanothece* sp. facilitated the non-diazotroph *Synechococcus* sp. through the release of fixed nitrogen. Furthermore, field studies have shown transfer of fixed nitrogen from large diazotrophic cyanobacteria to picoplankton in the Baltic Sea (Ohlendieck *et al.*, 2000) and in the Southwest Pacific (Garcia *et al.*, 2007). Similarly, blooms of diazotrophic *Trichodesmium* spp. are often succeeded by diatoms (Lenes *et al.*, 2001) or dinoflagellates (Walsh and Steidinger, 2001; Mulholland *et al.*, 2006), which may benefit from the nitrogen fixed by the diazotrophs.

It seems likely that marine N_2-fixing cyanobacteria supply nitrogen not only to other phototrophs but also to chemotrophic bacteria. Yet, not much is known about the interactions between these two groups of organisms. Although *Trichodesmium* colonies are typically associated with chemotrophic bacteria (Paerl *et al.*, 1989; Sheridan *et al.*, 2002), both positive and negative interactions of N_2-fixing cyanobacteria with chemotrophic bacteria have been described. For instance, Tseng *et al.* (2005) reported a higher abundance and productivity of chemotrophic bacteria during a *Trichodesmium* bloom. In contrast, Renaud *et al.* (2005) observed a decreased bacterial abundance and activity during a *Trichodesmium* bloom and also Nausch (1996) observed lower bacterial abundance and thymidine incorporation within a *Trichodesmium* bloom compared to the adjacent water.

The relationships between N_2-fixing cyanobacteria and chemotrophic bacteria may indeed be complex. On the one hand, N_2-fixing cyanobacteria and chemotrophic bacteria compete for dissolved nutrients such as phosphate. Chemotrophic bacteria are likely to be superior competitors for dissolved nutrients due to their small size and high substrate affinities (Currie and Kalff, 1984; Bratbak and Thingstad, 1985; Tambi *et al.*, 2009). On the other hand, N_2-fixing cyanobacteria can release substantial amounts of fixed nitrogen and organic carbon, which would facilitate chemotrophic bacteria (e.g. Glibert and Bronk, 1994; Mulholland *et al.*, 2004, 2006; Wannicke *et al.*, 2009; Dron *et al.*, 2012; but see Benavides *et al.*, 2013).

Furthermore, interactions within the microbial consortium are probably temperature dependent. N_2-fixing cyanobacteria of the open ocean occur in significant numbers only in the warm waters of the tropics and subtropics (Stal, 2009). Recently, we have demonstrated that temperatures below 21 °C hampered N_2-fixation and induced

nitrogen deficiency in the unicellular N_2-fixing *Cyanothece* sp. (Brauer *et al.*, 2013). The cost per molecule of N_2 fixed increased at low temperature, basically because the N_2-fixation rate declined while the cells still needed to invest in an oxygen-free environment to enable functionality of the nitrogenase enzyme. Moreover, below 21 °C the onset of nitrogenase activity was strongly delayed to the end of the night, probably because the *de novo* synthesis of nitrogenase takes more time at low temperature. These physiological mechanisms may explain why *Cyanothece* and other free-living unicellular N_2-fixing cyanobacteria grow well in warm waters only. Higher temperatures decreased the cost of N_2 fixation and stimulated growth and N_2-fixation rates (Brauer *et al.*, 2013). Hence, it is likely that increasing temperature also increases the amount of released nitrogen and organic carbon, thereby stimulating chemotrophic bacteria indirectly.

With this study we aim for a better insight into the functioning of a microbial consortium consisting of an N_2-fixing cyanobacterium and its associated chemotrophic bacteria. We formulate four testable hypotheses: 1) N_2-fixing cyanobacteria are strongly stimulated by temperature, but will respond much less to an increase in dissolved nitrogen or organic carbon as they can fix N_2 and CO_2. 2) Chemotrophic bacteria associated with N_2-fixing cyanobacteria are co-limited by dissolved nitrogen and organic carbon, and will strongly increase when dissolved nitrogen and organic carbon are either released by the diazotrophs or supplied in the growth medium. 3) Higher temperatures increase the abundance of chemotrophic bacteria because of enhanced nitrogen and organic carbon release by the N_2-fixing cyanobacteria. 4) The taxonomic composition of the chemotrophic community changes with both temperature and nutrient availability.

We tested these hypotheses by growing the marine unicellular N_2-fixing cyanobacterium *Cyanothece* sp. together with its accompanying community of chemotrophic bacteria in chemostats under different nitrogen, dissolved organic carbon and temperature conditions.

MATERIALS AND METHODS

Cyanothece strain

The marine unicellular cyanobacterium *Cyanothece* sp. strain Miami BG043511 (further named *Cyanothece*) is a facultative diazotroph that assimilates nitrate and switches to N_2-fixation when nitrate becomes scarce (Agawin *et al.*, 2007). The non-axenic but unialgal strain was obtained from the University of Hawaii Culture

Collection and maintained at room temperature under moderate light conditions in carbon and nitrogen-deficient mineral medium ("–C–N"; see below).

Chemostat experiments

Cyanothece was grown in chemostats together with its associated community of chemotrophic bacteria. Chemostats were made of glass tubes with a water jacket and had an inner diameter of 4 cm and a working volume of approximately 250 mL. The water jacket was connected to a refrigerating-heating circulator (F12-EH, Julabo GmbH, Seelbach, Germany), which guaranteed precise temperature control (± 0.1°C) of the culture. Light was supplied from one side at an alternating 12:12 hour light:dark cycle and an incident light intensity of 110 µmol photons m^{-2} s^{-1}, which is a saturating light level for the growth of *Cyanothece* (Brauer *et al.*, 2013). Chemostats were run at a dilution rate of 0.2 d^{-1} using a peristaltic pump (Minipuls 2, Gilson, Inc., Middleton, WI, USA). Bubbling of the culture vessels with air from a six-channel aquarium pump (ACO-9620, Guangdong Hailea Group Co., Ltd, Raoping, China) assured homogeneous mixing of the culture.

Cyanothece and its accompanying chemotrophic bacterial community were cultured at three temperatures (18, 23 and 28 °C) and four different nutrient regimes. The nutrient regimes were determined by the nitrogen and dissolved organic carbon (DOC) content of the growth medium, which contained either 0 or 100 µmol L^{-1} $NaNO_3$ and either 0 or 2 mmol L^{-1} carbon provided as glucose. The medium always contained 25 µmol L^{-1} KH_2PO_4. The concentrations of the nutrients were chosen such that DOC, nitrate, or phosphate may become growth limiting at steady-state. All other nutrients were available in excess (Supplementary Table 3.1). Hence, the molar C:N:P ratios in the four different nutrient treatments were 0:0:1 ("–C–N"), 0:4:1 ("–C+N"), 80:0:1 ("+C–N"), and 80:4:1 ("+C+N"). Sampling of the chemostats started the day after inoculation.

Unfortunately, one treatment (28 °C; –C+N) failed. *Cyanothece* cell density and the steady state measurements of particulate organic phosphorus were recovered from a previous pilot experiment performed under the same conditions but other data are missing.

Cell counts and biovolume

Samples (1.75 mL) for cell counts were taken almost every day and fixed with formaldehyde (1 % final concentration) for 30 min, flash-frozen with liquid nitrogen, and stored at -80 °C. Cells were stained with SYBR-Green 1 (Lumiprobe, FL, USA) and counted in triplicate by flow cytometry (FACS Calibur equipped with a 488 nm laser, Becton Dickinson, San Jose, CA, USA) using pre-calibrated counting beads (2.07 µm Nile Red, Spherotech, Inc., Lake Forest, Il, USA). The flow cytometer discriminated between cyanobacteria and other bacteria based on fluorescence and light scatter. Cell numbers of *Cyanothece* and chemotrophic bacteria are reported as the mean of the triplicate counts. Steady state cell numbers were calculated as the mean over the last 10 days of each experiment (day 22 to 32).

The total biovolume of *Cyanothece* and chemotrophic bacteria at steady state was calculated as the product of steady state cell number and the mean cell volume. Because volume data of individual cells were right-skewed, mean cell volume was estimated as the geometric mean of 30 (*Cyanothece*) or 100 (chemotrophic bacteria) cells. Individual cell volume was calculated from the measurements of length L and width W of SYBR-Green 1-stained cells with epifluorescence microscopy. Cell volume V_C of a prolate spheroid *Cyanothece* cell was calculated as $V_C = (\pi/6)\times W^2\times L$ (Hillebrand *et al.*, 1999). Cell volume V_b of a coccus or rod-shaped bacterium was calculated as $V_b = (\pi/4)\times W^2\times(L-W/3)$ (Bratbak, 1985).

Nutrient dynamics

For the determination of residual DOC (glucose), N (nitrate) and P (phosphate) concentrations 2 mL (for DOC) or 6 mL (for N and P) of culture were sampled almost every day and filtered over a sterile 0.2 µm membrane filter (Acrodisc; Pall Corporation, Port Washington, NY, USA; for C) or a glass fiber filter (GF/F, Whatman, Maidstone, UK; for N and P). The filtrates were stored at -20 °C. Nitrate and phosphate concentrations were analyzed by an autoanalyzer (SEAL QuAAtro, SEAL Analytical, ltd., Hampshire, UK). DOC (glucose) concentrations were determined with the glucose-oxidase assay (GAGO-20, Sigma-Aldrich, USA). Steady state nutrient concentrations were calculated as mean concentration between day 22 and day 32 of each experiment.

Elemental composition of the community

The elemental composition of the total community was determined from the concentrations of particulate organic carbon (POC), particulate organic nitrogen (PON) and particulate organic phosphorus (POP) at steady state. Measurements were done in triplicate by filtering 5 mL of culture over a pre-combusted glass fiber filter (Whatman GF/F; for POC and PON) or over a 0.45 µm nitrocellulose membrane filter (Millipore Corporation, Bedford, MA, USA; for POP), previously washed with 0.2 M HCl and rinsed with demineralized water. Filters were subsequently rinsed again with demineralized water and stored at -20 °C. Prior to analysis, filters were dried at 60 °C for 48 h. POC and PON were analyzed by an element analyzer (NA-2500 Thermo Analyzer, Thermo Fisher Scientific, Whaltham, MA, USA). POP was determined through digestion of the organic material with nitric acid at 200 °C and subsequent analysis at 213.6 nm with an inductively coupled plasma-optical emission spectrophotometer (iCap 6000 ICP-OES Analyzer, Thermo Fisher Scientific).

Chemotrophic bacteria clone library

The composition of the chemotrophic bacterial community at steady state was determined with the help of 16S rRNA gene clone libraries. A sample of 60-90 mL was taken from each chemostat and filtered over a glass fiber filter (Whatman GF/C; nominal pore size 1.2 µm) to remove *Cyanothece* cells. The smaller bacteria that passed through were collected on a 0.2 µm polycarbonate filter (Nuclepore Track-Etched Membrane, Whatman) and stored at -20 °C. Filters were cut into small pieces and bacterial DNA was extracted using the MOBIO UltraClean Soil DNA extraction kit (MOBIO Laboratories, Inc. Carlsbad, CA, USA) according to the manufacturer's protocol. The concentration of the isolated DNA was measured spectrophotometrically with a NanoDrop ND 1000 (Nanodrop Technologies, Inc. Wilmington, DE, USA). The nearly complete 16S rRNA gene was then amplified using the primers 8F (5' AGA GTT TGA TCM TGG CTC AG 3') and 1492R (5' GGT TAC CTT GTT ACG ACT T 3') (Weisburg *et al.*, 1991). The 25 µL PCR reaction mixture contained 3 % v/v dimethyl sulfoxide (Sigma-Aldrich, Munich, Germany), 0.01 % v/v bovine serum albumin (Fermentas, Hanover, MD, USA), 0.2 µmol of each primer, 0.2 µmol dNTP's (Roche Applied Science, Indianapolis, IN, USA), 1 x HotStarPCR buffer and 0.04 units HotStarTaq DNA Polymerase (Qiagen Inc., Valencia, CA, USA), and 10-20 ng DNA. Cycling conditions were 15 min at 95 °C, followed by 35 cycles with 1 min at 95 °C, 30 s at 55 °C, and 1 min and 50 s at 72 °C, and a final extension period of 7 min at 72 °C. PCR products were separated

by electrophoresis on a 1 % w/v agarose (Sigma-Aldrich) gel and stained with SYBR Gold (Invitrogen Corp., Carlsbad, CA, USA). Amplicon size was estimated by comparison with a Mass Ruler DNA Ladder (Fermentas) and purified using EZNA Cycle Pure Kit (Omega bio-tek Inc., Doraville GA, USA). The freshly purified amplicons were cloned with the help of the TOPO-TA cloning Kit (Invitrogen Corp.). White colonies were selected, suspended in 10 µL MilliQ water, and boiled for 10 min to free the vectors. The inserted 16S rRNA gene fragment was amplified with the vector primers M13F (5' GTA AAA CGA CGG CCA G 3') and M13R (5' CAG GAA ACA GCT ATG AC 3'). The 25µL PCR mixture contained 0.2 µmol of each primer, 0.2 µmol dNTP's, 1 x PCR reaction buffer and 0.03 units NEB Taq polymerase (New England Biolabs Inc., Ipswich , MA, USA), and 1 µL of sample DNA. Cycling conditions were 2 min at 94 °C, followed by 40 cycles with 1 min at 94 °C, 1 min at 55 °C, and 2 min at 72 °C, and a final extension period of 10 min at 72 °C. The PCR products were checked on a 1 % agarose gel. Amplicons were purified using Sephadex G-50 Superfine (Sigma-Aldrich) and DNA-concentrations were determined spectrophotometrically by NanoDrop. Amplicons were partially sequenced (400-600 bp) using the 1492R-primer and the BigDye Terminator chemistry (Big Dye Terminator v3.1 Cycle Sequencing Kit, Applied Biosystem, Foster City, CA, USA) according to the manufacturer's protocol, using a 3130 Genetic Analyzer (Applied Biosystems).

Nucleotide sequence accession numbers

The newly determined 16S rRNA sequences were deposited in NCBI GenBank under accession numbers KP325715 - KP326298.

Statistics and sequence analysis

To test the effects of temperature and nutrient treatment, a two-way ANOVA without replication (McDonald, 2009; Zar, 2010) was conducted on the mean of cell numbers and biovolumes measured between day 22 and 32 of the experiment (steady state). A normal two-way ANOVA was applied to the independent replicates of POC, PON, and POP. Because of the failed treatment (28 °C; –C+N) all ANOVAs were calculated using Type IV sum of squares, which are designed for the situation where there are missing cells. ANOVAs were performed in SPSS 22.0.0.

Sequences were manually inspected and corrected in MEGA 6.06 and analyzed for similarity in BLASTn (Basic Local Alignment Search Tool, National Center for Biotechnology Information, 8600 Rockville Pike, Bethesda, USA). To compare the community composition of associated chemotrophic bacteria between the treatments, a matrix of pairwise Euclidean distances was calculated based on shifted log-transformed (1+x) absolute taxon abundance. The distance matrix was subjected to a hierarchical agglomerative cluster analysis using the complete linkage algorithm. The cluster analysis was done in R 3.0.3.

RESULTS

Population dynamics

Regular microscopic inspection revealed that the microbial consortium in our experiments consisted of healthy non-senescent *Cyanothece* cells and free-living chemotrophic bacteria; we did not observe bacteria attached to *Cyanothece* cells or other forms of cell aggregates. The growth of *Cyanothece* was hardly affected by the nutrient treatment, but was strongly affected by temperature (Fig. 3.1). At 18 °C, the population density of *Cyanothece* remained at a low but constant level in three of the four treatments (–C–N, +C–N, –C+N; Fig. 3.1A-C), whereas it was continuously declining in the other treatment (+C+N; Fig. 3.1D). At 23 and 28 °C, the population density of *Cyanothece* initially increased and then approached a steady state after 10 to 18 days in all nutrient treatments (Fig. 3.1E-L).

Conversely, chemotrophic bacteria showed a weaker response to temperature but a strong response to the nutrient treatment, in particular to nitrate addition. When neither DOC nor nitrate was added to the medium (–C–N) chemotrophic bacteria density remained low throughout the experiment at all temperatures (Fig. 3.1A,E,I). Addition of DOC (+C–N) did not lead to an increase of chemotrophic bacteria at the lower temperatures (Fig. 3.1B,F) but stimulated bacteria at 28 °C (Fig. 3.1J). In response to nitrate addition (+C+N) bacteria exhibited strong growth and reached high population densities after 16-18 days at both 18 and 23 °C (Fig. 3.1C,G). Bacterial data are not available for the –C+N treatment at 28 °C. The simultaneous supply of DOC and nitrate (+C+N) generally stimulated bacteria, with higher population densities at a higher temperature (Fig. 3.1D,H,L). Bacterial densities in the

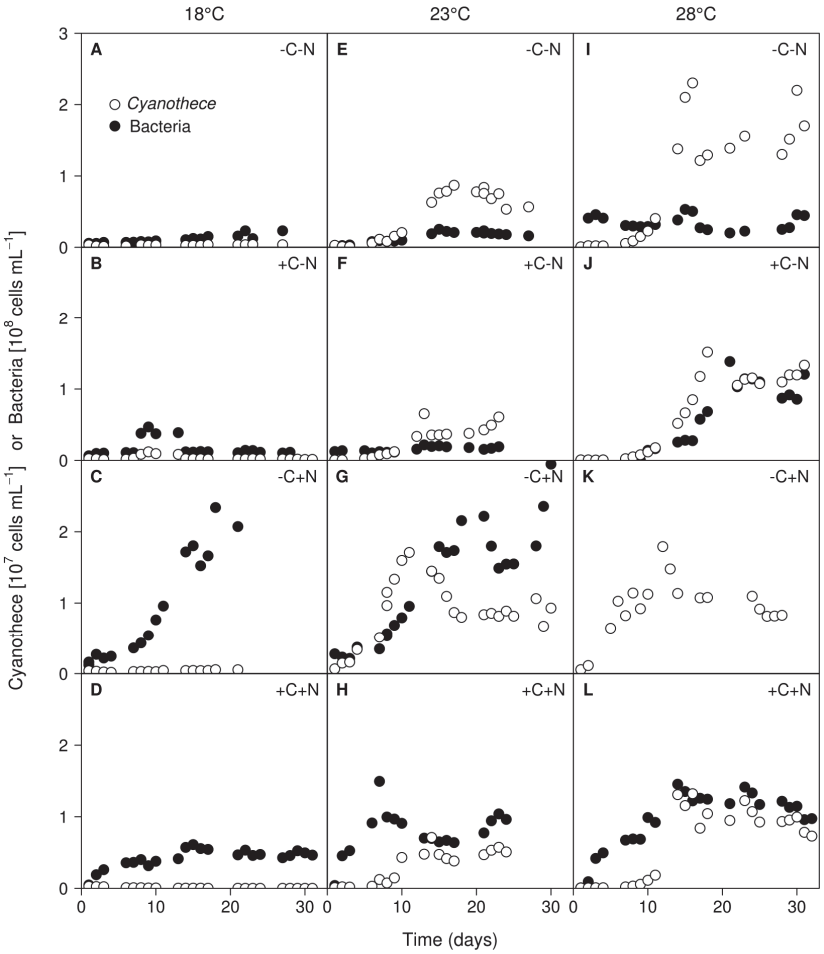

Figure 3.1: Time series of *Cyanothece* sp. and chemotrophic bacteria. *Cyanothece* sp. (open symbols) and chemotrophic bacteria (closed symbols) were grown together in chemostat experiments. Columns show temperature treatments at (A-D) 18 °C, (E-H) 23 °C and (I-L) 28 °C, rows show nutrient treatments with or without addition of DOC (C) and nitrate (N). Data of chemotrophic bacteria from the failed –C+N treatment at 28 °C (panel K) are missing.

+C+N treatment were generally lower than in the –C+N treatment (compare Fig. 3.1D,H,L with Fig. 3.1C,G,K).

The steady state population density of *Cyanothece* was significantly influenced by temperature but not by nutrient treatment (Fig. 3.2A; temperature: $F_{2,6} = 28.778$, $p < 0.001$; nutrient treatment: $F_{3,6} = 1.017$, $p = 0.448$). Conversely, the steady state

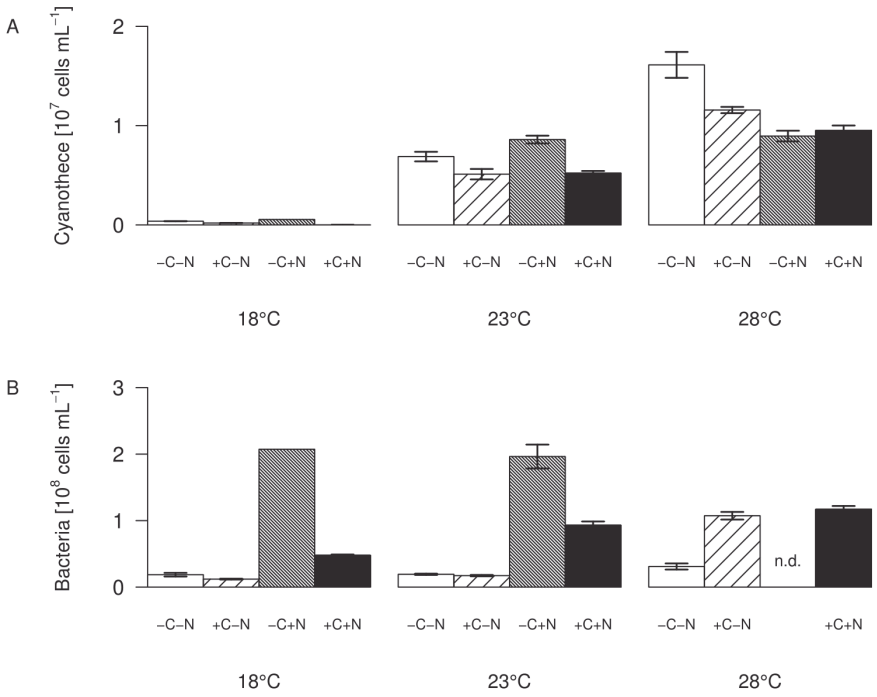

Figure 3.2: Steady-state population densities. (A) *Cyanothece* sp., (B) chemotrophic bacteria. Bars show the mean ± SE of the population densities measured between day 22 and day 32, for each temperature and nutrient treatment (see Fig. 3.1). Nutrient treatments: +C = with added DOC; +N = with added nitrate. Standard errors are not available for the –C+N treatment at 18 °C (n=1); n.d. = no data.

population density of chemotrophic bacteria was significantly affected by nutrient treatment but not by temperature (Fig. 3.2B; temperature: $F_{2,6}$ = 4.297, p = 0.082; nutrient treatment: $F_{3,6}$ = 26.015, p = 0.002). The steady state biovolume of *Cyanothece* and bacteria showed the same patterns as the steady state population density (Supplementary Fig. S3.1).

The contribution of chemotrophic bacteria to the total community was not affected by the nutrient treatment but was significantly reduced at higher temperatures (Fig. 3.3; temperature: $F_{2,6}$ = 10.675, p = 0.025; nutrient treatment: $F_{3,6}$ = 2.36, p = 0.213), from 7–18.5 % of the total community biovolume at 18 °C to <4 % at 23 and 28 °C. Hence, in terms of biomass, at higher temperatures the community was almost completely dominated by *Cyanothece*.

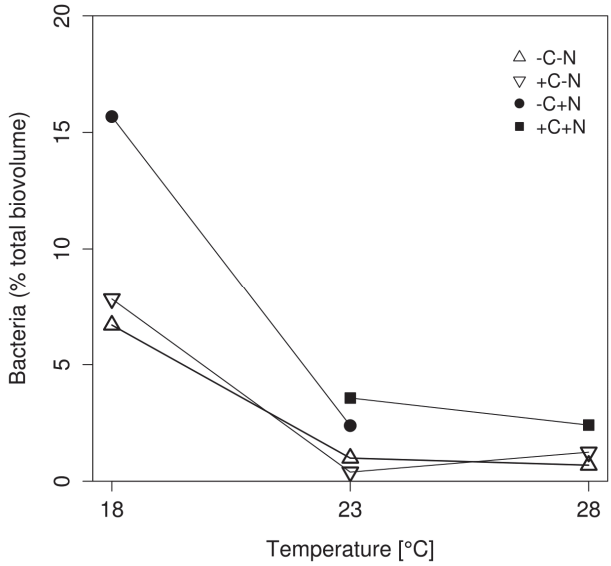

Figure 3.3: Effect of temperature on the relative abundance of chemotrophic bacteria. The relative abundance of chemotrophic bacteria is expressed as percentage of the total biovolume at steady state. Symbols indicate different nutrient treatments (+C = with added DOC; +N = with added nitrate). Data points are missing for the +C+N treatment at 18 °C because the *Cyanothece* abundance was too low to be accurately quantified, and for the failed –C+N treatment at 28 °C.

Nutrient dynamics

The growth of *Cyanothece* and chemotrophic bacteria led to the depletion of DOC, nitrate, and phosphate (Fig. 3.4). Nitrate concentrations were diminished to very low levels from the first day of sampling onwards in all treatments. At 18 °C phosphate concentrations remained high at ~10 µmol L^{-1} (Fig. 3.4A-D). In contrast, at 23 and 28 °C phosphate was depleted to <0.2 µmol L^{-1} within 1 to 10 days (Fig. 3.4E-L). In the +C–N treatment the DOC concentration remained high at 18 °C, and was only mildly depleted to 1.4 mmol C L^{-1} at 23 °C and to 0.9 mmol C L^{-1} at 28 °C (Fig. 3.4B,F,J). In contrast, in the +C+N treatment the DOC concentration was strongly depleted to 0.4 mmol C L^{-1} at 18 °C and to <0.15 mmol C L^{-1} at 23 and 28 °C (Fig. 3.4D,H,L). The nutrient concentrations at steady state are summarized in Supplementary Figure S3.2.

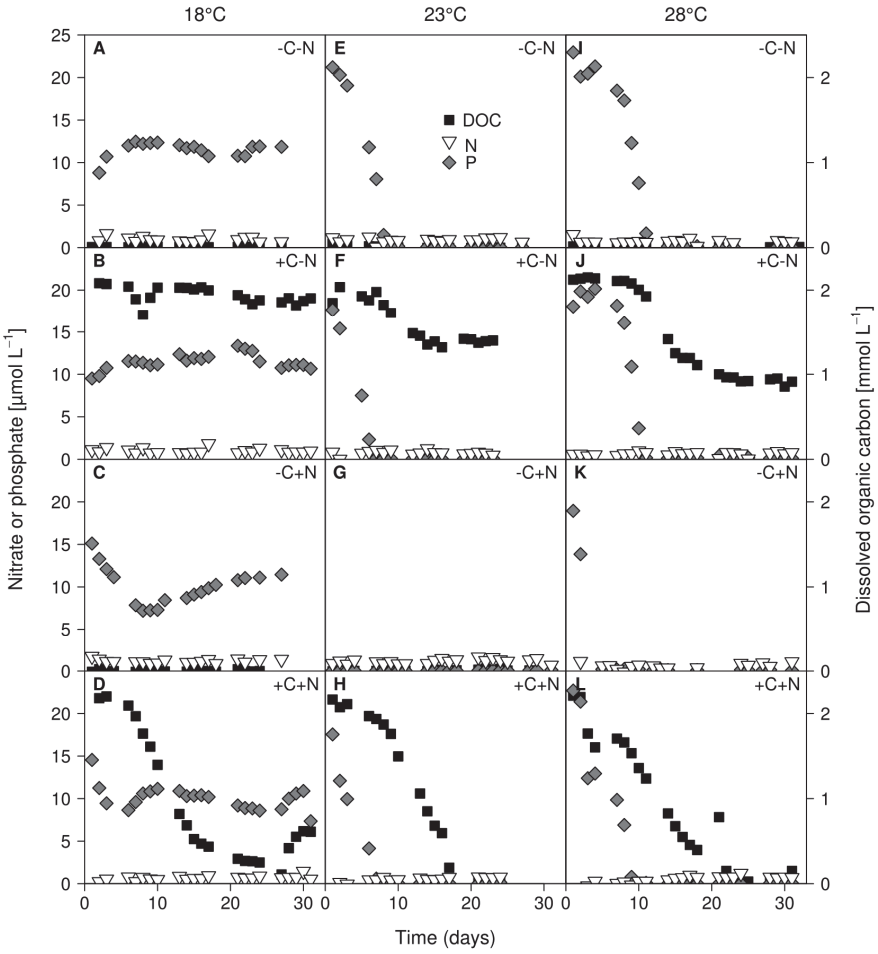

Figure 3.4: Time series of residual concentrations of DOC (black squares), nitrate (white inverted triangles) and phosphate (grey diamonds) during the experiments. Columns show temperature treatments at (A-D) 18 °C, (E-H) 23 °C and (I-L) 28 °C, rows show nutrient treatments with or without addition of DOC (C) and nitrate (N). DOC data from the failed –C+N treatment at 28 °C (panel K) are missing.

Elemental composition of the community

Both the POC and PON concentrations at steady state increased significantly with temperature but were not affected by nutrient treatment (Fig. 3.5A; temperature: $F_{2,6} = 90.77$, $p < 0.001$; nutrient treatment: $F_{3,6} = 1.691$, $p = 0.283$; Fig. 3.5B; temperature: $F_{2,6} = 83.5$, $p < 0.001$; nutrient treatment: $F_{3,6} = 1.853$, $p = 0.255$). POP concentrations were significantly affected by both temperature and nutrient treatment (Fig. 3.5C; temperature: $F_{2,6} = 218.025$, $p < 0.001$; nutrient treatment: $F_{3,6} = 11.151$,

p = 0.007). POP concentrations at 23 and 28 °C reached values close to the phosphate concentration of 25 µmol L^{-1} of the supplied growth medium. Hence, almost all available phosphate had been taken up by the organisms, consistent with the depleted phosphate concentrations in the cultures at 23 and 28 °C (Fig. 3.4E-L). POP

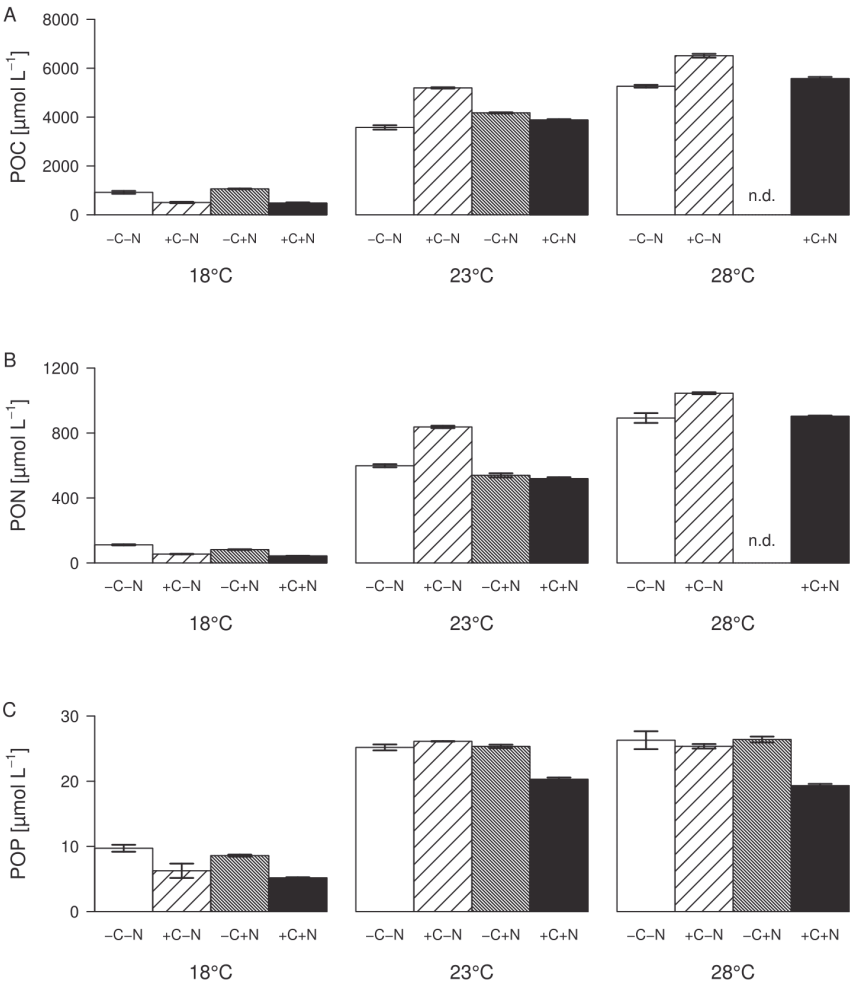

Figure 3.5: Elemental composition of the community. (A) POC, (B) PON, and (C) POP concentrations at steady state, for each temperature and nutrient treatment. Bars show means ± SE of triplicate measurements. Nutrient treatments: +C = with added DOC; +N = with added nitrate; n.d. = no data.

concentrations were slightly but significantly lower in the +C+N treatment than in the other treatments (post-hoc comparison of the means with Tukey HSD: $p < 0.01$ for +C+N vs -C-N; $p < 0.05$ for +C+N vs +C–N and for +C+N vs –C+N). The molar ratio of POC:PON at steady state decreased significantly with temperature but was

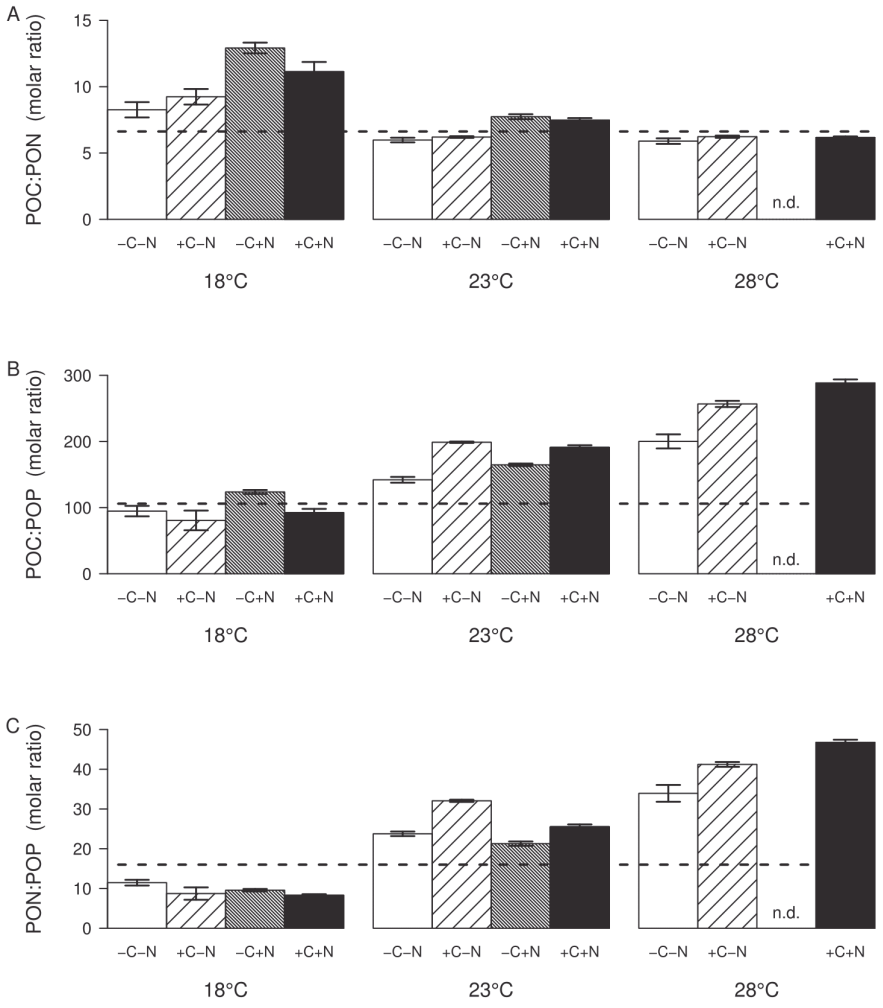

Figure 3.6: Steady-state elemental ratios (in mol/mol) of the entire community. (A) POC:PON ratio, (B) POC:POP ratio, and (C) PON:POP ratio. Bars show the mean ± SE of triplicate measurements, for each temperature and nutrient treatment. Horizontal dashed lines indicate the Redfield ratio of C:N:P = 106:16:1. Nutrient treatments: +C = with added DOC; +N = with added nitrate; n.d. = no data.

only marginally affected by nutrient treatment (Fig. 3.6A; temperature: $F_{2,6}$ = 22.016, p = 0.003; nutrient treatment: $F_{1,6}$ = 5.18, p = 0.054). Conversely, the POC:POP and PON:POP ratios both increased significantly with temperature, and were not affected by the nutrient treatment (Fig. 3.6B, temperature: $F_{2,6}$ = 26.649, p = 0.002; nutrient treatment: $F_{1,6}$ = 1.606, p = 0.3; Fig. 3.6C, temperature:$F_{2,6}$ = 35.548, p = 0.001; nutrient treatment: $F_{1,6}$ = 0.711, p = 0.586). As a consequence, the C:N:P stoichiometry of the community was invariant with respect to nutrient treatment but changed with temperature from 100:10:1 at 18 °C, to 174:26:1 at 23 °C, to 238:39:1 at 28 °C.

Community composition of chemotrophic bacteria

In total, 584 partial sequences of the bacterial 16S rRNA gene were analyzed by BLASTn, revealing 21 different OTUs. A separate PCR of the archaeal 16S rRNA gene yielded insignificant amounts of amplified DNA, indicating that archaea were not important in our experiments. Of the bacteria, 567 sequences revealed similarities between 97 % and 100 % with known organisms, while the other 17 sequences exhibited similarities between 93 % and 96 %. When possible, OTUs were grouped at the genus level, except the genera *Roseobacter*, *Labrenzia* and one unknown Rhodobacteriaceum, which were grouped as Rhodobacteriaceae. Furthermore, the genera *Alcanivorax*, *Halomonas* and one unknown Gammaproteobacterium were assigned as "other Gammaproteobacteria". The number of sequences analyzed per treatment varied between 22 and 72, which yielded 3-7 different taxonomic groups per treatment (Fig. 3.7A). Each chemotrophic community was co-dominated by 2-4 genera from three major taxonomic groups, i.e. the Alphaproteobacteria *Erythrobacter* and *Mesorhizobium*, the Gammaproteobacterium *Marinobacter*, and the Flavobacterium *Muricauda*. An additional clone library detected *nifH* genes belonging to the order Rhizobiales, which indicates that *Mesorhizobium* possessed the genetic equipment for N_2 fixation.

The bacterial community composition at steady state varied strongly with nutrient treatment but was less affected by temperature (Fig. 3.7A). In the treatments without nitrate (–C–N, +C–N), *Erythrobacter* and *Mesorhizobium* were co-dominant and the communities also contained a smaller but consistent proportion of Rhodobacteriaceae. Addition of DOC to the nitrate-free treatments increased the relative abundance of *Muricauda*. *Erythrobacter* and *Marinobacter* co-dominated the communities in treatments with nitrate (–C+N, +C+N). There was a small but consistent increase in

the proportion of *Mesorhizobium* in the +C+N treatments compared to the –C+N treatments. Cluster analysis grouped the bacterial communities according to nitrogen treatment at the highest level of the dendrogram and then further subdivided these communities according to the carbon and temperature treatment (Fig. 3.7B).

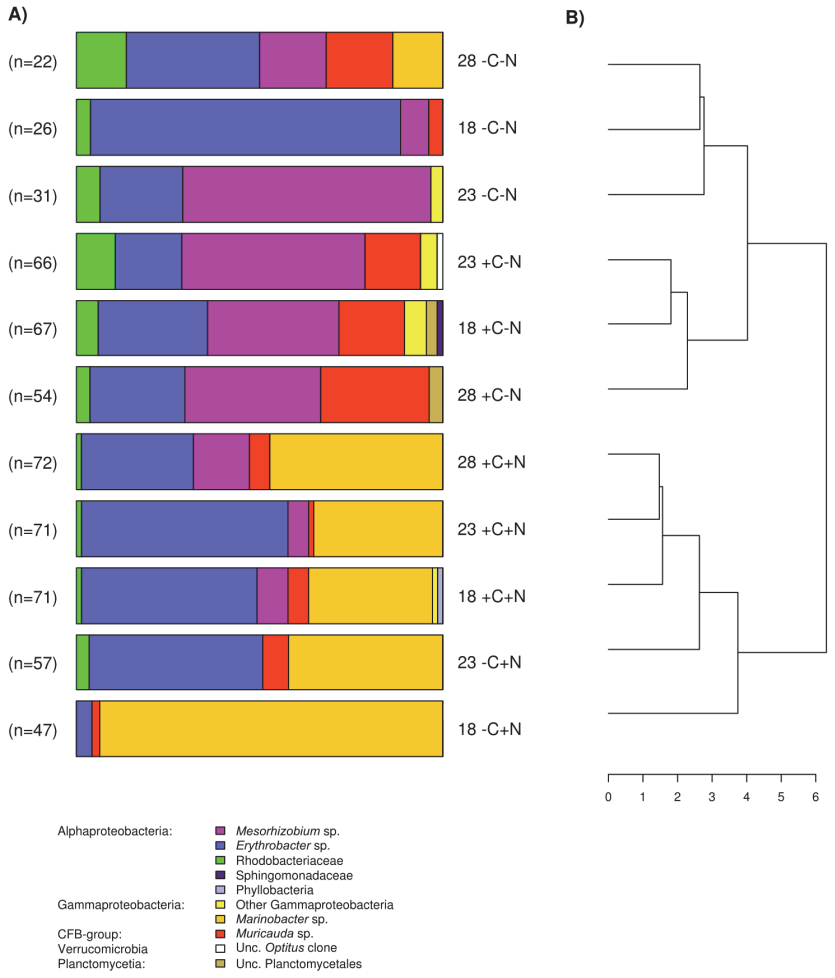

Figure 3.7: Community composition. (A) Community composition of the chemotrophic bacteria at steady state, for each temperature and nutrient treatment. Different colors indicate different taxonomic groups. Treatments were with or without addition of DOC (C) and nitrate (N) at three different temperatures (18, 23 and 28 °C). Data from the failed –C+N treatment at 28 °C are missing. (B) Dendrogram derived from cluster analysis of the community composition.

DISCUSSION

In this study we investigated the interactions between a small unicellular N_2-fixing cyanobacterium and its associated community of chemotrophic bacteria. All bacteria were free living according to our observations based on light and fluorescence microscopy, although this should be interpreted with some caution because higher-resolution methods such as scanning electron microscopy may have revealed bacteria attached to the *Cyanothece* cells. Nevertheless, it appears that there was little cell-to-cell contact that may have facilitated direct transfer of carbon and nutrients between the unicellular cyanobacteria and the other community members. In this sense, our study differs from earlier work on the bacterial communities of much larger filamentous diazotrophic cyanobacteria such as *Trichodesmium*, *Nodularia* and *Aphanizomenon*, where the bacteria were often attached to the filaments (Paerl, 1984; Paerl *et al.*, 1989, Salomon *et al.*, 2003; Tuomainen *et al.*, 2006; Ploug *et al.*, 2010, 2011; Hmelo *et al.*, 2012). We will now discuss our findings in relation to the four hypotheses that were formulated in the Introduction.

Hypothesis 1: Temperature and nutrient effects on *Cyanothece*

The chemostat experiments confirm our first hypothesis that the steady state abundance and biomass of *Cyanothece* depends strongly on temperature, and less on nutrient treatment (Fig. 3.2A). Moreover, *Cyanothece* largely dominated the microbial community in terms of biomass (Fig. 3.3). Hence, several community-wide parameters such as particulate carbon, nitrogen and phosphorus, as well as their elemental ratios were mainly driven by *Cyanothece* and therefore responded strongly to temperature but not to nutrient treatment (Fig. 3.5 and 3.6).

Interestingly, *Cyanothece* appeared to be limited by phosphorus at higher temperatures but by nitrogen at lower temperatures. At 18 °C phosphate was not depleted, the PON:POP ratio dropped below the Redfield ratio of 16 and the POC:PON ratio rose beyond the Redfield ratio of 6.6. Hence, at low temperature N_2 fixation did not meet the nitrogen demand of *Cyanothece*. This conclusion is consistent with previous results, which showed that temperatures below 21 °C hampered N_2 fixation and provoked a strong increase in the cellular C:N ratio of *Cyanothece* (Brauer *et al.*, 2013). Addition of nitrate at 18 °C did not alleviate nitrogen limitation of *Cyanothece* because nitrate was primarily taken up by chemotrophic bacteria. The increase in *Cyanothece* abundance with temperature coincided with an increase in the PON:POP ratio beyond the Redfield ratio and a drop in the POC:PON ratio below Redfield, which suggest that N_2 fixation met and even outreached the nitrogen demand (Fig. 3.2 and

3.6). At 23 and 28 °C virtually all phosphate was depleted and incorporated into particulate matter (Fig. 3.4 and 3.5). Thus, increasing temperature enhanced the N_2-fixation activity of *Cyanothece*, which alleviated *Cyanothece* from nitrogen limitation and caused a switch to phosphate limitation.

The temperature dependence of *Cyanothece* observed in our experiments is in agreement with the global distribution of marine photoautotrophic diazotrophs, which are largely confined to (sub)tropical oceans (Capone *et al.*, 1997; Staal *et al.*, 2003; Stal, 2009). Previously, we demonstrated that this global distribution might be caused by strong increases in the physiological cost of nitrogen fixation at temperatures below 21 °C (Brauer *et al.*, 2013). While this former study was conducted under nutrient-saturated conditions, we here show that the temperature dependence of diazotrophs also persists at low phosphate levels. Since iron and phosphate often limit N_2 fixation in the open ocean (Sañudo-Wilhelmy *et al.*, 2001; Mills *et al.*, 2004), our results provide additional support for the hypothesis that the global distribution of marine N_2-fixing cyanobacteria in the pelagic is limited by temperature (Staal *et al.*, 2003, Stal, 2009).

Hypothesis 2 and 3: Temperature and nutrient effects on chemotrophic bacteria

The strong growth response to nitrate addition and the weak response to DOC addition contradicted our second hypothesis that chemotrophic bacteria should be co-limited to a similar extent by both nitrogen and carbon. The bulk of chemotrophic bacteria were clearly limited by nitrogen. However, even though the DOC concentration was markedly depleted in the +C+N treatment (Fig. 3.4D,H,L), comparison with the –C+N treatment indicates that DOC addition had a negative impact on bacterial growth (Fig. 3.2B). Possibly the high DOC concentration had inhibitory effects on the growth of the chemotrophic bacteria.

The presence of chemotrophic bacteria in treatments without added nitrate or DOC indicates that *Cyanothece* facilitated its accompanying bacterial community through the release of dissolved nitrogen and carbon. Yet, it seems that *Cyanothece* released relatively more carbon than nitrogen in comparison to the C:N requirements of chemotrophic bacteria, because the bulk of chemotrophic bacteria were primarily limited by nitrogen. The C:N ratio of marine bacteria varies approximately from 4:1 under carbon limitation to 13:1 under nitrogen limitation (Goldman and Dennett, 2000). Little is known about the C:N release ratio of diazotrophs. However, it is

noteworthy that *Cyanothece* sp. CCY 0110 has one of the highest production rates of extracellular polymeric substances measured so far (Mota *et al.*, 2013), and our personal observations revealed that *Cyanothece* sp. Miami BG043511 has a tendency of high mucus production. This hints at a particularly high carbon release rate in the genus *Cyanothece*, which would be consistent with our hypothesis that *Cyanothece* released relatively more organic carbon than nitrogen.

The nitrogen release rates by *Cyanothece* also seemed to be low in absolute terms. Assuming a nitrogen content of 5 fg N $cell^{-1}$ (Allen *et al.*, 2005) chemotrophic bacteria in the nitrate-deficient cultures incorporated 0.7 – 8 % of the total particulate nitrogen, with an average of 3.4 %. Similarly low nitrogen release rates have recently been inferred from the quantification of external nitrogen pools in cultures of *Cyanothece* sp. Miami BG043511 (Benavides *et al.*, 2013). Yet, these low values disagree with many other studies demonstrating very high nitrogen release rates by the filamentous *Trichodesmium*, ranging between 12 and 82 % of recently fixed nitrogen (Mulholland, 2007). It is also in contrast with the study of Agawin *et al.* (2007) who found that *Cyanothece* sp. Miami BG043511 promoted a fourfold increase of the non-diazotrophic *Synechococcus* sp. through nitrogen release. One explanation for these contrasting findings might be that nitrogen release rates are generally less high in unicellular diazotrophs than in the filamentous *Trichodesmium* (Benavides *et al.*, 2013). Furthermore, in our study *Cyanothece* was limited by phosphorus, while in the study of Agawin *et al.* (2007) it was limited by light, which means that its physiological state differed between the two experiments. In *Trichodesmium* low phosphorus concentrations have been shown to decrease specific N_2-fixation rates (Fu and Bell, 2003; Mulholland and Bernhardt, 2005; but see Wannicke *et al.*, 2009). It is conceivable that in our experiments phosphorus limitation decreased the cellular N_2-fixation rate of *Cyanothece* as well, resulting in a relatively low nitrogen release rate.

Our third hypothesis, which states that higher temperature increases the amounts of released nitrogen and organic carbon and thus the number of chemotrophic bacteria, was supported only to a certain extent. One treatment (–C+N) did not show an increase of the chemotrophic bacteria from 18 to 23 °C, while we lack data at 28 °C. Hence, it is difficult to draw any final conclusions on the temperature response of the chemotrophic bacteria for this treatment. In the other three nutrient treatments, the chemotrophic bacteria increased with temperature as predicted by our hypothesis. However, they increased less strongly with temperature than *Cyanothece*. Hence, at higher temperatures, chemotrophic bacteria made up only a small fraction of the

entire community (Fig. 3.3), indicating that facilitation by *Cyanothece* did not significantly increase with temperature.

In our experiments resource competition between *Cyanothece* and chemotrophic bacteria played a minor role in the treatments without added nitrogen, since *Cyanothece* was primarily limited by phosphate, while chemotrophic bacteria were limited particularly by combined nitrogen and partly by organic carbon. Hence, both groups of organisms occupied rather distinct niches. However, in the +N treatments chemotrophic bacteria were partially alleviated from nitrogen limitation and may have shifted to P limitation, which will have brought them into more direct competition with the P-limited *Cyanothece* population. This is visible in the decline of *Cyanothece* and increase in chemotrophic bacteria from day 10 to day 18 in the –C+N treatment (Fig. 3.1G) and also in the lower steady-state abundance of *Cyanothece* in the +N treatments than in the –N treatments at 28 °C (Fig. 3.2A).

Hypothesis 4: Changes in community composition

The free-living chemotrophic bacteria in our experiments were dominated by *Erythrobacter*, *Mesorhizobium*, *Marinobacter* and *Muricauda*, which are common inhabitants of the marine pelagic and of phytoplankton cultures (Schäfer *et al.*, 2002; Kazamia *et al.*, 2012; Le Chevanton *et al.*, 2013). This suggests that the bacterial taxa were probably not specific for *Cyanothece*. This would be in line with Rooney-Varga *et al.* (2005), who showed that free-living bacteria found in association with phytoplankton are not very specific to these organisms. In contrast, bacteria attached to phytoplankton cells are often highly species-specific and may have evolved a long-term relationship with their hosts (Grossart *et al.*, 2005; Rooney-Varga *et al.*, 2005; Sison-Mangus *et al.*, 2014).

We do not know whether our consortium represents a natural association of N_2-fixing cyanobacteria and chemotrophic bacteria, or whether it is a laboratory artifact. However, a stable culture of a non-axenic cyanobacterium represents an excellent model system to study the interactions in this consortium. Moreover, most of the bacterial genera that we detected in our study are common in oceanic waters, and this gives confidence that the results obtained in this experimental study can be extrapolated to the natural environment.

Our results provide only partial support for Hypothesis 4. The taxonomic composition of the microbial community responded strongly to the nutrient

treatments, in particular to nitrate addition, but was less affected by temperature. *Marinobacter* exhibited the clearest signs of nitrate limitation, as it was mostly absent in the nitrate-deficient cultures but reached high numbers in the nitrate-amended cultures (Fig. 3.7). This is consistent with other studies describing *Marinobacter* as common nitrate-assimilating bacteria in marine habitats (Allen *et al.*, 2005; Cai and Jiao, 2008). *Marinobacter* was not affected by DOC or temperature.

Erythrobacter was generally the most successful species and the only one that was able to persist in all experimental treatments. This fits the observation that members of this genus are ubiquitous in the photic zone of the ocean (Hügler and Sievert, 2011). *Erythrobacter* seemed to be slightly stimulated by nitrate but not by DOC addition. However, it was also abundant in the nitrate-deficient cultures, which means that it was also able to utilize other, *Cyanothece*-derived nitrogen compounds. *Erythrobacter* spp. might be good competitors for dissolved organic carbon compounds as many of them belong to the aerobic anoxygenic phototrophs (AAPs), which are photoheterotrophs containing bacteriochlorophyll a (Kolber *et al.*, 2001; Koblížek *et al.*, 2003; but see Oh *et al.*, 2009). It has been shown that *Erythrobacter* sp. NAP1 uses light to increase its carbon use efficiency by substituting respiratory ATP-production with photophosphorylation (Hauruseu and Koblížek, 2012). Although similar observations have been made for the AAP-bacterium Roseobacter sp. COL2P belonging to the Rhodobacteriaceae (Hauruseu and Koblížek, 2012), the Rhodobacteriaceae in our study were much less successful than *Erythrobacter* (Fig. 3.7).

Mesorhizobium sp. was mainly present in the nitrate-free cultures, although small numbers of *Mesorhizobium* were still present when both nitrate and DOC were supplied (Fig. 3.7). The dominance of *Mesorhizobium* in nitrate-deficient environments and the presence of *nifH* genes belonging to the order Rhizobiales suggest that *Mesorhizobium* fixed dinitrogen. Hence, it was probably not limited by dissolved nitrogen but by organic carbon (energy-limited). This may also explain the presence of *Mesorhizobium* in the +C+N treatment. Although nitrate was added to the mineral medium, the nitrate concentration at steady state was depleted in the +C+N treatment (Fig. 3.4D,H,L), thus favoring suitable growth conditions for diazotrophic growth of *Mesorhizobium* when provided with sufficient organic carbon.

Muricauda was present in almost all cultures but only reached significant numbers in nitrate-deficient cultures when DOC was added (Fig. 3.7). This could hint at carbon-(energy) limitation. The abundance of *Muricauda* was stimulated by higher temperature, which agrees with its preference for aquatic environments between 25

and 30 °C (Bruns *et al.*, 2001; Hwang *et al.*, 2009). As *Muricauda* belongs to the Flavobacteria, it was possibly degrading the high-molecular mass fraction of the *Cyanothece*-derived organic matter (see e.g. Teeling *et al.*, 2012).

Thus, a closer look at the response of the individual species reveals that not all chemotrophic bacteria were nitrogen limited, but that different species were controlled by different limiting resources. These interspecific differences indicate that differential resource utilization played an important role in this community and contributed to the coexistence of chemotrophic bacteria from a variety of functional groups. This supports the view that niche differentiation is a major determinant of bacterial diversity in the relatively homogeneous habitat of the open oceans (Hutchinson, 1961; Stomp *et al.*, 2004; Hunt *et al.*, 2008; Teeling *et al.*, 2012). Hence, the bacterial species composition was neither neutral (sensu Hubbell, 2001) nor completely dictated by the diazotroph, but was structured by environmental conditions and species interactions in a similar way as many other ecological communities (Tilman, 1982; Prosser *et al.*, 2007; Fuhrman, 2009; Brauer *et al.*, 2012). An important implication is that changes in nitrogen and carbon availability due to, e.g., eutrophication and climate change are likely to induce shifts in the bacterial communities associated with N_2-fixing cyanobacteria.

Acknowledgments

We thank Sylvain Gandon for provision of chemostats, Myriam Boyer-Clavel, Cedric Mongellaz and Montpellier RIO Imaging for help with the flow cytometry analysis, Alain Hervé for support in the lab, and Lilian van der Linde and Henk Bolhuis for help with the clone library. The research of VSB and MS was supported by the Earth and Life Sciences Foundation (ALW), which is subsidized by the Netherlands Organization for Scientific Research (NWO). JH acknowledges the Turner-Kirk Charitable Trust for supporting his sabbatical at the Isaac Newton Institute for Mathematical Sciences of the University of Cambridge.

Supplementary Table 3.1: Composition of the growth medium

Compound	Concentration (µmol L^{-1})
Salts/Buffers:	
$MgSO_4•7H_20$	2.0 x 104
KCl	8.0 x 103
$CaCl_2•2H_2O$	2.5 x 103
NaCl	4.3 x 105
$NaHCO_3$	2.0 x 103
Macro nutrients:	
$C_6H_{12}O_6$	333; 0
$NaNO_3$	100; 0
$K_2HPO_4•3H_2O$	12.5
$Na_2SiO_3•9H_2O$	160
H_3BO_3	550
Micro nutrients:	
$FeSO_4•7H_20$	14
Na_2EDTA	35
$MnCl_2•4H_2O$	22
$ZnCl_2$	2.4
$Na_2MoO_4•2H_2O$	5.4
$CuSO_4•5H_2O$	0.2
$CoCl_2•4H_2O$	0.5
Vitamins:	
Thiamine•HCl (B1)	0.6
Biotin	4.0 x 10-3
Cyanocobalamin (B12)	7.4 x 10-3

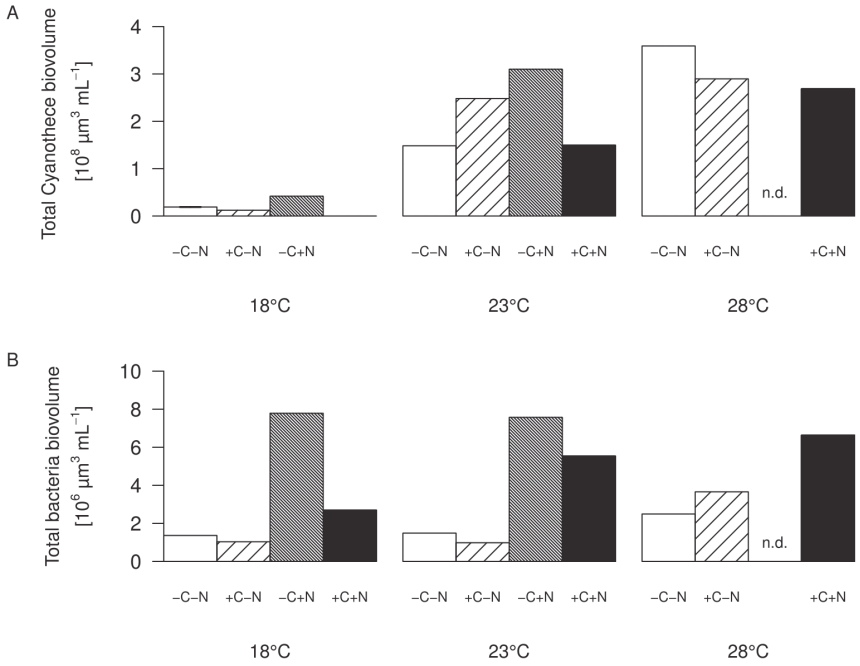

Supplementary Figure S3.1: Total biovolume of the community at steady-state. (A) *Cyanothece*, (B) chemotrophic bacteria. Bars show the geometric mean of the total biovolume measured between day 22 and day 32 of the experiment, for each temperature and nutrient treatment. Nutrient treatments: +C = with added DOC; +N = with added nitrate; n.d. = no data.

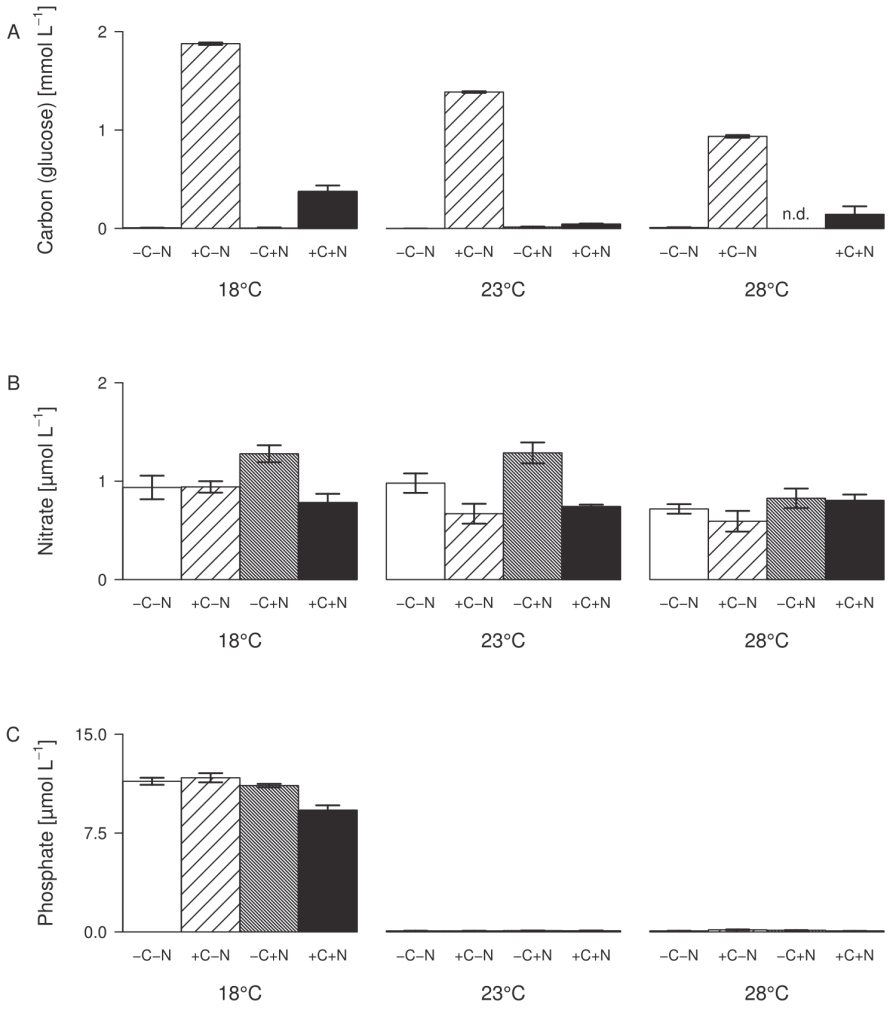

Supplementary Figure S3.2: Steady-state concentrations of the three major nutrients. (A) DOC, (B) nitrate, (C) phosphate. Bars show the mean ± SE of the nutrient concentrations measured between day 22 and day 32 of the experiment, for each temperature and nutrient treatment. Nutrient treatments: +C = with added DOC; +N = with added nitrate; n.d. = no data.

CHAPTER 4

The nutrient-load hypothesis: patterns of resource limitation and community structure driven by competition for nutrients and light

Verena S. Brauer, Maayke Stomp, Jef Huisman

The American Naturalist 179, 721-740, 2012

ABSTRACT

Resource competition theory predicts that the outcome of competition for two nutrients depends on the ratio at which these nutrients are supplied. Yet, there is considerable debate whether nutrient ratios or absolute nutrient loads determine the species composition of phytoplankton and plant communities. Here, we extend the classical resource competition model for two nutrients by including light as additional resource. Our results suggest the nutrient-load hypothesis, which predicts that nutrient ratios determine the species composition in oligotrophic environments, whereas nutrient loads are decisive in eutrophic environments. The underlying mechanism is that nutrient enrichment shifts the species interactions from competition for nutrients to competition for light, which favors the dominance of superior light competitors overshadowing all other species. Intermediate nutrient loads can generate high biodiversity through a fine-grained patchwork of two-species and three-species coexistence equilibria. Depending on the species traits, however, competition for nutrients and light may also produce multiple alternative stable states, suppressing the predictability of the species composition. The nutrient-load hypothesis offers a solution for several discrepancies between classical resource competition theory and field observations, explains why eutrophication often leads to diversity loss, and provides a simple conceptual framework for patterns of biodiversity and community structure observed in nature.

INTRODUCTION

Since its appearance in The American Naturalist, Tilman's (1980; 1985) resource-ratio hypothesis has become one of the leading conceptual theories on how competition for nutrients and light shapes the species composition of aquatic and terrestrial communities. The resource-ratio hypothesis predicts that the outcome of competition is determined by the ratios at which growth-limiting resources are supplied. This prediction is well founded in mathematical theory (León and Tumpson, 1975; Taylor and Williams, 1975; Tilman, 1980; 1982), and has been extensively tested in highly controlled competition experiments with bacteria (Smith, 1993), phytoplankton (Tilman, 1977; Sommer, 1985; van Donk and Kilham, 1990), zooplankton (Rothhaupt, 1988; Ciros-Pérez *et al.*, 2001), and terrestrial plants (Dybzinski and Tilman, 2007). The resource-ratio hypothesis received additional support from field studies in aquatic and terrestrial ecosystems (Inouye *et al.*, 1987; Sommer, 1989; 1993), and provided a major advance in the development of ecology as a theoretical and experimental science (Grover, 1997; Miller *et al.*, 2005).

Yet, there is still considerable debate on whether and to what extent nutrient ratios or absolute nutrient loads determine the species composition of natural communities. Numerous studies have shown that eutrophication often leads to diversity loss, and the dominance of only a few species in terrestrial vegetations (Grime, 1973; Stevens *et al.*, 2004; Harpole and Tilman, 2007; Hautier *et al.*, 2009). This indicates that absolute nutrient levels may have major effects on plant species composition. In freshwater and marine ecosystems, the question about absolute versus relative nutrient levels is of major importance for the prediction of harmful algal blooms. For instance, several cross-systems comparisons have revealed a strong relationship between the proportions of potentially harmful cyanobacteria in phytoplankton communities and ratios of total nitrogen (TN) to total phosphorus (TP) (Smith, 1983; Smith and Bennett, 1999; Havens *et al.*, 2003; Nõges *et al.*, 2008; Vrede *et al.*, 2009). However, just as much evidence has been provided that absolute concentrations of TN or TP are even better predictors for cyanobacterial dominance (Trimbee and Prepas, 1987; Canfield *et al.*, 1989; Jensen *et al.*, 1994; Reynolds, 1998; Downing *et al.*, 2001; McCarthy *et al.*, 2009). As Smith (2003, p. 130) noted, "this extremely important fundamental question remains unresolved, and is a key topic for future eutrophication research".

One plausible solution for this unresolved debate is that nutrient enrichment changes the species interactions from competition for nutrients to competition for light (Donald, 1958; Tilman, 1985; Aerts *et al.*, 1990; Olff *et al.*, 1993; Passarge *et al.*, 2006). High nutrient levels can support high plant and phytoplankton biomass, which

casts shade deeper down in the vegetation or water column. Hence, competition for light often plays a prominent role in eutrophic ecosystems (Huisman *et al.*, 2004; Hautier *et al.*, 2009). It is not immediately obvious, however, how shading will affect the species composition. Competition for light is conceptually more complex than competition for nutrients, because of the unidirectional nature of the light flux and the resulting vertical gradient in light availability (Weiner, 1990; Rees and Bergelson, 1997; Perry *et al.*, 2003).

In a series of papers, Huisman and Weissing (1994; 1995) developed a theory on competition for light that explicitly incorporated the unidirectional nature of the light gradient. They showed that competition for light in well-mixed waters can be investigated by a similar mechanistic approach as in Tilman's competition theory. The model predictions were supported by laboratory competition experiments with phytoplankton species (Huisman *et al.*, 1999; Passarge *et al.*, 2006; Agawin *et al.*, 2007; Van de Waal *et al.*, 2011), and have been applied in several field studies (Diehl *et al.*, 2002; Ptacnik *et al.*, 2003; Huisman *et al.*, 2004; Berger *et al.*, 2006; Jöhnk *et al.*, 2008). Subsequent work investigated other aspects of competition for light in phytoplankton communities, including incomplete mixing (Huisman *et al.*, 2004; 2006; Jäger *et al.*, 2008; Yoshiyama *et al.*, 2009; Ryabov *et al.*, 2010), fluctuating light conditions (Litchman and Klausmeier, 2001; Litchman *et al.*, 2004), photoinhibition (Gerla *et al.*, 2011), and the underwater light spectrum (Stomp *et al.*, 2004; 2007; Striebel *et al.*, 2009). The results also motivated several follow-up studies on competition for light in terrestrial plant communities (Dybzinski and Tilman, 2007; Vojtech *et al.*, 2007; Hautier *et al.*, 2009). However, the role of nutrient ratios versus absolute nutrients levels was not investigated further.

In this paper, we investigate how competition for light modifies nutrient-ratio effects on community structure. For this purpose, we extend Tilman's (1980; 1982) graphical-mechanistic approach on competition for two nutrients by incorporating competition for light (Huisman and Weissing, 1994; 1995). We keep our model as simple as possible to focus on the essentials of competition for nutrients and light. For instance, the model assumes complete mixing, with a spatially homogeneous distribution of nutrients and species. This assumption is particularly relevant for phytoplankton communities in well-mixed waters. However, many of our findings may also be of interest for competition studies in other ecosystems such as terrestrial plant communities.

COMPETITION MODEL

We use essentially the same model structure as in earlier work (Tilman, 1982; Huisman and Weissing, 1994; 1995), but now extended to competition for two nutrients and light. The model considers a vertical water column, illuminated from above, in which nutrients and several phytoplankton species are homogeneously mixed.

Light enters the water column from above, and light intensity decreases exponentially with depth due to light absorption by water and various other components (e.g., dissolved organic matter, suspended clay particles). Light is also absorbed by the phytoplankton community itself. More specifically, let $I(z)$ denote the light intensity at depth z, where z ranges from 0 at the water surface to the maximum depth z_M at the bottom of the water column. According to Lambert-Beer's law:

$$I(z) = I_{in} e^{-[K_{BG} + \sum_{j=1}^{n} k_j N_j]z}, \qquad (4.1)$$

where I_{in} is the incident light intensity at the water surface, K_{BG} is the background turbidity due to light absorption by water and other non-phytoplankton components, k_j is the specific light attenuation coefficient of phytoplankton species j, N_j is the population density of phytoplankton species j, and n is the number of phytoplankton species. We define I_{out} as the light intensity at the bottom of the water column (i.e., $I_{out} = I(z_M)$). Note that the vertical light gradient is dynamic in time. A growing phytoplankton population will absorb more light, and thereby reduces light availability in the water column.

The specific growth rates of the phytoplankton species depend on ambient nutrient and light availability. More precisely, we assume that the local specific growth rate of a species at a given depth in the water column, $\mu_j(z)$, is determined by the most limiting resource at that depth, as in Von Liebig's (1840) 'Law of the Minimum':

$$\mu_j(z) = \mu_{\max,j} \min[f_{1j}(R_1), f_{2j}(R_2), g_j(I(z))] \qquad (4.2)$$

where $\mu_{max,j}$ is the maximum specific growth rate of species j, min is the minimum operator, and the functions $f_{1j}(R_1)$, $f_{2j}(R_2)$ and $g_j(I(z))$ describe growth limitation by nutrient 1, nutrient 2, and light, respectively. The exact shape of the functions $f_{1j}(R_1)$, $f_{2j}(R_2)$ and $g_j(I(z))$ may depend on the species and environmental conditions. Here, we describe the resource-limited growth rate of species j as an increasing saturating

function of the local nutrient and light availability using Monod's (1950) equation. That is, for nutrient-limited growth

$$f_{ij}(R_i) = \frac{R_i}{M_{ij} + R_i}, \tag{4.3}$$

and for light-limited growth

$$g_j(I(z)) = \frac{I(z)}{H_j + I(z)}, \tag{4.4}$$

where M_{ij} is the half-saturation constant for nutrient i of species j, and H_j is its half-saturation constant for light.

The depth-averaged specific growth rate of a species, $\overline{\mu_j}$, is then obtained by integrating the local specific growth rates of all individuals of this species over the entire depth of the water column:

$$\overline{\mu_j} = \frac{1}{z_M}\int_0^{z_M} \mu_j(z)\, dz$$

$$= \frac{1}{z_M}\int_0^{z_M} \mu_{\max,j} \min[f_{1j}(R_1), f_{2j}(R_2), g_j(I(z))]\, dz \tag{4.5}$$

The net rate of change of a species depends on the balance of its growth and loss rate. Hence, the population dynamics of n phytoplankton species is described by

$$\frac{dN_j}{dt} = \left(\overline{\mu_j} - l_j\right) N_j \qquad j=1,\ldots,n \tag{4.6}$$

where l_j is the specific loss rate of species j due to cell death, grazing, viruses, and so on.

Nutrients enter the water column from surface run-off, river inflow, or the sediment below, and are taken up by the phytoplankton species. Accordingly, changes in the ambient concentrations of the two nutrients, R_1 and R_2, are described as

$$\frac{dR_i}{dt} = \frac{F}{z_M}(R_{in,i} - R_i) - \sum_{j=1}^{n} c_{ij}\overline{\mu_j} N_j \qquad i=1,2. \tag{4.7}$$

The first term on the right-hand side describes the influx and efflux of nutrients into and from the water column. Here, $R_{in,i}$ is the concentration of nutrient i in the influx, and will henceforth be called the nutrient load, and F is the flow rate of the influx and efflux. The nutrient flux is mixed over the entire depth of the water column, which is accounted for by the depth z_M. The second term describes nutrient consumption by the phytoplankton community, where c_{ij} is the content of nutrient i in species j.

Parameter values were chosen to be within a realistic range for freshwater and marine phytoplankton species (Huisman *et al.*, 1999; Passarge *et al.*, 2006; Agawin *et al.*, 2007). The model variables and parameters are summarized in Table 4.1.

RESULTS

In the following sections, we first investigate the growth of a single species on two nutrients and light. As a next step, we extend the model to analyze competition for nutrients and light between different sets of species. Throughout our analysis, we consider an incident light intensity high enough to support population growth at low population densities.

Dynamics of a single species

Figure 4.1 illustrates depth profiles of the local specific growth rate of a phytoplankton species. Because both nutrients are homogeneously mixed, the nutrient-limited growth rates $f_{ij}(R_i)$ are constant over depth. In contrast, light availability decreases with depth, and hence the light-limited growth rate $g_j(I(z))$ decreases with depth as well.

It is useful to define the light intensity $I_{co,j}$ and depth $z_{co,j}$ at which the local specific growth rate switches from nutrient-limited to light-limited growth (Fig. 4.1B). This light intensity is implicitly given by $g_j(I_{co,j})=\min[f_{1j}(R_1),f_{2j}(R_2)]$. In view of Equations (4.3) and (4.4), this yields

$$I_{co,j} = H_j \min\left(\frac{R_1}{M_{1j}}, \frac{R_2}{M_{2j}}\right) \tag{4.8}$$

Inserting $I_{co,j}=I(z_{co,j})$ and $I_{out}=I(z_M)$ into Equation (4.1), the depth $z_{co,j}$ at which the local specific growth rate switches from nutrient-limited to light-limited growth is given by:

Table 4.1: Symbols with their interpretation and dimension.

Symbol	Interpretation	Dimension	Value
Independent variables:			
t	Time	day	-
z	Depth	m	-
Dependent variables:			
N_j	Population density of species j	million cells mL^{-1}	-
R_i	Environmental concentration of nutrient i	µmol L^{-1}	-
$I(z)$	Light intensity at depth z	µmol photons m^{-2} s^{-1}	-
I_{out}	Light intensity at bottom of water column	µmol photons m^{-2} s^{-1}	-
Species parameters and functions:			
$\overline{\mu_j}$	Depth-averaged specific growth rate of species j	day^{-1}	-
$f_{ij}(R_i)$	Specific growth rate of species j when limited by	day^{-1}	-
$g_j(I)$	Specific growth rate of species j when limited by light	day^{-1}	-
$\mu_{max,j}$	Maximum specific growth rate of species j	day^{-1}	0.8–1
l_j	Specific loss rate of species j	day^{-1}	0.25
M_{ij}	Half-saturation constant of species j for nutrient i	µmol L^{-1}	0.001–5
H_j	Half-saturation constant of species j for light	µmol photons m^{-2} s^{-1}	15–60
c_{ij}	Cellular content of nutrient i in species j	fmol $cell^{-1}$	2–160
k_j	Specific light attenuation coefficient of species j	μm^2 $cell^{-1}$	0.5–10
R_{ij}^*	Critical concentration of nutrient i for species j	µmol L^{-1}	-
$I_{out,j}^*$	Critical light intensity for species j	µmol photons m^{-2} s^{-1}	-
Environmental parameters:			
$R_{in,i}$	Load of nutrient i	µmol L^{-1}	0–800
F	Flow rate	m day^{-1}	0.1–0.25
I_{in}	Incident light intensity	µmol photons m^{-2} s^{-1}	100–600
z_M	Total depth of water column	m	1–100
K_{BG}	Background turbidity	m^{-1}	0.05–0.1

$$z_{co,j} = z_M \left(\frac{\ln(I_{in}) - \ln(I_{co,j})}{\ln(I_{in}) - \ln(I_{out})} \right). \tag{4.9}$$

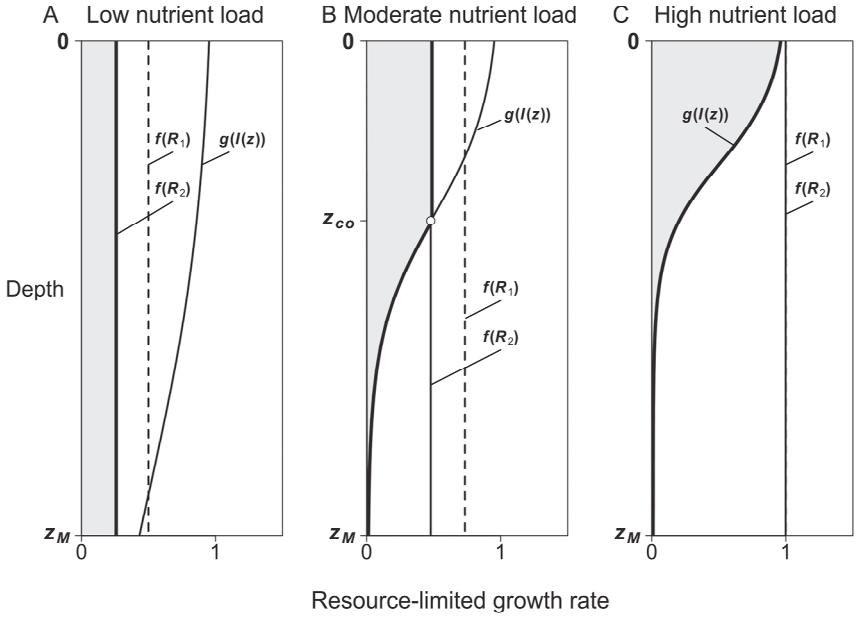

Figure 4.1: Depth profiles of the local specific growth rate. Nutrient-limited growth is uniform over depth, as described by the functions $f(R_1)$ and $f(R_2)$. Light-limited growth, $g(I(z))$, decreases with depth. At each depth, the local specific growth rate (bold line) is determined by the most limiting resource. The depth-averaged specific growth rate is obtained by integrating these local specific growth rates over depth, as indicated by the shaded area. (A), At low nutrient load, the specific growth rate is nutrient-limited throughout the water column. (B), At intermediate nutrient load, the specific growth rate is nutrient-limited in the upper part and light-limited in the lower part of the water column. The depth zco marks the transition from nutrient limitation to light limitation. (C), At high nutrient load, the specific growth rate is light-limited throughout the water column.

Figure 4.2 displays which resource limits the depth-averaged growth rate of a species as function of both nutrient loads. The different regions in this graph can be interpreted in terms of the three depth profiles of Figure 4.1:

Nutrient limitation: At low nutrient loads, sufficient light reaches the bottom of the water column (i.e., $I_{out} > I_{co,j}$). In this case, the specific growth rate is either limited by nutrient 1 or limited by nutrient 2 throughout the entire water column (as in Fig. 4.1A):

$$\overline{\mu_j} = \mu_{\max,j} \min[f_{1j}(R_1), f_{2j}(R_2)] \tag{4.10}$$

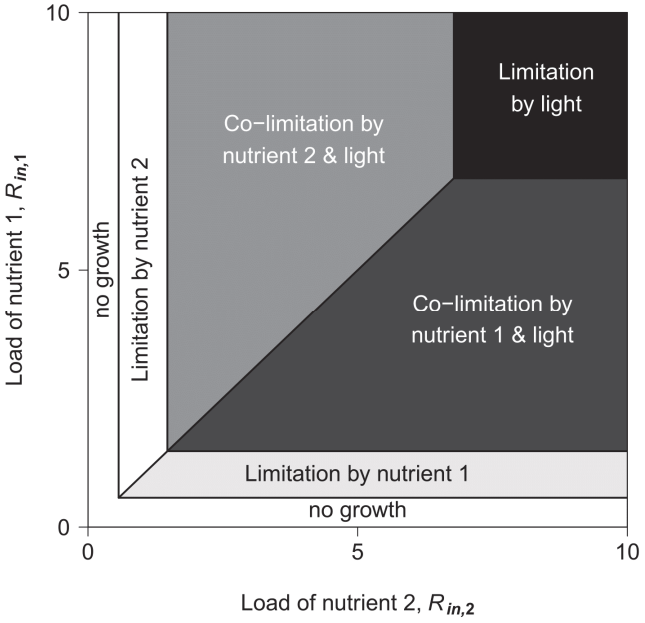

Figure 4.2: Resource limitation of a single species. In the 'no growth' regions, nutrient availability is too low to support a phytoplankton population. At low nutrient loads, the growth rate is limited by either nutrient 1 or nutrient 2, depending on the ratio of the nutrient loads. At intermediate nutrient loads, growth is co-limited either by nutrient 1 and light or by nutrient 2 and light, depending on the ratio of the nutrient loads. At high nutrient loads, growth is limited by light irrespective of the nutrient ratios. Parameter values are given in Appendix C.

In this case, a species can establish a population only if the nutrient loads of both nutrients exceed a critical threshold value R_{ij}^* (Fig. 4.2). These critical nutrient concentrations, R_{1j}^* and R_{2j}^*, can be derived by solving Equation (4.6) for zero. With the help of Equations (4.3) and (4.10), this yields (Tilman, 1982):

$$R_{ij}^* = \frac{M_{ij} l_j}{\mu_{\max,j} - l_j}, \qquad i=1,2. \tag{4.11}$$

Hence, the values of these critical nutrient concentrations depend on species traits such as the maximum specific growth rate, loss rate and half-saturation constants. In Figure 4.2, the horizontal boundary line between the region of 'no growth' and the region where the species is limited by nutrient 1 is given by $R_{in,1}=R_{1j}^*$. Likewise, the vertical boundary line between the region of 'no growth' and the region where the species is limited by nutrient 2 is given by $R_{in,2}=R_{2j}^*$.

The region where growth is limited by nutrient 1 is separated from the region where growth is limited by nutrient 2 by a diagonal boundary line (Fig. 4.2). At this diagonal boundary, both nutrients limit growth. Hence, the diagonal boundary line can be obtained by solving Equations (4.6) and (4.7) at equilibrium, assuming $R_1=R_{1j}^*$ and $R_2=R_{2j}^*$. This yields:

$$R_{in,1} = R_{1j}^* + \frac{c_{1j}}{c_{2j}}[R_{in,2} - R_{2j}^*] \tag{4.12}$$

This equation shows that the slope of the diagonal boundary line is given by the ratio c_{1j}/c_{2j}. Assuming $R_{in,i} >> R_{ij}^*$ for both nutrients, it follows that if $R_{in,1}/R_{in,2} > c_{1j}/c_{2j}$, the species is limited by nutrient 2. Conversely, if $R_{in,1}/R_{in,2} < c_{1j}/c_{2j}$, the species is limited by nutrient 1. In other words, the ratio at which the two nutrients are supplied determines which of the two nutrients limits phytoplankton growth. This reasoning lies at the heart of Tilman's resource-ratio hypothesis.

Co-limitation: At intermediate nutrient loads, the upper part of the water column receives sufficient light such that local growth is nutrient-limited, while growth deeper down in the water column is light-limited (i.e., $I_{out} < I_{co,j} < I_{in}$). This scenario is shown in Figure 4.1B. In this case, one might say that the depth-averaged phytoplankton growth rate experiences co-limitation by nutrients and light (Fig. 4.2). That is, the depth-averaged specific growth rate of species j depends on the weighted average of nutrient-limited growth in the upper part and light-limited growth in the lower part of the water column:

$$\overline{\mu_j} = \mu_{\max,j} \frac{1}{z_M} \left(\int_0^{z_{co,j}} \min[f_{1j}(R_1), f_{2j}(R_2)]dz + \int_{z_{co,j}}^{z_M} g_j(I(z))dz \right) \tag{4.13}$$

The two depth integrals in this equation can be solved with the help of Equations (4.1), (4.4) and (4.9). This yields:

$$\overline{\mu_j} = \mu_{\max,j} \min[f_{1j}(R_1), f_{2j}(R_2)] \left(\frac{\ln(I_{in}) - \ln(I_{co,j})}{\ln(I_{in}) - \ln(I_{out})} \right) + \mu_{\max,j} \left(\frac{\ln(H_j + I_{co,j}) - \ln(H_j + I_{out})}{\ln(I_{in}) - \ln(I_{out})} \right) \tag{4.14}$$

where $I_{co,j}$ is given by Equation (4.8) and I_{out} is the light intensity at the bottom of the light gradient.

The two regions of nutrient limitation are separated from the two regions of co-limitation by nutrients and light by two boundary lines (Fig. 4.2). Appendix A shows that these two boundary lines are given by:

$$R_{in,1} = R^*_{1j} + \frac{c_{1j} l_j}{k_j F}\left(\ln(I_{in}) - \ln(H_j R^*_{1j} / M_{1j}) - K_{BG} z_M\right) \qquad (4.15A)$$

$$R_{in,2} = R^*_{2j} + \frac{c_{2j} l_j}{k_j F}\left(\ln(I_{in}) - \ln(H_j R^*_{2j} / M_{2j}) - K_{BG} z_M\right) \qquad (4.15B)$$

Equation (4.15A) is independent of $R_{in,2}$. Hence, in Figure 4.2, Equation (4.15A) specifies the horizontal boundary line at the transition from limitation by nutrient 1 to co-limitation by nutrient 1 and light. Likewise, Equation (4.15B) specifies the vertical boundary line at the transition from limitation by nutrient 2 to co-limitation by nutrient 2 and light. This implies that the transition from nutrient limitation to co-limitation is not determined by nutrient ratios, but by absolute nutrient loads (Fig. 4.2). The diagonal boundary line separating the two co-limitation regions indicates that the nutrient ratio does determine which of the two nutrients co-limits growth.

Light limitation: At high nutrient loads, the specific growth rate is limited by light throughout the entire water column (i.e., $I_{co,j} > I_{in}$). In this case, illustrated in Figure 4.1C, the depth-averaged growth rate can be written as (Huisman and Weissing, 1994):

$$\overline{\mu_j} = \mu_{\max,j} \frac{1}{z_M} \int_0^{z_M} g_j(I(z))dz = \mu_{\max,j}\left(\frac{\ln(H_j + I_{in}) - \ln(H_j + I_{out})}{\ln(I_{in}) - \ln(I_{out})}\right). \qquad (4.16)$$

It can be shown that, under light-limited conditions, the phytoplankton population will continue to increase until it has reduced the light intensity at the bottom of the water column to a critical light intensity $I_{out,j}^*$ (Huisman and Weissing, 1994; 1995). The critical light intensity has a similar interpretation as the critical nutrient concentrations R_{ij}^*. Different species have different critical light intensities, depending on their traits (Huisman *et al.*, 1999). Contrary to R^*, the critical light intensity does not have an explicit analytical solution, but it can be solved numerically (i.e., by evaluating $\overline{\mu_j} - l_j = 0$ with the help of Equation (4.16)).

The boundary lines separating the regions of co-limitation by nutrients and light from the region of light limitation are given by (App. A):

$$R_{in,1} = \frac{M_{1j}}{H_j} I_{in} + \frac{c_{1j} l_j}{k_j F} \left(\ln(I_{in}) - \ln(I^*_{out,j}) - K_{BG} z_M \right) \quad (4.17A)$$

$$R_{in,2} = \frac{M_{2j}}{H_j} I_{in} + \frac{c_{2j} l_j}{k_j F} \left(\ln(I_{in}) - \ln(I^*_{out,j}) - K_{BG} z_M \right) \quad (4.17B)$$

Equation (4.17A) specifies a horizontal boundary line, while Equation (4.17B) specifies a vertical boundary line. Hence, the transition from co-limitation to limitation by light is again determined by absolute nutrient loads (Fig. 4.2).

In total, these results show that, at low to intermediate nutrient loads, the ratio of the nutrient loads determines which of the two nutrients will limit growth. However, the absolute nutrient loads determine the transition from nutrient limitation to co-limitation by nutrients and light and also the transition from co-limitation to light limitation. Furthermore, the boundary lines separating the different resource limitation regions also depend on species traits, and on physical parameters affecting the underwater light field such as incident light intensity (I_{in}), background turbidity (K_{BG}) and mixing depth (z_M). More specifically, since the value of $I^*_{out,j}$ decreases with I_{in} (Huisman and Weissing, 1994), the nutrient thresholds specified by Equations (4.15) and (4.17) increase with incident light intensity. This is illustrated in Figure 4.3A-C, which shows that the transitions from nutrient to co-limitation and from co-limitation to light limitation will occur at higher nutrient loads in ecosystems exposed to higher incident light intensities (e.g., tropical latitudes). Conversely, since $I^*_{out,j}$ is independent of K_{BG} and z_M (Huisman and Weissing, 1994), the nutrient thresholds specified by Equations (4.15) and (4.17) decrease linearly with mixing depth and background turbidity. This is illustrated in Figure 4.3D-F, which shows that the transitions from nutrient to co-limitation and from co-limitation to light limitation occur at lower nutrient loads in deeply mixed waters than in shallow waters. Qualitatively similar results are obtained for changes in background turbidity. Accordingly, patterns of resource limitation show many similarities across ecosystems, yet quantitatively the values of the critical nutrient loads at which systems will shift from nutrient to light limitation will strongly depend on the local environmental setting.

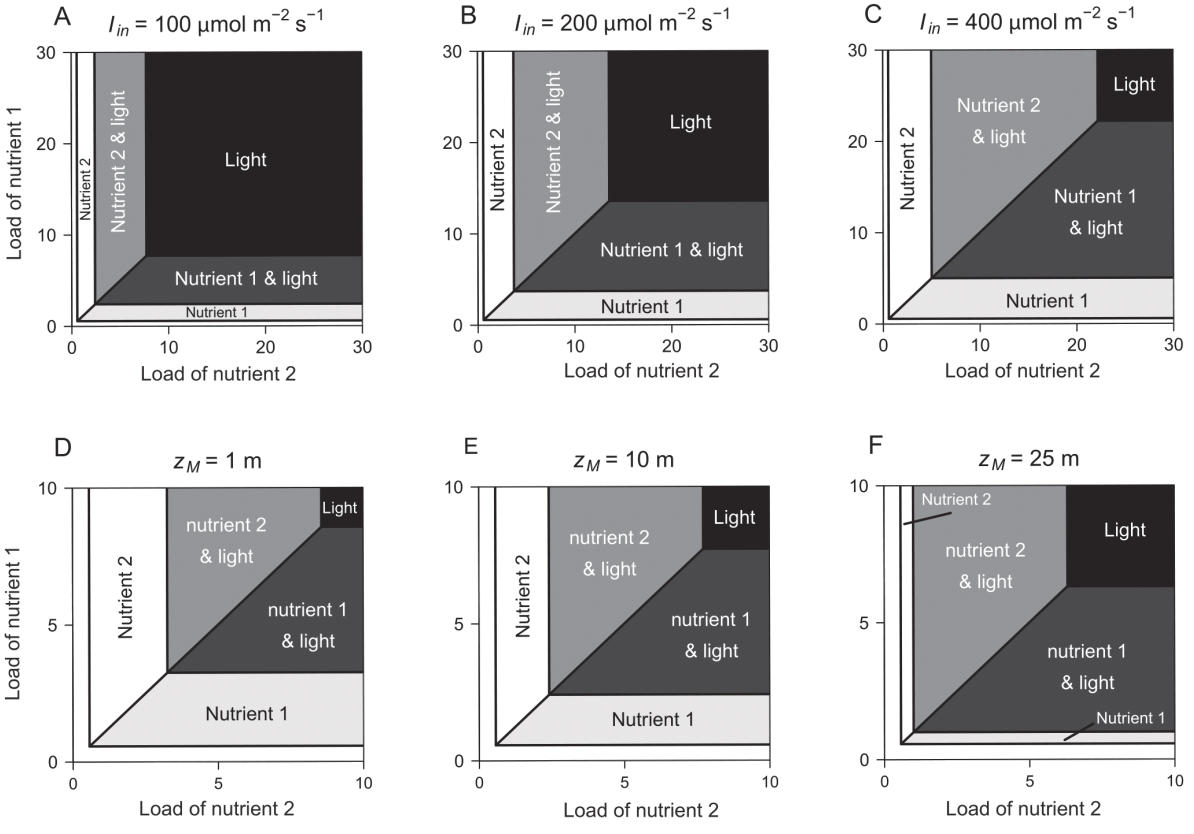

Figure 4.3: Resource limitation of a single species at different incident light intensities and mixing depths. (A-C), With increasing incident light intensities, the transition from nutrient limitation to co-limitation by nutrients and light and, also, the transition from co-limitation to light limitation will occur at higher nutrient loads. (D-F), With increasing mixing depths, the transition from nutrient limitation to co-limitation and from co-limitation to light limitation will occur at lower nutrient loads. Parameter values are given in Appendix C.

Competition between two species

Resource competition among two species is well understood. If both species are limited by the same nutrient, the species with lowest R^* for that nutrient will be the superior competitor and will eventually exclude the other species (Armstrong and McGehee, 1980; Tilman, 1982). Likewise, under light limitation, the species with lowest I_{out}^* will be the superior competitor for light (Huisman and Weissing, 1994; Huisman *et al.*, 1999). When two resources are limiting, two species can coexist if each species is the superior competitor for another resource. The coexistence equilibrium is stable if each species consumes relatively more of that resource for which it is an inferior competitor (León and Tumpson, 1975; Tilman, 1982; Huisman and Weissing, 1995). Conversely, the coexistence equilibrium is unstable, and the winner will depend on the initial conditions, if each species consumes relatively more of that resource for which it is a superior competitor.

For our model, the presence of a vertical light gradient complicates the mathematical analysis. Therefore, we first consider a simplified version of the model, in which the depth-averaged growth rate of Equation (4.5) is replaced by:

$$\overline{\mu_j} = \mu_{\max,j} \min\left[f_{1j}(R_1), f_{2j}(R_2), \frac{1}{z_M} \int_0^{z_M} g_j(I(z))\, dz \right] \qquad (4.18)$$

This equation differs from Equation (4.5) in that the integral term is inside rather than outside the minimum function. Hence, the 'Law of the Minimum' now acts at the global scale rather than at each local depth. This assumption may particularly apply to terrestrial vegetation, where individual plants can integrate their photosynthetic activity over the entire depth of the canopy. The resource limitation pattern predicted by this simplified model resembles Figure 4.2, but without co-limitation of nutrients and light (Fig. B4.1 in App. B). The simplified model has the advantage that the boundaries between different regions of competitive dominance can be derived analytically (see App. A). However, Equation (4.5) is a more accurate description of local phytoplankton growth. Hence, we will return to the full model based on Equation (4.5) at the end of this section, to compare the predictions of the simplified and full model.

We investigate three competition scenarios. The species parameters are chosen such that two-species coexistence is stable whenever it occurs (see App. C for parameter values). In the first scenario, species 1 is the superior competitor for nutrient 1 and light, and species 2 is the superior competitor for nutrient 2 (Fig. 4.4A). In the

intermediate region, the two species coexist because each species becomes limited by the resource for which it is an inferior competitor (Fig. 4.4A). At low nutrient loads, the shape of this coexistence region resembles the classical cone form predicted by Tilman's (1982) resource-ratio hypothesis. Within this cone, species 1 is limited by nutrient 2, and species 2 is limited by nutrient 1. At high nutrient loads, the coexistence region extends vertically. Here, species 1 is still limited by nutrient 2, but species 2 has become limited by light. Hence, the change in orientation of the coexistence region occurs when the competitive interactions shift from competition for two nutrients to competition for nutrient 2 and light. Consequently, at low nutrient loads the outcome of competition depends on the ratio of the nutrient loads, but at high nutrient loads the outcome is determined by the absolute load of nutrient 2.

In the second scenario, species 1 is the superior competitor for nutrient 1 and species 2 is the superior competitor for nutrient 2 and light. The results resemble the first scenario. At high nutrient loads, however, the coexistence region now extends horizontally, where the two species compete for nutrient 1 and light (Fig. 4.4B).

In the third scenario, species 1 is the superior competitor for both nutrients and species 2 is the superior competitor for light. In this case, the different regions are separated by L-shaped boundary lines that run parallel to the axes (Fig. 4.4C). Species 1 wins at low nutrient loads, while species 2 wins at high nutrient loads. The two species coexist in the intermediate region, where they are co-limited either by nutrient 1 and light or by nutrient 2 and light. Hence, in this scenario, the outcome of competition is never determined by the nutrient ratios. Instead, the species composition is determined by the absolute nutrient loads. The boundary lines in Figure 4 are derived in Appendix A.

Appendix B investigates the same competition scenarios, with the same parameter values as in Figure 4, but now for the full model based on Equation (4.5). Quantitatively, the predictions of the simplified and full model show several differences, but qualitatively their predictions are very similar (compare Fig. 4.4 and Fig. B4.2 in App. B). At low nutrient levels, the two species compete primarily for nutrient 1 and 2, and the outcome of competition is determined by the ratio of the nutrient loads. At high nutrient levels, the two species compete mainly for light, and the outcome of competition is determined by the absolute nutrient loads.

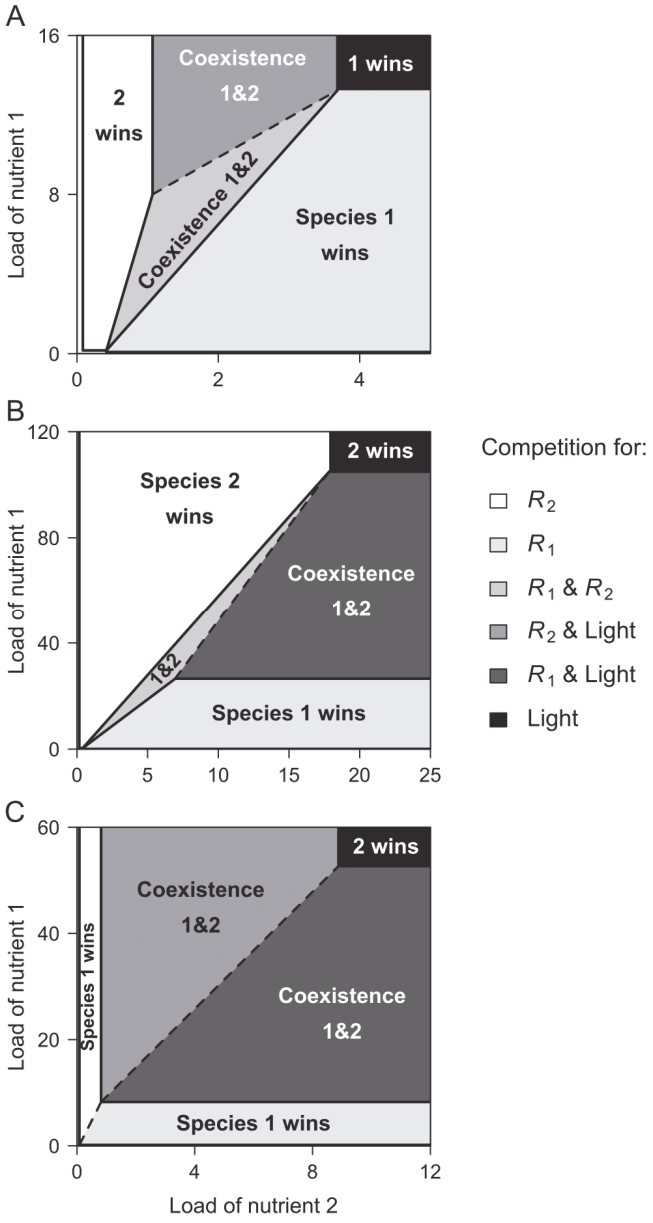

Figure 4.4: The outcome of competition between two species for two nutrients and light, predicted by the simplified model. (A), Species 1 is the superior competitor for nutrient 1 and light, whereas species 2 is the superior competitor for nutrient 2. (B), Species 1 is the superior competitor for nutrient 1, whereas species 2 is the superior competitor for nutrient 2 and light. (C), Species 1 is the superior competitor for both nutrients, whereas species 2 is the superior competitor for light. Close to the x-axis and y-axis, there is a region of 'no growth' (as in Fig. 4.2), but this region is often too narrow to be visible. Parameter values are given in Appendix C.

Competition between three species

This section investigates competition between three species for two nutrients and light. The number of theoretically possible scenarios is overwhelming. As Huisman and Weissing (2001) pointed out, three species can be ordered in 6 different ways according to their R^* values for a single resource. Hence, there are 63 = 216 different ways to order the R^* values of three species for three resources. The stability of the coexistence equilibria depends on the resource consumption parameters of the species (i.e., the values of c_{1j}, c_{2j} and k_j), and there are also 216 different ways to order the resource consumption parameters of three species for three resources. In case of three species competing for three resources one can thus distinguish 216 x 216 = 46,656 different model scenarios. Although some of these scenarios will be mathematically equivalent, it is clear that we cannot treat all possible scenarios here. Instead, we confine our analysis by the assumption that species 1 is the superior competitor for nutrient 1, species 2 is the superior competitor for nutrient 2, and species 3 is the superior competitor for light. We consider three cases with different configurations of the consumption parameters (Fig. 4.5A-C). With the help of the simplified model based on Equation (4.18), the boundary lines can again be derived analytically (see App. A).

The results show that species 1 wins if all species are limited by nutrient 1, species 2 wins if all are limited by nutrient 2, and species 3 wins if all are limited by light (Fig. 4.5A-C). Adjacent to these single-species regions are regions with either stable coexistence of two competitors (Fig. 4.5A,B) or alternative stable states of two competitors (Fig. 4.5C). In the center of each graph, where all three resources are limiting simultaneously, there is a stable or unstable three-species coexistence region (Fig. 4.5A-C). Huisman and Weissing (2001) demonstrated earlier that, in case of competition for three nutrients, the stability of the three-species coexistence equilibrium depends on the configuration of the consumption parameters. Our simulation results indicate that their 'rules of thumb' also apply if three species compete for two nutrients and light. Coexistence of all three species is stable if each species consumes most of the resource for which it is the inferior competitor (Fig. 4.5A). If each species consumes most of the resource for which it is the intermediate competitor, competition produces non-transitive interactions characterized by sustained species oscillations in the form of limit cycles (Fig. 5B). This is an interesting case, because these non-equilibrium dynamics may enable the coexistence of many species on a few limiting resources (Huisman and Weissing, 1999). If each species consumes most of the resource for which it is the best competitor, the species tend to

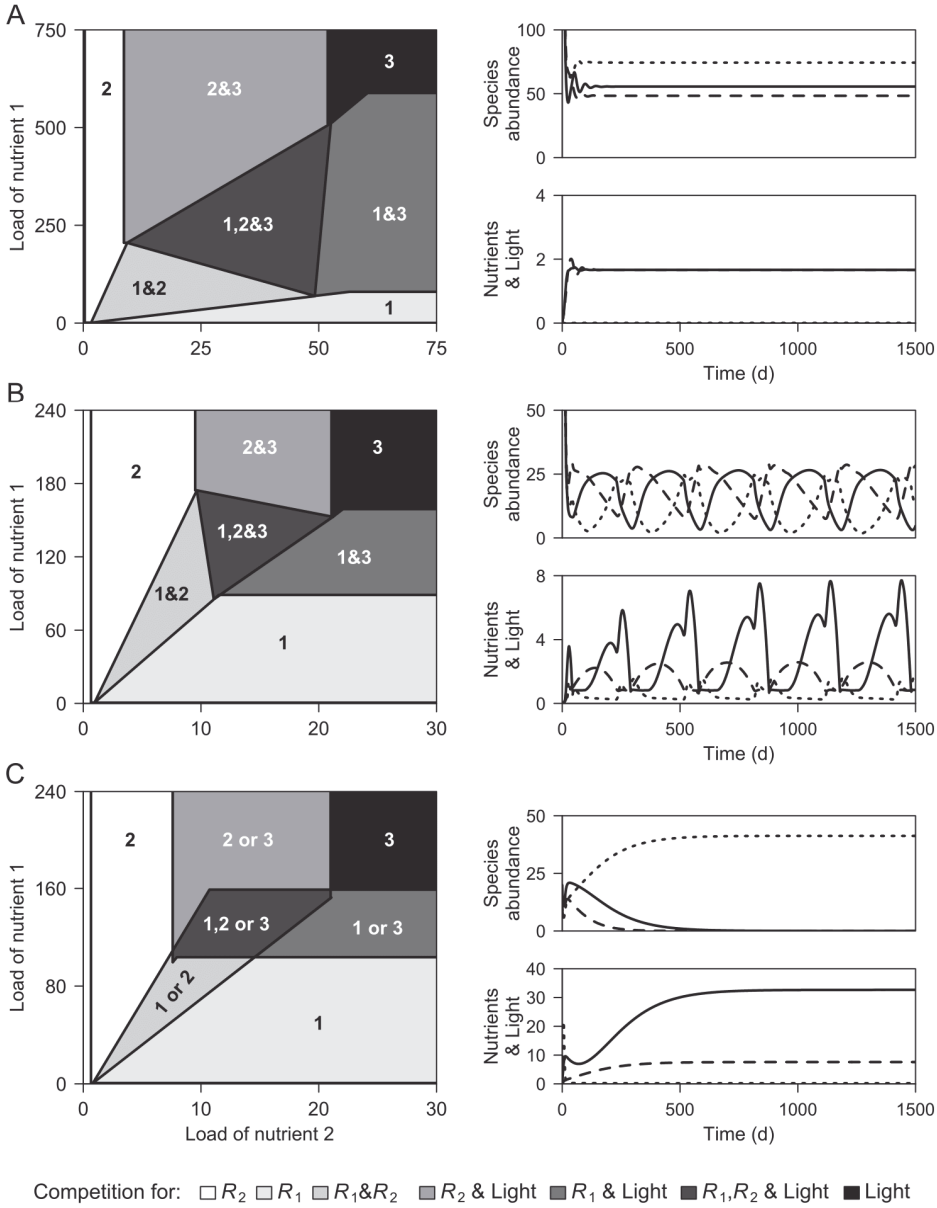

Figure 4.5: Competition between three species for two nutrients and light, predicted by the simplified model. Species 1 is the superior competitor for nutrient 1, species 2 for nutrient 2, and species 3 for light. Left panels show the winners of competition as function of the nutrient loads. Right panels show time series of species abundances, nutrient and light availability for the center region (region '1,2&3' in A,B; region '1,2 or 3' in C). Upper right panels show abundances of species 1 (solid line), species 2 (dashed line) and species 3 (dotted line). Lower right panels show concentrations of nutrient 1 (solid line), nutrient 2 (dashed line) and light penetration I_{out} (dotted line). The graphs consider three scenarios: (A), Each species consumes most of the resource for which it is the inferior competitor; this produces stable

coexistence. (B), Each species consumes most of the resource for which it is the intermediate competitor; this produces limit cycles in the center region. (C), Each species consumes most of the resource for which it is the superior competitor; this produces alternative stable states. Parameter values are given in Appendix C.

monopolize the limiting resource, which leads to competitive exclusion where the winner depends on the initial conditions (Fig. 4.5C).

Figure 4.6 investigates the same model scenarios, but now for the full model. In comparison to the simplified model, the boundaries separating the different dominance regions shift to other nutrient loads in the full model. Furthermore, several boundaries lines predicted by the full model are not linear but curved, reflecting the more gradual transition from nutrient to light limitation. Qualitatively, though, the predictions of the simplified and full model are again similar (compare Fig. 4.5 and Fig. 4.6). Species 1 wins if all species compete only for nutrient 1, species 2 wins if they all compete for nutrient 2, species 3 wins if they all compete for light, competition for two resources leads to stable or unstable two-species coexistence, and there is a stable or unstable three-species coexistence region in the center.

Interestingly, however, we did not find limit cycles in the full model, at least not for the parameter values that generated limit cycles in the simplified model. Instead, the full model predicts stable coexistence of all three species (Fig. 4.6B). A plausible explanation for this difference is that, in the simplified model, the growth rate of a species is limited by the same resource across the entire depth of the water column. Hence, non-transitive interactions between species play out over the entire depth of the water column. In contrast, in the full model, resource limitation is determined at each local depth. Accordingly, the species' growth rates will remain nutrient-limited in the upper part and light-limited in the lower part of the water column, while their growth rates may fluctuate between nutrient and light limitation only at intermediate depth. Hence, any tendency for fluctuations in resource limitation generated by non-transitive interactions will be restricted to this narrow depth range only. We conjecture that this has a stabilizing effect on the population dynamics, suppressing the species oscillations in the full model.

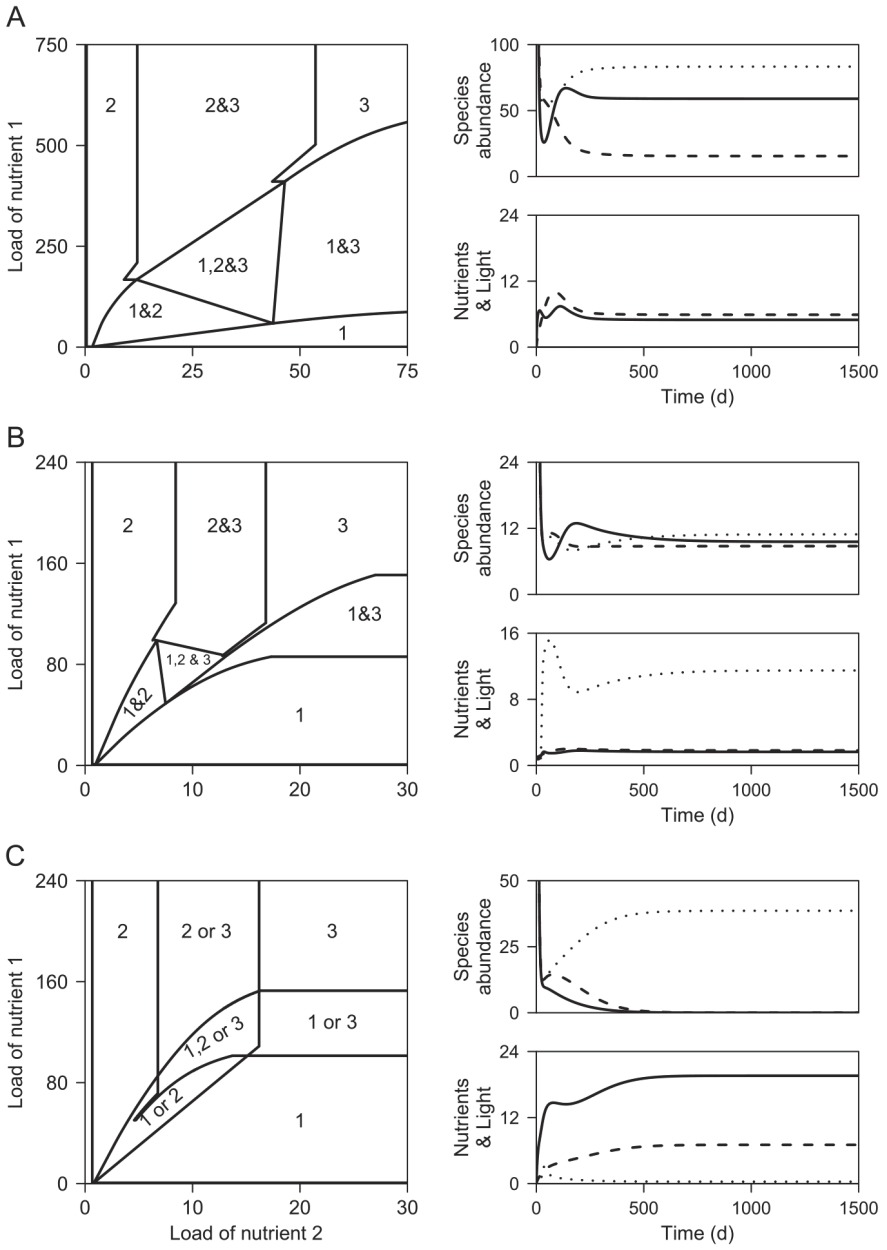

Figure 4.6: Competition between three species for two nutrients and light, predicted by the full model. Figure lay-out and parameter values are the same as in Figure 4.5. The graphs consider three scenarios: (A), Each species consumes most of the resource for which it is the inferior competitor; this produces stable coexistence. (B), Each species consumes most of the resource for which it is the intermediate competitor; in the full model, this produces stable coexistence instead of limit cycles. (C), Each species consumes most of the resource for which it is the superior competitor; this produces alternative stable states.

Trait combinations and species distributions

Natural communities often contain numerous species. This section therefore uses the full model to explore multispecies competition. Although the number of possible scenarios is daunting, some species traits may be physiologically or ecologically more plausible than others. Therefore, we confined our analysis to the following set of trait combinations:

Assumption 1: A three-way trade-off between competitive abilities for nitrogen, phosphorus and light (see Fig. C4.1A in App. C). In total, we consider nine species. Species 1-5 are superior competitors for nutrients but inferior competitors for light, with species 1 the superior competitor for nitrogen (lowest R^* for nitrogen) and species 5 the superior competitor for phosphorus (lowest R^* for phosphorus). Species 6-8 are intermediate competitors for nutrients and light, with species 6 the better competitor for nitrogen and species 8 the better competitor for phosphorus. Species 9 is the superior competitor for light but an inferior competitor for both nutrients. The existence of a trade-off between competitive abilities for nitrogen and phosphorus is supported by the recent meta-analysis of Edwards *et al.* (2011), who showed that strong competitors for nitrogen are generally weak competitors for phosphorus, and vice versa. Less is known about trade-offs between competitive abilities for nutrients versus light (e.g., Passarge *et al.*, 2006), although the existence of such trade-offs is suggested by the common observation that the species composition of phytoplankton communities changes along environmental gradients of nutrient and light availability (Sommer, 1993; Reynolds, 1997).

Assumption 2: Strong nutrient competitors (species with low R^* values) have low cellular contents of these nutrients (low c_{ij}'s), reflecting the common observation that species of nutrient-poor habitats generally have higher nutrient use efficiencies than those of nutrient-rich habitats (e.g., Sterner *et al.*, 1997). We incorporated this assumption through a positive correlation between the half-saturation constants for nutrient-limited growth and the cellular nutrient contents of the species, in line with empirical data reported by Litchman *et al.* (2007).

Assumption 3: Two different scenarios for the relationship between competitive ability for light and the light attenuation coefficients of species. The first scenario assumes that strong competitors for light (species with low I_{out}^*) have low light attenuation coefficients, while weak competitors for light have high light attenuation coefficients (Fig. C4.1B). Conversely, the second scenario assumes that strong competitors for

light have high light attenuation coefficients, while weak competitors have low light attenuation coefficients (Fig. C4.1C).

The results show that the species composition predicted by this multispecies competition model is sensitive to changes in both nutrient ratios and nutrient loads (Fig. 4.7). At low nutrient loads, species compete for nutrients and the species composition is largely determined by the N:P ratio. Species 1 and 2 are superior nitrogen competitors, and win at low N:P ratio. Species 4 and 5 are superior phosphorus competitors and win at high N:P ratio. At high nutrient loads, community biomass increases and the competitive interactions are shifted towards competition for light. Here, species 9 is the superior light competitor, and wins. At intermediate nutrient loads, multispecies competition generates a patchwork of different species combinations. The stability of the local coexistence equilibria within this patchwork depends on the two scenarios of Assumption 3.

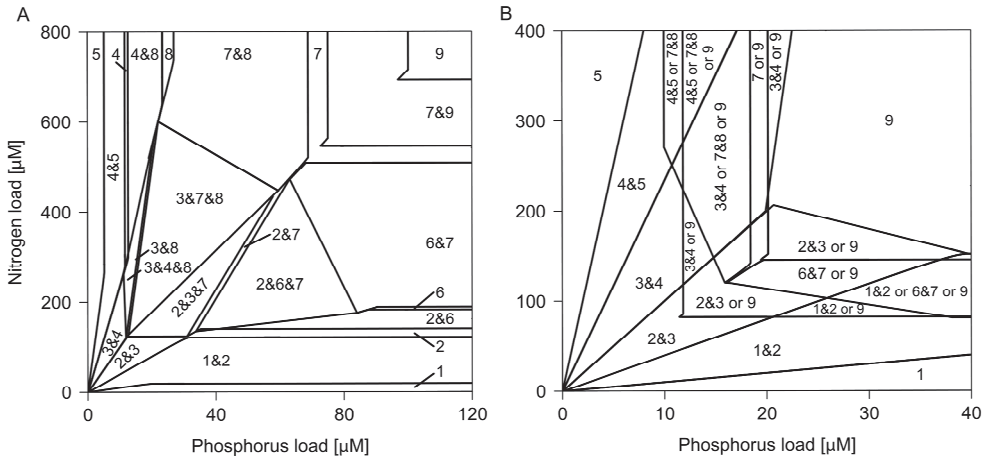

Figure 4.7: Competition between nine species for nitrogen, phosphorus and light, predicted by the full model. The graphs show the winners of competition as function of the nitrogen and phosphorus loads, for two different scenarios: (A), Strong competitors for light have low light attenuation coefficients (see Fig. C4.1B). This produces a patchwork of local regions with stable coexistence of two or three species. (B), Strong competitors for light have high light attenuation coefficients (see Fig. C4.1C). This produces a patchwork of alternative stable states in species composition. Parameter values are given in Appendix C, with a graphical illustration of the main traits of the species in Figure C4.1.

In the first scenario, strong competitors for light have low light attenuation coefficients, while weak competitors have high light attenuation coefficients. This trait combination has a stabilizing effect, generating a patchwork of stable two-species and three-species coexistence regions (Fig. 4.7A).

In the second scenario, strong competitors for light have high light attenuation coefficients. This trait combination generates a patchwork of local alternative stable states in species composition (Fig. 4.7B). In one state, the superior competitor for light creates low-light conditions that favor its own dominance and prevent invasion by strong nutrient competitors. In the alternative state, strong nutrient competitors deplete ambient nutrients to low levels preventing invasion by the superior light competitor. In some regions, we even found three alternative stable states, where two intermediate competitors generated light conditions too low for invasion of stronger nutrient competitors, but nutrient conditions too low for invasion of stronger light competitors. Hence, the species composition in this scenario depends not only on the nutrient loads, but is also sensitive to the initial species abundances.

DISCUSSION

This paper proposes the nutrient-load hypothesis to explain changes in species composition along productivity gradients. The nutrient-load hypothesis predicts that ratios of nutrient loads and absolute nutrient loads both have a major impact on the species composition of primary producers. Nutrient ratios are predicted to be a key determinant of the species composition in oligotrophic ecosystems, consistent with earlier resource competition theory (Tilman, 1982; Grover, 1997) and experiments (e.g., Tilman, 1977; Sommer, 1985; van Donk and Kilham, 1990; Smith, 1993). In contrast, absolute nutrient loads are predicted to be decisive for the outcome of competition in eutrophic ecosystems. High nutrient loads can produce high biomass, shifting the species interactions to competition for light. This favors the dominance of a superior light competitor that overshadows and excludes all other species. In mesotrophic ecosystems, communities can become co-limited by two nutrients and light. This may enable stable coexistence of species, but may also generate non-equilibrium coexistence or alternative stable states depending upon the traits of the competing species. These results were obtained for two alternative formulations of the specific growth rate (Equations (4.5) and (4.18)). This indicates that, qualitatively, the nutrient-load hypothesis does not depend on highly specific model assumptions, but

reflects more general principles. Several insights suggested by our model results will be discussed below.

Nutrient ratios versus nutrient loads

Our findings may help to reconcile the controversy over the role of nutrient ratios versus absolute nutrient levels in controlling the community composition of primary producers. For instance, several field studies have shown that the relative abundance of cyanobacteria in phytoplankton communities correlates well with the nitrogen-to-phosphorus ratio (Smith, 1983; Smith and Bennett, 1999; Havens *et al.*, 2003; Nõges *et al.*, 2008; Vrede *et al.*, 2009), whereas other studies have shown that cyanobacterial dominance is more strongly associated with absolute nutrient concentrations (Trimbee and Prepas, 1987; Canfield *et al.*, 1989; Jensen *et al.*, 1994; Reynolds, 1998; Downing *et al.*, 2001; McCarthy *et al.*, 2009). To illustrate how our model predictions may explain these contrasting field observations, we consider a hypothetical scenario in which cyanobacteria compete against eukaryotic phytoplankton at different nitrogen and phosphorus supply concentrations. Our scenario assumes that eukaryotic phytoplankton are superior competitors for phosphorus (e.g., diatoms; Grover, 1997), whereas cyanobacteria are superior competitors for nitrogen (Smith, 1986; Tyrrell, 1999) and for light (Mur *et al.*, 1977; Schwaderer *et al.*, 2011).

The outcome of competition between cyanobacteria and eukaryotic phytoplankton predicted from this hypothetical scenario is plotted in Figure 4.8. The arrows indicate three gradients of nutrient enrichment. Interestingly, the replacement of eukaryotes by cyanobacteria is very similar along all three gradients (bottom panels in Fig. 4.8). At low nutrient levels, enhanced phosphorus loads lead to an increase of the ambient P:N ratio, which shifts the species interactions from competition for phosphorus to competition for nitrogen. This favors the dominance of cyanobacteria at the expense of eukaryotic phytoplankton (gradient I). At high nutrient levels, the model also predicts that enhanced phosphorus loads lead to an increased P:N ratio, which again favors cyanobacteria over eukaryotic phytoplankton (gradient II). In this case, however, the correlation between the species composition and the P:N ratio is spurious, because the species interactions shift from competition for phosphorus to competition for light rather than to competition for nitrogen. The third gradient shows that cyanobacterial dominance also increases with combined nitrogen and phosphorus enrichment, even if the P:N ratio remains constant (gradient III). In this case, cyanobacteria become dominant again because of their superior competitive

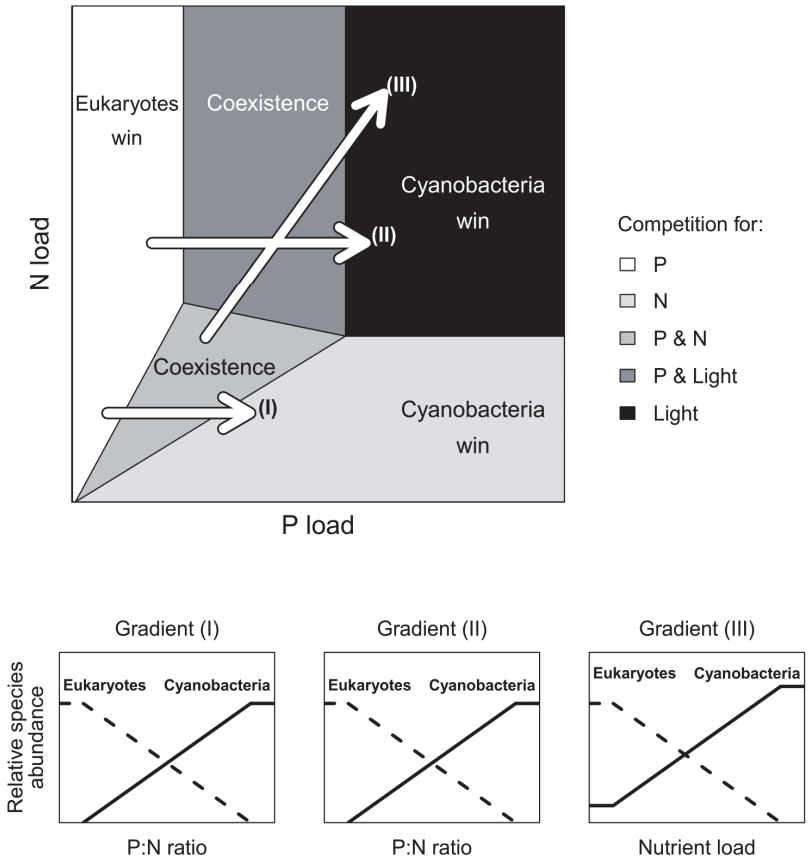

Figure 4.8: Competition between eukaryotic phytoplankton and cyanobacteria for nitrogen, phosphorus and light. The graph assumes that eukaryotes are superior competitors for phosphorus, while cyanobacteria are superior competitors for nitrogen and light. The upper panel shows the outcome of competition as function of the nutrient loads; the arrows indicate environmental gradients. Gradient I: As the P load increases, the P:N ratio increases, and the species interaction shifts from competition for phosphorus to competition for nitrogen. Gradient II: As the P load increases, the P:N ratio again increases, but now the species interaction shifts from competition for phosphorus to competition for light. Gradient III: The nitrogen and phosphorus loads both increase without changing the P:N ratio, shifting the species interaction from competition for nitrogen and phosphorus to competition for light. The three lower panels show the changes in species composition along these gradients (solid line, cyanobacteria; dashed line, eukaryotes).

ability for light. In total, our model thus predicts that cyanobacteria will be favored by low N:P ratios (high P:N ratios), and also by combined N+P enrichment (Fig. 4.8). This offers a simple and straightforward solution for the long-standing controversy

whether cyanobacterial dominance should be attributed to low N:P ratios or high nutrient loads (Smith, 2003).

These predictions are supported by the few experimental studies that have investigated competition for two nutrients and light. Yang and Jin (2008) investigated competition between the non-nitrogen-fixing cyanobacterium *Microcystis* aeruginosa, a green alga and a diatom at different N:P:light levels. At low light levels, the cyanobacterium became dominant irrespective of the N:P ratio. At high light levels, the cyanobacterium coexisted with the green alga, and the relative abundances of the two species depended on the N:P ratio. De Tezanos Pinto and Litchman (2010) performed similar experiments with the nitrogen-fixing cyanobacterium *Anabaena* flos-aquae and several other species of cyanobacteria, green algae, diatoms and cryptophytes. At low light levels, *Anabaena* became dominant irrespective of the N:P ratio. At high light levels, *Anabaena* dominated at low N:P ratios, while high N:P ratios resulted in a mixture of green algae. Hence, consistent with our model predictions, both studies found that nutrient ratios affected the species composition at high light conditions, but not at low light conditions where light limitation controlled the competitive outcome.

Productivity and diversity

Relations between productivity and biodiversity have been investigated in numerous theoretical and empirical studies. In this sense, our study builds upon previous work, and integrates elements from several earlier theoretical studies (e.g., Tilman, 1982; Huisman and Weissing, 1995). Yet, our model study is the first to analyze competition for two nutrients and light in a systematic manner. It is therefore interesting to assess to what extent the model predictions can capture observed productivity-diversity relationships.

Figure 4.7 illustrates how different nutrient loads are predicted to affect the number of coexisting species. Dominance by one or two species is expected at low nutrient levels, where species compete for one or two nutrients but not for light. At intermediate nutrient loads, species compete for both nutrients and light, which can generate a patchwork of many local two-species and three-species coexistence areas (Fig. 4.7A). In natural habitats, spatial heterogeneity or non-equilibrium conditions may span several of these local two-species and three-species areas, which will further enhance species diversity at larger spatial and temporal scales (cf. Tilman, 1982). High nutrient loads lead to the lowest biodiversity, because the superior light competitor excludes all

other species such that ultimately only a single species remains. Hence, in total, the model predicts that intermediate loads of both nutrients will favor high biodiversity, while high nutrient loads will strongly suppress biodiversity due to intense competition for light.

These model predictions are consistent with the unimodal productivity-diversity relationship observed for primary producers of many terrestrial, freshwater and marine ecosystems (Grime, 1973; Tilman and Pacala, 1993; Mittelbach *et al.*, 2001; Irigoien *et al.*, 2004; Stomp *et al.*, 2011). They are also in line with field observations documenting a positive relation between the species diversity of primary producers and the number of limiting resources (Interlandi and Kilham, 2001; Grover and Chrzanowski, 2004; Harpole and Tilman, 2007; Harpole and Suding, 2011). Moreover, these model predictions may help to understand why eutrophication of ecosystems often leads to diversity loss, and the dominance of only a few species (Grime, 1973; Carpenter *et al.*, 1998; Hautier *et al.*, 2009). The nutrient-load hypothesis may thus offer a simple conceptual framework to describe and understand how changes in productivity affect biodiversity.

Interestingly, however, our model results point out that intermediate nutrient loads do not necessarily yield high diversity. Instead of species coexistence, competition for two nutrients and light may also produce alternative stable states in species composition (Fig. 4.5C and 4.6C). The latter occurs if strong competitors for light absorb more light per unit biomass than other species (as in Fig. C4.1C), such that they can create the light-limited conditions that favor their own competitive dominance. Such a scenario seems physiologically quite plausible, since species with high light absorption per unit biomass will be able to cast substantial shade on other competitors while still capturing sufficient light energy themselves to survive under low-light conditions. Indeed, in laboratory experiments with five freshwater phytoplankton species, Passarge *et al.* (2006) found that the species with the highest light attenuation coefficients were the strongest competitors for light. In a multispecies context, this scenario produces a patchwork of alternative stable states, including regions with two and sometimes even three alternative stable states (Fig. 4.7B). The presence of a patchwork of multiple alternative stable states implies that small differences in nutrient loads and initial species abundances will determine which species will ultimately gain the upper hand. This makes the species composition at intermediate nutrient loads rather unpredictable.

Suggestions for future work

Our model can be interpreted as a model of intermediate complexity. It adds further realism to classic resource competition theory by incorporation of competition for light. Yet, the model still makes many simplifying assumptions. Our findings therefore suggest several avenues for further theoretical and experimental work.

One important simplification is the use of Von Liebig's (1840) 'Law of the Minimum'. As a consequence, species shift abruptly from nutrient-limited to light-limited growth. We introduced this assumption because it facilitated the mathematical analysis. Yet, rates of photosynthesis are known to be sensitive to the nutrient status of organisms. Conversely, assimilation of nutrients into a wide range of cellular functions requires energy provided by photosynthesis. Hence, from a physiological perspective, it would be more realistic to assume interactive effects of light and nutrient availability on growth (Healey, 1985; Evans, 1989; Aguirre von Wobeser *et al.*, 2011). This would result in a more gradual transition from nutrient to light limitation (Huisman and Weissing, 1995). More detailed physiological models could certainly contribute to a better understanding of the interactions between competition for nutrients and competition for light.

Another important simplification is the assumption that species and nutrients are all homogeneously mixed. In a strict sense, this limits the applicability of our model to phytoplankton in turbulent waters, while incomplete mixing may lead to deviations from our model predictions. For instance, incomplete mixing may select for species that can exploit spatial variation in nutrient and light conditions (Huston and DeAngelis, 1994; Huisman *et al.*, 2006; Yoshiyama *et al.*, 2009; Ryabov and Blasius, 2011). Furthermore, species that overtop others will profit from enhanced light access while leaving competitors in their shade, which may foster founder control in terrestrial plant communities (Rees and Bergelson, 1997; Perry *et al.*, 2003). It will be interesting to investigate how such spatially extended growth strategies will affect the competitive interactions for nutrients and light.

Previous theory has shown that competition for three limiting resources can generate species oscillations induced by non-transitive interactions between the species (Huisman and Weissing, 1999; 2001). These non-equilibrium dynamics may in turn favor high biodiversity (Huisman and Weissing, 1999; Kerr *et al.*, 2002; Laird and Schamp, 2006). One might expect that competition for two nutrients and light would produce similar species oscillations. This was confirmed by the simplified model (Fig. 4.5B), but surprisingly numerical simulations did not show species oscillations in the

full model (Fig. 4.6B). We conjecture that the vertical light gradient in combination with localized growth restricts non-transitive interactions to a narrow depth range, which has a stabilizing effect on the species dynamics. However, we have not explored this issue in further detail, and more rigorous theoretical analysis may shed more light on this issue.

Testing predictions of resource competition models is laborious but relatively straightforward. Species can be grown in monoculture to measure their growth kinetics, and subsequently the competitive interactions between these species can be studied at a range of different nutrient and light conditions (Tilman, 1977; Sommer, 1985; Huisman *et al.*, 1999; Passarge *et al.*, 2006). Surprisingly, only a few experimental studies investigated the three-way interaction of competition for two nutrients and light (Yang and Jin, 2008; De Tezanos Pinto and Litchman, 2010). As discussed above, these studies confirmed that nutrient ratios affect the species composition at high light conditions, but not under light-limited conditions. However, these studies were not a priori designed to test the theory developed here, and more systematic tests of the theoretical predictions in controlled competition experiments would therefore certainly be warranted.

One aspect deserves particular attention. Theory predicts that competition for nutrients and light can produce either stable species coexistence (Fig. 4.7A) or alternative stable states in species composition (Fig. 4.7B), depending on the trait combinations of the competing species. Some empirical evidence indicates that strong competitors for light tend to have higher light attenuation coefficients (Passarge *et al.*, 2006), which would favor alternative stable states. However, we still lack sufficient data to fully assess whether stable coexistence or alternative stable states will be more likely in natural communities. Moreover, in reality, the trait combinations might be fuzzier than the neat alignment of species traits assumed in our model simulations (Fig. C4.1). In that case, the model predicts a complex mixture of the patterns in Figure 4.7A and 4.7B, with some stable coexistence regions and other regions where alternative stable states prevail. These different scenarios have important implications for our general understanding of the productivity-diversity relationship and for the predictability of the species composition of natural communities. It will therefore be an important challenge for experimental studies to unravel which of these theoretically feasible scenarios are biologically most plausible.

Concluding remarks

Human activities have modified nutrient availability in many aquatic and terrestrial ecosystems, for instance through eutrophication, changes in land use and climate change. The nutrient-load hypothesis offers a simple conceptual framework to interpret and communicate how such human-driven changes in nutrient availability may affect the biodiversity and species composition of aquatic and terrestrial plant communities. In particular, this hypothesis incorporates the important role of nutrient ratios in oligotrophic environments, provides a mechanistic explanation for the high biodiversity commonly observed in mesotrophic environments, and helps to explain why reduction of nutrient loads is essential to suppress superior light competitors and restore high biodiversity in ecosystems exposed to long-term eutrophication.

Acknowledgments

We thank the anonymous reviewers for their constructive comments, which have been of great help to improve the manuscript. The research of V.S.B., M.S. and J.H. was supported by the Earth and Life Sciences Foundation (ALW), which is subsidized by the Netherlands Organization for Scientific Research (NWO).

Appendix A: ANALYTICAL DERIVATION OF TRANSITIONS IN RESOURCE LIMITATION AND SPECIES COMPOSITION

The boundary lines in our graphs represent transitions in resource limitation and species composition, plotted as function of the nutrient loads $R_{in,1}$ and $R_{in,2}$. For instance, these boundary lines indicate at which nutrient load the species interactions will shift from competition for nutrients to competition for light, or at which nutrient load the species composition will change drastically. Assuming Liebig's Law of the Minimum, expressions for these boundary lines can be derived analytically, by solving the differential Equations (4.6) and (4.7) for equilibrium. The derivations are presented in this appendix.

Resource limitation of a single species

At equilibrium, the depth-averaged growth rate of a single species j will be limited by one of the two nutrients (Fig. 4.1A), co-limited by a nutrient and light (Fig. 4.1B), or exclusively limited by light (Fig. 4.1C). We assume that the incident light intensity is high enough to support population growth at low population densities (i.e., $I_{out}>I_{out,j}^{*}$ at $N\approx 0$). Therefore, the only requirement for net population growth at low population densities is that the nutrient loads exceed the critical nutrient concentrations R_{1j}^{*} and R_{2j}^{*}. Hence, in Figure 2, the horizontal boundary line between 'no growth' and 'limitation by nutrient 1' and the vertical boundary line between 'no growth' and 'limitation by nutrient 2' are given by

$$R_{in,1} = R_{1j}^{*} \quad for \;\; R_{in,2} > R_{2j}^{*} \tag{A4.1A}$$

$$R_{in,2} = R_{2j}^{*} \quad for \;\; R_{in,1} > R_{1j}^{*}. \tag{A4.1B}$$

At the diagonal boundary line between the regions 'limitation by nutrient 1' and 'limitation by nutrient 2', the specific growth rate is co-limited by nutrient 1 and 2. Hence, at this boundary line,

$$R_1 = R_{1j}^{*} \text{ and } R_2 = R_{2j}^{*}. \tag{A4.2}$$

Inserting these values in Equation (4.7), and solving $dR_1/dt=0$ and $dR_2/dt=0$ yields an equation for the diagonal boundary line in Figure 4.2:

$$R_{in,1} = R_{1j}^{*} + \frac{c_{1j}}{c_{2j}}[R_{in,2} - R_{2j}^{*}]. \tag{A4.3}$$

Co-limitation of nutrients and light occurs at intermediate nutrient loads, where $I_{out} \le I_{co,j} \le I_{in}$. Hence, the horizontal line separating the region of 'limitation by nutrient 1' from the region of 'co-limitation by nutrient 1 and light' is characterized by

$$R_1 = R_{1j}^{*} \text{ and } I_{out} = I_{co,1j}^{*} \tag{A4.4}$$

Here $I_{co,1j}^{*} = H_j R_{1j}^{*} / M_{1j}$, in accordance with Equation (4.8) when nutrient 1 is limiting at equilibrium. Similarly, the vertical line separating the region of limitation by nutrient 2 from the region of co-limitation by nutrient 2 and light is characterized by

$$R_2 = R_{2j}^{*} \text{ and } I_{out} = I_{co,2j}^{*} \tag{A4.5}$$

Inserting Equations (A4.4) and (A4.5) into Equations (4.1), (4.6), and (4.7) and solving for zero yields explicit equations for the horizontal and vertical line separating the two regions of nutrient limitation from the two regions of co-limitation by nutrients and light:

$$R_{in,1} = R_{1j}^{*} + \frac{c_{1j} l_j}{k_j F}\left(\ln(I_{in}) - \ln(I_{co,1j}^{*}) - K_{BG} z_M\right) \tag{A4.6A}$$

$$R_{in,2} = R_{2j}^{*} + \frac{c_{2j} l_j}{k_j F}\left(\ln(I_{in}) - \ln(I_{co,2j}^{*}) - K_{BG} z_M\right) \tag{A4.6B}$$

When nutrient loads are raised further, such that $I_{co,j} \ge I_{in}$, the depth-averaged growth rate shifts from co-limitation by nutrients and light to light limitation only. The horizontal and vertical line separating the two regions of co-limitation by nutrients and light from the region of light limitation are characterized by

$$I_{co,j} = I_{in} \text{ and } I_{out} = I_{out,j}^{*}. \tag{A4.7}$$

In view of Equation (4.8), $I_{co,j} = I_{in}$ implies $R_1 = (M_{1j}/H_j) I_{in}$ for nutrient 1 and $R_2 = (M_{2j}/H_j) I_{in}$ for nutrient 2. Hence, the horizontal and vertical line separating the regions of co-limitation by nutrients and light from the region of light limitation are given by

$$R_{in,1} = \frac{M_{1j}}{H_j} I_{in} + \frac{c_{1j} l_j}{k_j F}\left(\ln(I_{in}) - \ln(I_{out,j}^{*}) - K_{BG} z_M\right) \tag{A4.8A}$$

$$R_{in,2} = \frac{M_{2j}}{H_j} I_{in} + \frac{c_{2j} l_j}{k_j F}\left(\ln(I_{in}) - \ln(I_{out,j}^{*}) - K_{BG} z_M\right) \tag{A4.8B}$$

We were not able to find an analytical solution for the diagonal boundary separating the region of co-limitation by nutrient 1 and light from the region of co-limitation by nutrient 2 and light (Fig. 4.2). The equation describing this boundary resembles Equation (A4.3):

$$R_{in,1} = R_{co,1j} + \frac{c_{1j}}{c_{2j}}[R_{in,2} - R_{co,2j}]. \qquad \text{(A4.9)}$$

where $R_{co,1j}$ and $R_{co,2j}$ are now the equilibrium solutions of R_1 and R_2 obtained by inserting growth Equation (4.14) into dN_j/dt = 0. This gives

$$R_{co,ij} = \frac{M_{ij}\mu_{\max,j}[\ln(H_j + I_{co,j}) - \ln(H_j + I_{out})] - M_{ij}l_j[\ln(I_{in}) - \ln(I_{out})]}{l_j[\ln(I_{in}) - \ln(I_{out})] - \mu_{\max,j}[\ln(I_{in}) - \ln(I_{co,j})] - \mu_{\max,j}[\ln(H_j + I_{co,j}) - \ln(H_j + I_{out})]} \qquad \text{(A4.10)}$$

The terms $I_{co,j}$ and I_{out} in this equation depend on the equilibrium population density N_j, which is in turn a complex function of $R_{in,1}$ and $R_{in,2}$. We therefore solved this diagonal boundary numerically in Figure 4.2.

Competition between two species

For our mathematical analysis of competition between species, we consider a simplified model in which the depth-averaged specific growth rate is written as:

$$\overline{\mu_j} = \mu_{\max,j} \min\left[f_{1j}(R_1), f_{2j}(R_2), \frac{1}{z_M}\int_0^{z_M} g_j(I(z))\, dz \right]. \qquad \text{(A4.11)}$$

According to this equation, the depth-averaged growth rate of a species is limited by either nutrient 1, or nutrient 2, or light (Fig. B4.1). We first consider competition among two species, where each species is the superior competitor for another resource. It can be shown that the coexistence equilibrium occurs for the nutrient and light availability at which each species is limited by the resource for which it is the inferior competitor (see Huisman and Weissing, 2001 for a formal proof).

Scenario 1: Species 1 is the superior competitor for nutrient 1 and light, and species 2 is the superior competitor for nutrient 2 (Fig. 4.4A). The coexistence equilibrium then occurs either at the point where species 1 is limited by R_2 and species 2 by R_1, or at the point where species 1 is limited by R_2 and species 2 by light. That is,

$R_2=R_{21}^*$ and $R_1=R_{12}^*$, or

$R_2=R_{21}^*$ and $I_{out}=I_{out,2}^*$. (A4.12)

At the boundary between the region where species 2 wins and the coexistence region, we have N_1 = 0 and N_2 > 0. The boundary line is obtained by inserting these conditions and Equation (A4.12) into Equations (4.1), (4.6) and (4.7) and subsequent solving for zero. This yields:

$$R_{in,1} = R_{12}^* + \frac{c_{12}}{c_{22}}[R_{in,2} - R_{21}^*] \; for \;\; R_{21}^* \le R_{in,2} \le R_{21}^* + \frac{c_{22}l_2}{k_2}L_2$$
$$R_{in,2} = R_{21}^* + \frac{c_{22}l_2}{k_2}L_2 \qquad for \;\; R_{in,1} \ge R_{11}^* + \frac{c_{12}l_2}{k_2}L_2 \tag{A4.13}$$

where we defined

$$L_j = \frac{1}{F}\left(\ln(I_{in}) - \ln(I_{out,j}^*) - K_{BG}z_M\right) \tag{A4.14}$$

Conversely, inserting N_1 > 0, N_2 = 0 and Equation (A4.12) into Equations (4.1), (4.6) and (4.7), and subsequent solving for zero, yields the boundary line between the region where species 1 wins and the coexistence region:

$$R_{in,1} = R_{12}^* + \frac{c_{11}}{c_{21}}[R_{in,2} - R_{21}^*] \; for \;\; R_{21}^* \le R_{in,2} \le R_{21}^* + \frac{c_{21}l_1}{k_1}L_2$$
$$R_{in,2} = R_{21}^* + \frac{c_{21}l_1}{k_1}L_2 \qquad for \;\; R_{in,1} \ge R_{11}^* + \frac{c_{11}l_1}{k_1}L_2 \tag{A4.15}$$

Equations (A4.13) and (A4.15) show that the two boundary lines in Figure 4.4A consist of two distinct parts. This is due to the assumption of Von Liebig's 'Law of the Minimum'. The first lines in Equations (A4.13) and (A4.15) describe the diagonal legs of the boundary lines, representing the conditions for coexistence on two nutrients. The second lines in Equations (A4.13) and (A4.15) describe the vertical legs of the boundary lines, representing the conditions for coexistence on nutrient 2 and light.

Scenario 2: The derivation of the boundary lines for scenario 2 is similar to that for scenario 1, but the boundary lines extend horizontally instead of vertically (Fig. 4.4B).

Scenario 3: Species 1 is the superior competitor for nutrient 1 and 2, and species 2 is the superior competitor for light (Fig. 4.4C). The two-species equilibrium occurs either at the point where species 1 is limited by light and species 2 by R_1, or at the point where species 1 is limited by light and species 2 by R_2. That is:

$I_{out}=I_{out,1}^*$ and $R_1=R_{12}^*$, or

$I_{out}=I_{out,1}^*$ and $R_2=R_{22}^*$. (A4.16)

At the boundary between the region where species 1 wins and the coexistence region, we have $N_2 = 0$ and $N_1 > 0$. The equation for this boundary line is obtained by inserting these conditions and Equation (A4.16) into Equations (4.1), (4.6) and (4.7) and subsequent solving for zero. This yields:

$$R_{in,1} = R_{12}^* + \frac{c_{11}l_1}{k_1}L_1 \quad for \quad R_{in,2} \geq R_{22}^* + \frac{c_{21}l_1}{k_1}L_1$$

$$R_{in,2} = R_{22}^* + \frac{c_{21}l_1}{k_1}L_1 \quad for \quad R_{in,1} \geq R_{12}^* + \frac{c_{11}l_1}{k_1}L_1 \quad . \qquad \text{(A4.17)}$$

Conversely, inserting $N_1 > 0$, $N_2 = 0$ and Equation (A4.16) into Equations (4.1), (4.6) and (4.7), and subsequent solving for zero, yields the boundary line between the region where species 2 wins and the coexistence region:

$$R_{in,1} = R_{12}^* + \frac{c_{12}l_2}{k_2}L_1 \quad for \quad R_{in,2} \geq R_{22}^* + \frac{c_{22}l_2}{k_2}L_1$$

$$R_{in,2} = R_{22}^* + \frac{c_{22}l_2}{k_2}L_1 \quad for \quad R_{in,1} \geq R_{12}^* + \frac{c_{12}l_2}{k_2}L_1 \quad . \qquad \text{(A4.18)}$$

The first lines in Equations (A4.17) and (A4.18) describe the horizontal legs of the boundary lines in Figure 4.4C, representing the conditions for coexistence on nutrient 1 and light. The second lines in Equations (A4.17) and (A4.18) describe the vertical legs, representing the conditions for coexistence on nutrient 2 and light.

Stability conditions: The stability of the coexistence equilibrium on two nutrients is determined by the consumption parameters of the competing species. More specifically, previous studies have shown that competition for two nutrients yields stable coexistence, if each species consumes relatively more of the nutrient for which it is the inferior competitor (León and Tumpson, 1975; Taylor and Williams, 1976;

Tilman, 1980). That is, if species 1 is the superior competitor for nutrient 1 and species 2 the superior competitor for nutrient 2, then stable coexistence requires:

$$\frac{c_{11}}{c_{21}} < \frac{c_{12}}{c_{22}}. \tag{A4.19}$$

The stability condition for the coexistence equilibrium on a single nutrient and light is quite similar. However, it depends not only on the consumption characteristics of the competing species, but also on their loss rates. More specifically, if species 1 is the superior competitor for nutrient 1 and species 2 the superior competitor for light, then stable coexistence requires (Huisman and Weissing, 1995):

$$\frac{c_{11}l_1}{k_1} < \frac{c_{12}l_2}{k_2}. \tag{A4.20}$$

If the inequality in Equation (A4.19) or Equation (A4.20) is reversed, the coexistence equilibrium is unstable. In that case, one species will exclude the other species, but which of the two species wins depends on the initial conditions (León and Tumpson, 1975; Tilman, 1980; Huisman and Weissing, 1995).

Competition between three species

We now consider competition between three species, again using the simplified model (Equation (A4.11)). We assume that species 1 is the superior competitor for nutrient 1, species 2 is the superior competitor for nutrient 2, and species 3 is the superior competitor for light. More precisely, the three species are ranked according to their competitive abilities as follows:

$$\begin{aligned} &R_{11}^* < R_{12}^* < R_{13}^* \\ &R_{22}^* < R_{23}^* < R_{21}^* \\ &I_{out,3}^* < I_{out,1}^* < I_{out,2}^*. \end{aligned} \tag{A4.21}$$

The boundary lines between the regions where a single species wins and the two-species coexistence equilibria, shown in Figure 4.5, are as described in the previous section. The three-species equilibrium exists only if each species is limited by the resource for which it is the inferior competitor (see Huisman and Weissing, 2001 for a formal proof). Consequently, in our case, the three-species equilibrium occurs at

$$R_1=R_{13}^*,\ R_2=R_{21}^* \text{ and } I_{out}=I_{out,2}^*. \tag{A4.22}$$

The region where all three species coexist is described by three boundary lines (Fig. 5A,B). To obtain analytical expressions for these three boundary lines, we make use of the matrix **C**, which describes the 3x3 matrix of resource consumption parameters:

$$\mathbf{C} = \begin{bmatrix} c_{11}l_1 & c_{12}l_2 & c_{13}l_3 \\ c_{21}l_1 & c_{22}l_2 & c_{23}l_3 \\ k_1 & k_2 & k_3 \end{bmatrix}. \qquad \text{(A4.23)}$$

We define $\det(c_{ij})$ as the determinant of the smaller matrix c_{ij}, which is the 2x2 matrix resulting from deletion of row i and column j of matrix **C**.

The first boundary line describes the transition from the three-species equilibrium to the coexistence region of species 1 and 2. At this boundary line, we have $N_1>0$, $N_2>0$, and $N_3=0$. Inserting these conditions and Equation (A4.22) into Equations (4.1), (4.6) and (4.7), and solving for equilibrium, yields an explicit equation for the boundary line:

$$R_{in,1} = R_{13}^* + \frac{\det(\mathbf{C_{23}})}{\det(\mathbf{C_{13}})}[R_{in,2} - R_{21}^*] - \frac{\det(\mathbf{C_{33}})}{\det(\mathbf{C_{13}})}L_2, \qquad \text{(A4.24)}$$

where L_2 is described by Equation (A4.14) and the boundary line is restricted to the interval

$$R_{21}^* + \frac{c_{22}l_2}{k_2}L_2 > R_{in,2} > R_{21}^* + \frac{c_{21}l_1}{k_1}L_2 .$$

At the second boundary line, which describes the transition from the three-species equilibrium to the coexistence region of species 1 and 3, we have $N_1>0$, $N_2=0$, and $N_3>0$. Inserting these conditions and Equation (A4.22) into Equations (4.1), (4.6) and (4.7), and solving these equations for equilibrium, yields:

$$R_{in,1} = R_{13}^* + \frac{\det(\mathbf{C_{22}})}{\det(\mathbf{C_{12}})}[R_{in,2} - R_{21}^*] - \frac{\det(\mathbf{C_{32}})}{\det(\mathbf{C_{12}})}L_2, \qquad \text{(A4.25)}$$

restricted to the interval

$$R_{21}^* + \frac{c_{21}l_1}{k_1}L_2 > R_{in,2} > R_{21}^* + \frac{c_{23}l_3}{k_3}L_2 .$$

Likewise, we can find the third boundary line, which describes the transition from the three-species equilibrium to the coexistence region of species 2 and 3. Inserting the

conditions N_1=0, N_2>0, N_3>0 and Equation (A4.22) into Equations (4.1), (4.6) and (4.7), and solving these equations for equilibrium, yields:

$$R_{in,1} = R_{13}^* + \frac{\det(\mathbf{C_{21}})}{\det(\mathbf{C_{11}})}[R_{in,2} - R_{21}^*] - \frac{\det(\mathbf{C_{31}})}{\det(\mathbf{C_{11}})}L_2, \qquad \text{(A4.26)}$$

restricted to the interval

$$R_{21}^* + \frac{c_{22}l_2}{k_2}L_2 > R_{in,2} > R_{21}^* + \frac{c_{23}l_3}{k_3}L_2 .$$

The boundary lines in Figures 4.5C, 4.6, 4.7 and B4.2 are more complicated, and were calculated numerically with MATLAB package MATCONT 2.4 (Dhooge *et al.*, 2003).

Given the ranking of the competitive abilities of the species, in Equation (A4.21), the local stability of the three-species coexistence equilibrium depends on the structure of the consumption matrix C. The stability conditions are similar to those described in detail in Huisman and Weissing (2001; see their App. B), and we used MATCONT 2.4 to verify the stability of all three-species equilibria using numerical simulations of the time course of competition.

APPENDIX B: COMPARISON BETWEEN THE SIMPLIFIED AND FULL MODEL

In this appendix we compare some of the predictions of the simplified and full model. In the full model, Von Liebig's Law of the Minimum applies at each local depth

$$\overline{\mu_j} = \frac{1}{z_M}\int_0^{z_M} \mu_{\max,j} \min[f_{1j}(R_1), f_{2j}(R_2), g_j(I(z))]\, dz \qquad \text{(B4.1)}$$

Accordingly, the specific growth rate can be limited by nutrients near the water surface, but limited by light deeper down in the water column (Fig. 4.1B). Therefore, one might say that the depth-averaged specific growth rate is co-limited by nutrients and light.

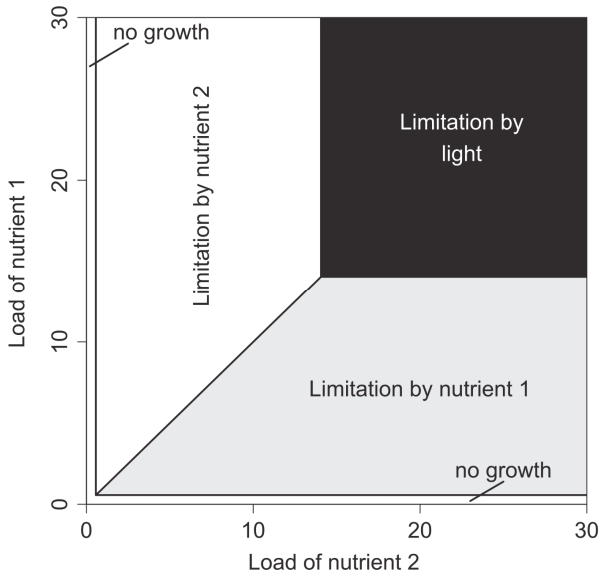

Figure B4.1: Resource limitation of a single species growing on two nutrients and light, predicted by the simplified model. In the 'no growth' regions, nutrient availability is too low to support a phytoplankton population. At low nutrient loads, the growth rate is limited by either nutrient 1 or nutrient 2, depending on the ratio of the nutrient loads. At high nutrient loads, growth is limited by light irrespective of the nutrient ratios. Parameter values are the same as in Figure 4.2 of the main text (see App. C).

In contrast, in the simplified model, the Law of the Minimum applies at once over the entire water column:

$$\overline{\mu_j} = \mu_{\max,j} \min\left[f_{1j}(R_1), f_{2j}(R_2), \frac{1}{z_M} \int_0^{z_M} g_j(I(z))\, dz \right] \qquad \text{(B4.2)}$$

Hence, in the simplified model, the growth rate is either limited by nutrient 1, or by nutrient 2, or by light over the entire depth; co-limitation does not occur. This is illustrated in Figure B4.1. This figure resembles Figure 4.2 of the main text, in that nutrient ratios determine whether nutrient 1 or nutrient 2 is limiting, while absolute nutrient loads determine the transition from nutrient limitation to light limitation. However, Figure B4.1 differs from Figure 4.2 in that the simplified model does not predict a region of co-limitation by nutrients and light.

Figure B4.2 shows the outcome of two-species competition predicted by the full model. Comparison with the outcome of competition predicted by the simplified

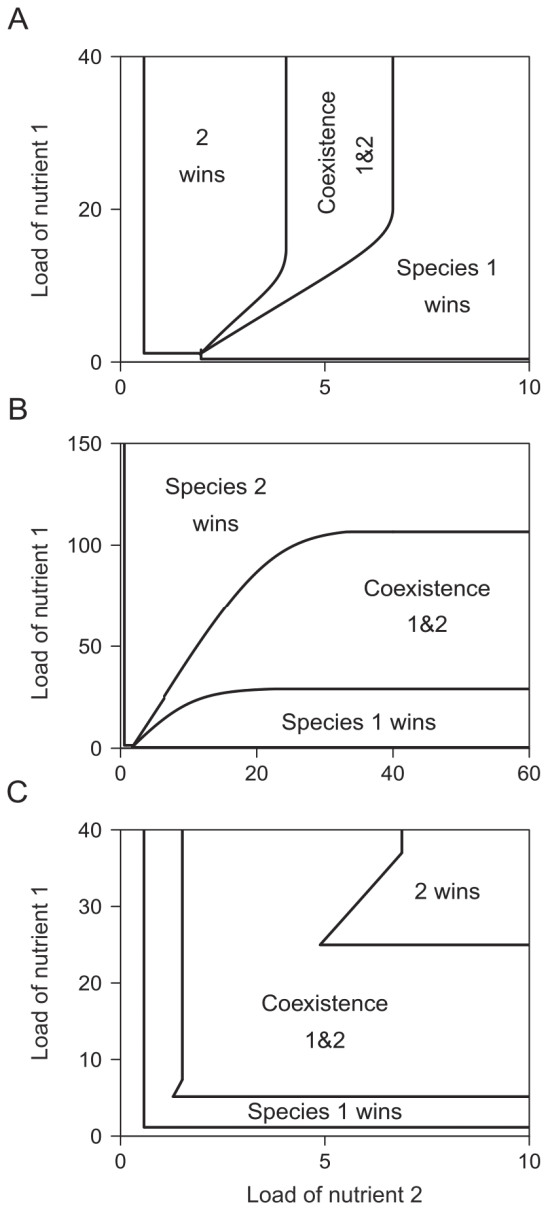

Figure B4.2: The outcome of competition between two species for two nutrients and light, predicted by the full model. (A), Species 1 is the superior competitor for nutrient 1 and light, whereas species 2 is the superior competitor for nutrient 2. (B), Species 1 is the superior competitor for nutrient 1, whereas species 2 is the superior competitor for nutrient 2 and light. (C), Species 1 is the superior competitor for both nutrients, whereas species 2 is the superior competitor for light. Parameter values are the same as in Figure 4 of the main text (see App. C).

model (Fig. 4.4 in the main text) shows that, qualitatively, the predictions of the simplified and full model are similar. At low nutrient levels, the outcome of competition is determined by the nutrient ratio. At high nutrient levels, the outcome of competition is determined by the absolute nutrient loads.

Quantitatively, however, the results are different. For instance, the boundary lines characterizing the transition from 'no growth' to species 1 or 2 wins may occur at higher nutrient loads in the full model than in the simplified model (compare Fig. B4.2 versus Fig. 4.4), even though both models make use of exactly the same parameter values. The underlying reason is that the model simulations of Figure B4.2 and Figure 4.4 consider a deep water column, and the full model predicts that phytoplankton growth will be limited by light deeper down in the water column even at low nutrient levels. Hence, in this case, co-limitation by nutrients and light suppresses the depth-averaged growth rate in the full model, such that the establishment of a phytoplankton population requires higher nutrient loads in the full model than in the simplified model.

APPENDIX C: PARAMETER VALUES

If not stated otherwise, the default values for the physical parameters in our simulations were: I_{in} = 600 µmol photons m^{-2} s^{-1}, z_M = 20 m, K_{BG} = 0.1 m^{-1}, F = 0.25 m day^{-1}.

The default parameters for the maximum specific growth rates and specific loss rates were: $\mu_{max,j}$ = 1 day^{-1}, l_j = 0.25 day^{-1} (where j = 1,…,n).

Figure 4.2: $\mu_{max,1}$ =0.8 day^{-1}, M_{11} = 1.25 µmol L^{-1}, M_{21} = 1.25 µmol L^{-1}, H_1 = 50 µmol photons m^{-2} s^{-1}, c_{11} = 6 fmol $cell^{-1}$, c_{21} = 6 fmol $cell^{-1}$, k_1 = 8 μm^2 $cell^{-1}$, F = 0.1 m day^{-1}, I_{in} = 100 µmol photons m^{-2} s^{-1}, K_{BG} = 0.1 m^{-1}, z_M = 10 m.

Figure 4.3: Same parameter values as in Figure 4.2, but K_{BG} = 0.05 m^{-1}.

Figure 4.3A: I_{in} = 100 µmol photons m^{-2} s^{-1}; Figure 4.3B: I_{in} = 200 µmol photons m^{-2} s^{-1}; Figure 4.3C: I_{in} = 400 µmol photons m^{-2} s^{-1}; Figure 4.3D: z_M = 1 m; Figure 4.3E: z_M = 10 m; Figure 4.3F: z_M = 25 m.

Figure 4.4: The half-saturation constants for the two nutrients, M_{ij} (µmol L^{-1}), and the half-saturation constants for light, H_j (µmol photons m^{-2} s^{-1}), are summarized in matrix **M**. Rows represent nutrient 1, nutrient 2 and light. Columns represent species 1 and 2:

$$\mathbf{M} = \begin{bmatrix} M_{11} & M_{12} \\ M_{21} & M_{22} \\ H_1 & H_2 \end{bmatrix}.$$

Analogously, the cellular nutrient contents, c_{ij} (fmol $cell^{-1}$), and the specific light attenuation coefficients, k_j (µm^2 $cell^{-1}$), are summarized in matrix **C**:

$$\mathbf{C} = \begin{bmatrix} c_{11} & c_{12} \\ c_{21} & c_{22} \\ k_1 & k_2 \end{bmatrix}.$$

Figure 4.4A:

$$\mathbf{M} = \begin{bmatrix} 0.25 & 0.5 \\ 1.25 & 0.25 \\ 30 & 40 \end{bmatrix}, \quad \mathbf{C} = \begin{bmatrix} 48 & 72 \\ 12 & 6 \\ 4 & 10 \end{bmatrix}.$$

Figure 4.4B:

$$\mathbf{M} = \begin{bmatrix} 0.25 & 1.25 \\ 1.25 & 0.5 \\ 30 & 20 \end{bmatrix}, \quad \mathbf{C} = \begin{bmatrix} 48 & 96 \\ 12 & 16 \\ 4 & 2 \end{bmatrix}.$$

Figure 4.4C:

$$\mathbf{M} = \begin{bmatrix} 0.5 & 1.25 \\ 0.25 & 0.75 \\ 40 & 20 \end{bmatrix}, \quad \mathbf{C} = \begin{bmatrix} 72 & 96 \\ 6 & 16 \\ 10 & 2 \end{bmatrix}.$$

z_M = 100 m, F = 0.1 m day^{-1}.

Figure 4.5:

Figure 4.5A:

$$\mathbf{M} = \begin{bmatrix} 1 & 3 & 5 \\ 5 & 1 & 3 \\ 20 & 30 & 15 \end{bmatrix}, \quad \mathbf{C} = \begin{bmatrix} 20 & 80 & 100 \\ 14 & 3 & 10 \\ 3 & 4 & 2 \end{bmatrix}.$$

The time series in Figure 4.5A are shown for $R_{in,1}$ = 250 µmol L^{-1}, $R_{in,2}$ = 35 µmol L^{-1}.

Figure 4.5B:

$$\mathbf{M} = \begin{bmatrix} 2 & 2.5 & 2.9 \\ 2.9 & 2 & 2.5 \\ 55 & 60 & 45 \end{bmatrix}, \quad \mathbf{C} = \begin{bmatrix} 100 & 160 & 120 \\ 12 & 8 & 16 \\ 9 & 7 & 6 \end{bmatrix}.$$

The time series in Figure 4.5B are shown for $R_{in,1}$ = 130 µmol L^{-1}, $R_{in,2}$ = 13 µmol L^{-1}.

Figure 4.5C:

$$\mathbf{M} = \begin{bmatrix} 2 & 2.3 & 2.5 \\ 2.5 & 2 & 2.3 \\ 55 & 60 & 50 \end{bmatrix}, \quad \mathbf{C} = \begin{bmatrix} 160 & 120 & 130 \\ 10 & 16 & 9 \\ 8 & 6 & 10 \end{bmatrix}.$$

The time series in Figure 4.5C are shown for $R_{in,1}$ = 140 µmol L^{-1}, $R_{in,2}$ = 15 µmol L^{-1}.

Figure 4.6: This figure is based on the full model instead of the simplified model, with the same parameter values as in Figure 4.5.

The times series in Figure 4.6A are shown for $R_{in,1}$ = 220 µmol L^{-1}, $R_{in,2}$ = 40 µmol L^{-1}.

The times series in Figure 4.6B are shown for $R_{in,1}$ = 75 µmol L^{-1}, $R_{in,2}$ = 9 µmol L^{-1}.

The times series in Figure 4.6C are shown for $R_{in,1}$ = 120 µmol L^{-1}, $R_{in,2}$ = 14 µmol L^{-1}.

Figure 4.7:

Figure 4.7A:

$$\mathbf{M} = \begin{bmatrix} 0.008 & 0.032 & 0.13 & 0.45 & 1.3 & 0.16 & 0.32 & 0.63 & 0.5 \\ 0.2 & 0.041 & 0.008 & 0.002 & 0.001 & 0.063 & 0.025 & 0.01 & 0.05 \\ 60 & 44 & 52 & 48 & 56 & 38 & 30 & 34 & 25 \end{bmatrix}$$

$$\mathbf{C} = \begin{bmatrix} 15 & 24 & 40 & 70 & 100 & 25 & 45 & 68 & 50 \\ 15 & 6 & 4 & 3 & 2 & 12 & 6 & 2.5 & 7 \\ 6 & 1.5 & 2.5 & 2 & 3 & 1.2 & 0.8 & 0.9 & 0.5 \end{bmatrix}$$

Figure 4.7B:

$$\mathbf{M} = \begin{bmatrix} 0.008 & 0.032 & 0.13 & 0.45 & 1.3 & 0.16 & 0.32 & 0.63 & 0.5 \\ 0.2 & 0.041 & 0.008 & 0.002 & 0.001 & 0.063 & 0.025 & 0.01 & 0.05 \\ 60 & 44 & 52 & 48 & 56 & 34 & 30 & 38 & 25 \end{bmatrix}$$

$$\mathbf{C} = \begin{bmatrix} 15 & 24 & 40 & 70 & 100 & 25 & 45 & 68 & 50 \\ 15 & 6 & 4 & 3 & 2 & 12 & 6 & 2.5 & 7 \\ 0.5 & 1.2 & 1.5 & 0.9 & 0.8 & 2.5 & 3 & 2 & 6 \end{bmatrix}$$

These parameter sets can be used to calculate important species traits, such as their competitive abilities for nutrients and light. These traits are illustrated in Figure C4.1.

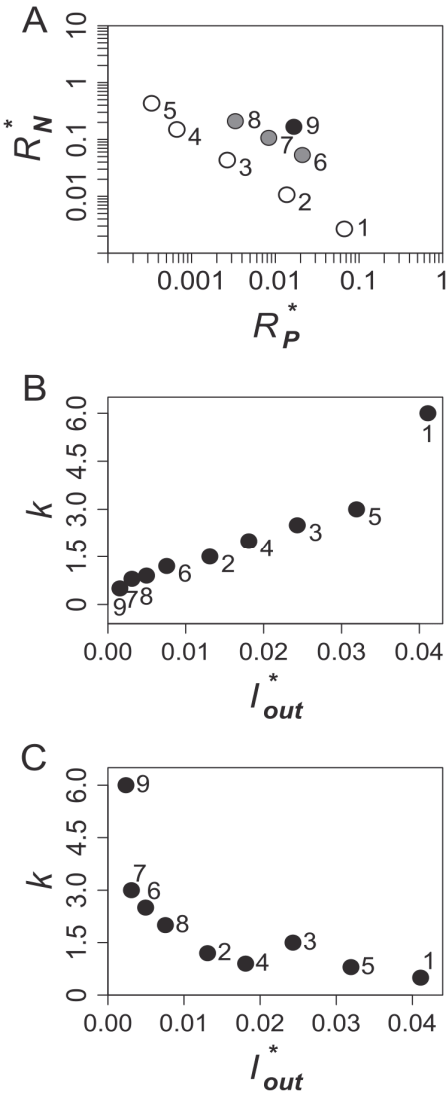

Figure C4.1: Species traits used in the multispecies competition model (see Fig. 4.7 in the main text). The nine species are indicated by different numbers. (A), Three-way trade-off between competitive ability for nitrogen, phosphorus and light. Open, gray and black circles indicate weak, intermediate, and strong competitors for light, respectively. Hence, species 1-5 are superior competitors for nutrients but inferior competitors for light, with species 1 the superior competitor for nitrogen (lowest R_N^* for nitrogen) and species 5 the superior competitor for phosphorus (lowest R_P^* for phosphorus). Species 6-8 are intermediate competitors for nutrients and light. Species 9 is the superior competitor for light but an inferior competitor for both nutrients. B and C illustrate two alternative scenarios. (B), Strong competitors for light (species with low Iout*) have low light attenuation coefficients (k); this assumption is used in Figure 4.7A. (C), Strong competitors for light have high light attenuation coefficients; this assumption is used in Figure 4.7B. Parameter values are given in Appendix C.

Chapter 5

Does universal temperature dependence apply to communities? - An experimental test using natural marine plankton assemblages

Verena S. Brauer, Victor N. de Jonge, Anita G. J. Buma, Franz J. Weissing

Oikos 118, 1102-1108, 2009

ABSTRACT

The metabolic theory of ecology (MTE) is an intriguing but controversial theory that tries to explain ecological patterns at all scales on the basis of first principles. Temperature plays a pivotal role in this theory. According to MTE, the Arrhenius relationship that describes the effect of temperature on biochemical reactions extends to a 'universal temperature dependence' that encompasses all kinds of processes and scales up to the cellular, the organismal, and the community level. In this study we test the prediction that community growth rate is temperature dependent in an Arrhenius-like way. First, we performed a literature review of the scanty data on the temperature dependence of the rates of metabolism, photosynthesis and growth of communities. In contrast to the predictions of MTE, the community activation energies did not cluster around 0.32 eV, the activation energy of photosynthesis and primary production or around 0.65 eV, the activation energy of metabolism. However, in none of the published studies the conditions were sufficiently controlled to allow firm conclusions. We therefore also performed replicated and controlled experiments using natural assemblages of marine plankton. As predicted by MTE, the maximal growth rates of community biomass increased linearly in an Arrhenius plot, with a slope close to 0.32 eV. However, a diversity of other models for the temperature dependence of community growth rates fit our data equally well. Hence, our results are at best a weak confirmation of MTE.

INTRODUCTION

Virtually all aspects of life are influenced by temperature. Based on the laws of thermodynamics, we have a fairly good understanding of how the reaction rates of enzymes are affected by temperature. In contrast, it is still largely debated how temperature influences vital rates at higher levels of organization, such as the growth rates of individuals, populations or communities. The authors of the metabolic theory of ecology (MTE) claim that the thermodynamical principles governing simple biochemical reactions can be extrapolated in a straightforward manner to individual metabolism, and from there to all kinds of biological rates at all levels of organisation (Gillooly *et al.*, 2001; Brown *et al.*, 2005). Accordingly, MTE makes the strong prediction that the temperature dependence of virtually any biological rate r can be described by an Arrhenius relationship of the form:

$$r(T) = r_0 \cdot e^{-\frac{E}{k \cdot T}}. \qquad (5.1)$$

Here T is temperature in Kelvin, r_0 is a normalization constant, k=8.618*10^{-5} eV K^{-1} is Boltzmann's constant, and E is the so-called activation energy in electron volts (Gillooly *et al.*, 2001; Brown *et al.*, 2004). Equivalently, MTE predicts that in an Arrhenius-plot, where the natural logarithm of r is plotted against the inverse of temperature $1/kT$, a linear relationship results with slope $-E$ and intercept $\ln(r_0)$:

$$\ln(r(T)) = \ln(r_0) - E \cdot (1/kT). \qquad (5.2)$$

In addition, MTE makes the more specific prediction that the 'activation energy' E of metabolism is generally close to 0.65 eV (Gillooly *et al.*, 2001). However, it has been argued that activation energies corresponding to photosynthesis and primary production should be lower and close to 0.32 eV (Allen *et al.*, 2005, López-Urrutia *et al.*, 2006).

MTE is an intriguing theory, for at least two reasons. First, proponents of the theory argue that it can be used to explain all kinds of thermal trends, including the temperature dependence of resource consumption (Enquist *et al.*, 2003), the maximum per capita growth rate (Savage *et al.*, 2004), the rates of predation and parasitism (Brown *et al.*, 2004), the rate of biomass turnover and energy flux of ecosystems (Enquist *et al.*, 2003), and even global carbon flux (Allen *et al.*, 2005). Second, the theory makes quantitative a priori predictions that can be tested both in the lab and in the field.

Not surprisingly, an all-encompassing theory like MTE has attracted a lot of criticism, both concerning its theoretical foundation and its empirical support. On the theoretical side, it is not at all clear whether, and to what extent, the thermal properties of single biochemical reactions are reflected in the temperature dependence of individual metabolism (Precht *et al.*, 1973; Clarke, 2004; Clarke and Fraser, 2004). Even if individual metabolism were related to temperature in an Arrhenius-like fashion, the extrapolation to higher levels of organization is far from straightforward (Cottingham and Zens, 2004; Marquet *et al.*, 2004; O'Connor *et al.,* 2007), since additional factors like resource limitation or temperature acclimation are undoubtedly of major importance for the temperature response of an organism (Rhee and Gotham, 1981; Vasseur and McCann, 2005; Clarke, 2006; López-Urrutia and Morán, 2007; Terblanche *et al.*, 2007). On the empirical side, it is important to realize that so far virtually all evidence is either based on field studies or on data compiled from the literature. The mechanisms supposedly underlying the thermal properties of biological rates have thus far not been exposed to thorough experimental testing (Brown *et al.*, 2004; Cottingham and Zens, 2004; Cyr and Walker, 2004; Marquet *et al.*, 2004; Van der Meer, 2006). Still, the Arrhenius relationship seems to provide a good phenomenological description, at least at the individual and the population level. This holds, for example, for the temperature dependence of individual metabolism (e.g. Gillooly *et al.*, 2001; Brown *et al.*, 2004) and population growth rates (Savage *et al.*, 2004). It has not yet been investigated whether this is also the case at the community level. We therefore screened the literature for empirical studies and meta-analyses on the effect of temperature on community rates of metabolism, growth, and photosynthesis. In addition, we performed replicated and temperature-controlled experiments on natural assemblages of marine plankton. In both cases the aim was to test whether 1) the temperature dependence of community growth rate is indeed described by an Arrhenius relationship, and 2) whether the corresponding activation energy is close to the predicted values of either 0.32 or 0.65 eV.

LITERATURE DATA

We systematically searched the literature for quantitative studies on the dependence of community metabolism, photosynthesis and/or growth rate on temperature. We focused on studies that either reported the results in terms of activation energies (e.g., in terms of an Arrhenius relationship) or in terms of Q_{10}-values (e.g., Raven and Geider, 1988), since the latter can be translated into activation energies (e.g., Vasseur and McCann, 2005). Surprisingly, not a single controlled experiment could be found

where a community had been exposed to a series of previously defined temperatures (Tab. 5.1). All studies encountered refer to some kind of a field experiment where measurements were done either directly in the field or by taking natural samples and simulating the natural conditions. A few of these studies actively controlled for either thermal acclimation or limitation by a certain resource, but most studies did apparently not consider these and other potentially confounding factors. To standardize the results we transformed all reported values for temperature dependence into activation energies in electron volts (eV). In cases where the activation energy was directly estimated in a given study, the corresponding R^2-value (when available) gives an indication of the goodness-of-fit with the Arrhenius relationship. In cases where Q_{10}-values were reported, the R^2-values are given in brackets in Table 5.1, since the goodness-of-fit refers to an exponential relationship with temperature rather than an Arrhenius relationship. From Table 5.1 we conclude that based on published studies little can be said about whether and to what extent the natural logarithm of community rates is linearly related to the inverse of temperature. The studies in Table 5.1 do certainly not support the more specific prediction that activation energies should cluster around either 0.32 eV or 0.65 eV. However, it is questionable whether far-reaching conclusions on the applicability of MTE to the community level can be drawn from such a compilation of data. As indicated above, none of the studies refers to controlled experiments that were specifically set up to test the thermal predictions of MTE. We therefore performed such a controlled and replicated study ourselves.

Table 1: Compilation of literature date on the temperature dependence of rates of metabolism, photosynthesis and/or growth of planktonic, soil microbial, or forest communities. Temperature dependence is quantified by activation energy E in electron volts (eV), which according to MTE is predicted to be close to 0.65 eV for metabolism and close to 0.32 eV for photosynthesis and primary production. Original estimates in terms of Q_{10}-values were translated into activation energies. All studies either present field or *in situ* measurements or a meta-analysis of field data. If not stated differently in column six, the systems studied were probably affected by long-term acclimation to ambient temperature and by some sort of resource limitation. R^2-values in brackets refer to goodness-of-fit to an exponential model, i.e., to a model differing from an Arrhenius relationship.
([a] Q_{10}--values were converted to activation energies by $E(\text{eV})=0.1*(kT^2)*\ln(Q_{10}\text{-})$, where T_0 is the median temperature (in K) of the temperature range from which Q_{10}-was calculated (e.g., Vasseur and McCann, 2005); [b] activation energies converted from kJ/mol by $E(\text{eV})=1.037*10^{-2}\ E$ (kJ/mol); [c] activation energies converted by multiplying original estimates (corresponding to E/k) with Boltzmann's constant; [d] no long-term acclimation but medium-term acclimation during 60 and 110 days).

Rate	Community	E(eV)	Q_{10}	R^2	Control for acclimation/ resource limitation	Reference
Metabolism	soil bacteria	0.31		0.99	acclimation	Pietikäinen (2005)
		0.65	2.42	(0.83)		Yan *et al.* (2006)
		0.64	2.39	(0.88)		
		0.60	2.28	(0.83)		
		[a] 0.23	1.35	-	[d] acclimation	Niklinska and Klimek (2007)
		[a] 0.53	2.22	-		
		[a] 0.77	2.93	-		
		[b] 0.93		0.82		Gaumont-Guay *et al.* (2006)
		[a] 0.41	1.8	(0.7)	[d] acclimation	Yuste *et al.* (2007)
		[a] 0.77	3.1	(0.8)	water limitation	
	Marine bacterioplankton	0.75		0.66		Apple *et al.* (2006)
		[b] 0.52		-	acclimation	Hancke (2004)
		[b] 0.35		-		
		[b] 0.58		-		

		0.59	0.20		López-Urrutia and Morán (2007)
	Marine autotrophic plankton	0.33	0.97		López-Urrutia *et al.* (2006)
	Marine heterotrophic plankton	0.56	0.85		López-Urrutia *et al.* (2006)
	Freshwater phytoplankton	0.06	0.53		De Castro and Gaedke (2008)
	Freshwater zooplankton	0.32	0.82		De Castro and Gaedke (2008)
	Different microbial communities	[b] 1.14	-		Price (2004)
	Forests	[c] 0.61	0.48		Enquist *et al.* (2003)
		[c] 1.02	0.61		
		[c] 0.62	0.32		
		[c] 0.75	0.23		
		[c] 0.67	0.43		
		[c] 0.68	0.23		
Photosynthesis	Microphytobenthos	[b] 0.24	-	acclimation	Hancke (2004)
		[b] 0.52	-	light limitation	
		[b] 0.32	-		
Growth	Marine bacterioplankton	[a] 0.42	1.9	-	Kirchman *et al.* (2005)
		[a] 0.74	3.1	-	

CONTROLLED EXPERIMENTS: MATERIAL AND METHODS

Experimental setup

The idea underlying the experimental study was to let natural marine phytoplankton-dominated communities grow for a certain time period to quantify the temperature dependence of the maximum community growth rate. Factors like thermal acclimation and light limitation should be prevented as far as possible.

A large sample of surface water was taken on February 15th 2006 from the Dutch Wadden Sea (53° 33.547 N, 6° 39.671 E; water temperature 2.1 °C) and immediately portioned out to smaller bottles yielding 15 one-litre subsamples. In the lab the 15 communities were randomly assigned to five subsets with three replicates each. Each subset was brought to the experimental temperatures of 6, 9, 12, 16, or 20 °C overnight. During the warming phase the communities were stored in darkness.

Subsequently we kept them under constant temperature and continuous light (approximately 200 µmol photons m^{-2} s^{-1}) for eight days. Before the start of the experiment, at the beginning of the warming phase, we added nutrients and vitamins in high amounts to yield concentrations of f2-sea water (for details see Andersen, 2005). This was done to ensure resource saturation and to create conditions for exponential growth. Once a day we diluted the communities with 230 mL fresh f2-medium. This semi-continuous dilution started at day two for the higher temperatures and at day three for the 6 and 9 °C-treatment. The daily removed volume was used for subsequent biomass and nutrient analyses. In total the sampling procedure of the 15 cultures, i.e. the 15 nutrient enriched communities, resulted in six 6-days biomass time series for the lower temperatures, 6 and 9 °C, and in nine 7-days biomass time series for the higher temperatures.

Sample analysis

In order to determine biomass we measured the amounts of organic carbon (C_{org}), organic nitrogen (N_{org}) and chlorophyll-a (chl-a). For the analysis of C_{org} and N_{org} samples we used 100 mL of culture concentrated on GF/F filters (Whatman®). C_{org} and N_{org} were measured with the help of the CN-element analyser (Flash 1112 EA Element Analyser, National Institute for Coastal and Marine Management/ RIKZ Middelburg). To determine chl-a concentrations 100 mL of culture were concentrated on a GF/F filter. The filter was then put into 4 mL of 90 % acetone. After an

extraction time of 48 hours we determined the concentration of chl-a with a fluorometer at excitation- and emission wavelength of 436 and 668 nm. Fluorescence readings occurred before ("R_b") and 10 min after ("R_a") sample acidification with 150 µL of 10 % HCl. We calculated chl-a in µg/L as $chl-a = \frac{R_b - R_a}{0.77} \cdot \frac{V_e}{V_f} \cdot 3.74$ (V_e is extraction volume, V_f is filtered volume). Multiplication factors stem from spectrophotometric calibration using a chl-a standard (Lorenzen, 1967).

Estimation of maximum growth rates

For any given temperature, T, we assume that the community was growing exponentially at a rate $r = r(T)$. Let B_t denote the biomass at day t before a fraction D of the culture was removed and replaced by fresh medium. Then the biomass at the following day is given by $B_{t+1} = (1-D)*B_t*e^r$. In our case $1-D = 0.77 \approx e^{-0.26}$. As a consequence biomass growth was assumed to be governed by $B(t) = B_0*e^{(r-0.26)*t}$ or, on a logarithmic scale $\ln(B(t)) = \ln(B_0)+(r-0.26)*t$. Hence, r could be estimated by linear regression of $\ln(B(t))$ against time and adding 0.26 to the regression coefficient.

In the experiment the replicate communities developed in a highly consistent way throughout the growth period at all temperatures, showing remarkably little variation even towards the end. For each measurement we therefore pooled the three replicates by taking their average. These averages form the basis for all further calculations. Subsequently, we estimated community growth rate r by means of linear regression of the ln-transformed biomass data as described above. The activation energy of community growth rate, E, was calculated as the slope of the linear regression of $\ln(r)$ against the inverse of temperature $1/kT$.

Throughout, R^2-values are used for judging the goodness-of-fit between our data and various models. These were calculated from the residual sum of squares obtained from non-linear curve fitting on non-transformed data using Newton's method. All statistics were done using R 2.5.0.

CONTROLLED EXPERIMENTS: RESULTS

Biomass dynamics

The natural logarithms of the absolute amounts of C_{org}, N_{org} and chl-a increased linearly over time, indicating that the communities were indeed growing exponentially

(Fig. 5.1). A preliminary comparison of the biomass dynamics between temperatures also indicates that the rate of increase was positively related to temperature. Interestingly, the C_{org} and N_{org} data provide parallel lines while the slope of the chl-a data is steeper. Note that at 16 °C and 20 °C the logarithms of the three measured variables do not seem to increase linearly over the whole time-period, indicating some growth-limiting effects at these temperatures.

Temperature-dependence of community growth rate

As predicted by MTE, the community growth rates show a roughly linear relationship when plotted against the inverse of temperature, indicating an Arrhenius-like relationship (Fig. 5.2). Since the samples contained not only phytoplankton but also zooplankton and bacteria, we consider the estimation of r based on the C_{org} data as the most relevant indicator of community biomass, although phytoplankton was the most dominant fraction. Nevertheless, we also present estimations of r based on N_{org} and chl-a, since these quantities are often used as proxies for biomass. For C_{org}, the community activation energy (which corresponds to the slope of the regression line in the Arrhenius plot) equals 0.33 eV (95 % confidence interval: (0.22 eV, 0.44 eV), $p < 0.005$, $R^2 = 0.93$). This estimation of E is remarkably close to the predicted value of 0.32 eV for photosynthesis and primary production (Allen *et al.*, 2005). N_{org} data exhibited an activation energy of 0.27 eV (95 % confidence interval: (0.01 eV, 0.53 eV), $p < 0.05$, $R^2 = 0.93$), which is quite similar. In contrast to this, community growth based on chl-a data seems to be temperature independent (E= 0.001 eV, 95 % confidence interval: (-0.27 eV, 0.26 eV), $R^2 < 0.001$).

Alternative temperature relationships

Obtaining a good fit between data and a model does not necessarily mean that the model is correct, since alternative models might fit the data as well. To check this, we fitted our data not only to the Arrhenius-relationship but also to three other temperature models that are frequently used (Ahlgren, 1987). The models and their

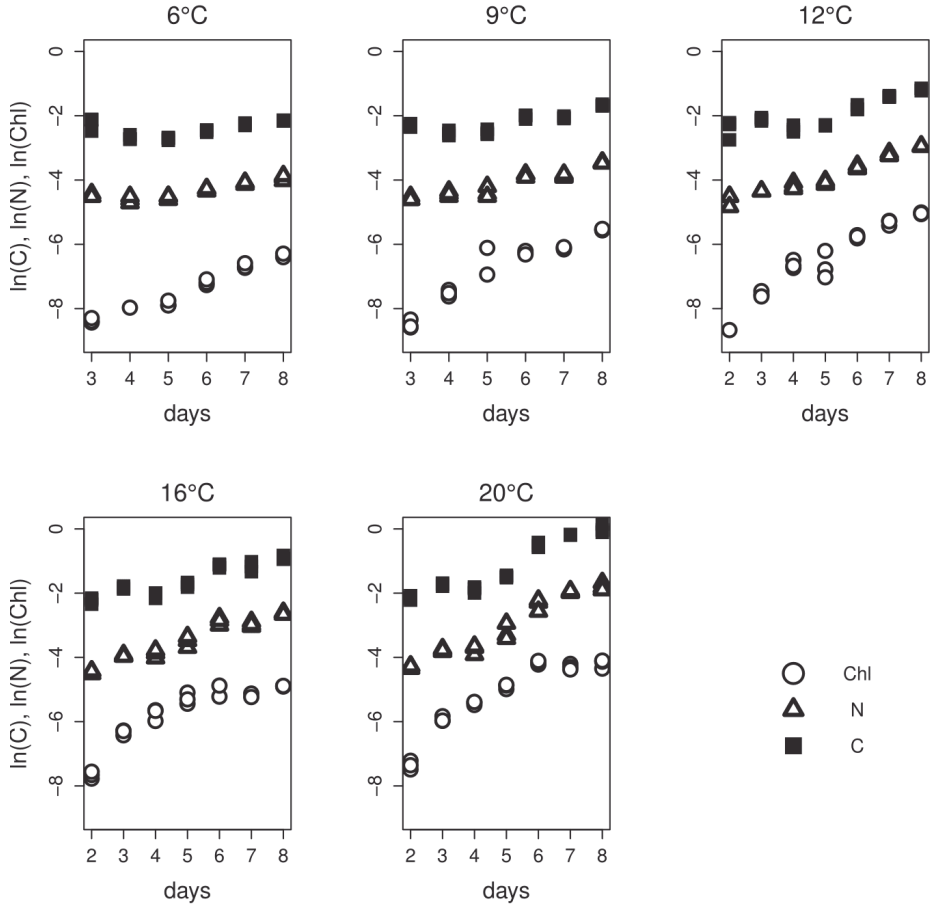

Figure 5.1: Log-linear plots of the time-series of biomass ("C_{org}", squares), organic nitrogen ("N_{org}", triangles) and chlorophyll-a ("chl-a", circles) [mg] of natural plankton communities grown at 6, 9, 12, 16, and 20 °C in the lab. Plankton samples were taken from the field in February 2006 one day before the start of the experiment and grew for a week in semi-continuous cultures. Nutrient concentrations and irradiance were non-limiting in order to achieve maximum growth conditions.

R^2–values are listed in Table 5.2. The linear relationship serves as a null model, the Arrhenius-relationship and the Berthelot-relationship reflect different biochemical principles, and the Belehradek-relationship is derived from physical considerations. Intriguingly, all four models fit the temperature relationship equally well for all the three measurements C_{org}, N_{org} and chl-a. In other words, the Arrhenius relationship does not provide a better description of our data than the other three models.

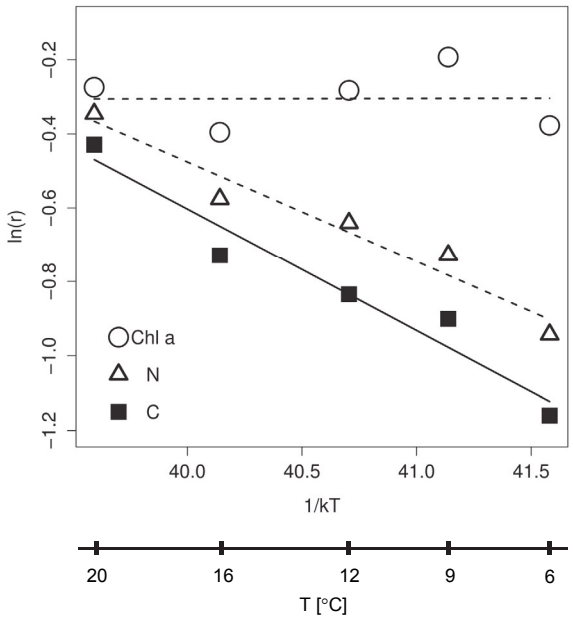

Figure 5.2: Arrhenius-plots of community growth rate r [day^{-1}], where ln(r) is plotted against the inverse of temperature $1/kT$. r was estimated by the slope of the regression lines of the log-linear plots for C_{org} (squares), N_{org} (triangles), or chl-a (circles) in Figure 5.1. The temperature dependence of community growth rate, estimated on the basis of C_{org}, corresponds to a linear relationship in the Arrhenius-plot with activation energy 0.33 eV. N_{org} data show a similar trend, with a slightly lower activation energy of 0.27 eV. Chl-a data indicated higher absolute values of community growth rate, which appear to be temperature-independent (E = 0.001 eV).

DISCUSSION

There is consensus that in order to judge the validity of the predictions of the metabolic theory of ecology (MTE) controlled and replicated experiments are urgently needed (Brown *et al.*, 2004, Cottingham and Zens, 2004, Cyr and Walker, 2004, Marquet *et al.*, 2004, Van der Meer, 2006). Our study is a step in this direction. At first glance the results seem to confirm the prediction of MTE on temperature dependence: the growth rate of community biomass (C_{org}) does indeed show an Arrhenius-type relationship (as indicated by the straight line in the Arrhenius plot of Fig. 5.2), and the slope of this relationship closely reflects the activation energy of photosynthesis and primary production (i.e., 0.32 eV). A similar agreement with the thermal predictions of MTE was obtained when using intracellular nitrogen (N_{org}) as a proxy for biomass. In this sense our results support the view of MTE that the

Table 5.2: Comparison of the R^2-values for the fit of the experimental Corg, Norg, and chl-a data to four different models of temperature dependence (Ahlgren, 1987). Temperature T is measured in Kelvin. All models have two parameters a and b. Optimal fits were based on the non-transformed growth rate data and obtained by minimizing residual sum of squares resulting from non-linear curve fittings using Newton's method. The R^2-values for the growth rates of carbon and nitrogen are above 0.90 for all models, but close to zero for chl-a growth rates.

Model	R^2		
	C_{org}	N_{org}	chl-a
linear: $r(T) = a + b \cdot (T - 273)$	0.93	0.95	0.0005
Arrhenius: $r(T) = a \cdot e^{-b(1/kT)}$	0.95	0.95	0.0004
Belehradek: $r(T) = a \cdot (T - 273)^b$	0.91	0.94	0.001
Berthelot: $r(T) = a \cdot b^{T-273}$	0.95	0.95	0.0005

behaviour of complex systems can to a remarkable degree be explained on the basis of quite simple fundamental principles. In contrast to C_{org} and N_{org}, our chl-a data did not exhibit temperature dependence. One might have expected that just these data, which represent the autotrophic part of the community only, should have a slope of about 0.32 eV in the Arrhenius plot, whereas the overall community should have a slope between 0.32 eV and 0.65 eV, However, chl-a is generally considered a less reliable measure of biomass, since intracellular chl-a concentrations are often not constant (de Jonge, 1980). It is conceivable that the more rapid growth of phytoplankton at higher temperatures is associated with a decrease in intracellular chl-a levels. Alternatively, higher temperatures might induce a shift in community composition (from autotrophs to heterotrophs). Both factors might mask the increase in community growth rate with temperature that is predicted by MTE.

We are aware of the fact that our study will not be the final word on the applicability of MTE to whole communities. In fact, our study exemplifies some of the limitations encountered when testing the seemingly straightforward thermal prediction. For instance it turned out to be very difficult to obtain a reliable estimate of maximum growth rates. Apparently, growth at maximal rate only occurred during a rather short initial period. At a later stage, community growth was apparently already limited. Moreover, the size distribution of individuals might have changed during our experiments in a temperature- dependent way. MTE predicts that metabolic rate (and other biological rates) does not only depend on temperature but also on body mass, implying that a reliable estimate of activation energy E requires a correction for

changes in body mass (Gillooly *et al.*, 2001). For natural communities like ours such a correction seems a forbidding task, since one would have to consider size changes in many different organisms, ranging from bacteria to zooplankton (Enquist *et al.*, 2003, de Castro and Gaedke, 2008). At best, one might hope to arrive at better estimates of *E* by simple rules of thumb, such as the empirical finding of Atkinson *et al.* (2003) that each additional °C rise in temperature leads to a size reduction in protists by about 2.5 %. Applying this rule of thumb to our data would raise the community activation energies to 0.49 eV for C_{org}, 0.43 eV for N_{org}, and 0.16 eV for chl-a.

Our results illustrate that a linear relationship of a biological rate with temperature in an Arrhenius plot is by far not sufficient as a 'proof' that the Arrhenius relationship can be upscaled from simple biochemical reactions to higher levels of organisation. There are many reasons why biological rates should increase with temperature, each leading to a different model for temperature dependence. As our study shows (see Tab. 5.2), the same set of data can be fitted equally well to a variety of quite different models, some of which also having a plausible mechanistic underpinning. Hence, focussing on just a single model may give rise to misleading conclusions, since the observed trends might be even better 'explained' by an alternative model.

There are at least two possibilities to discriminate between the different models for temperature dependence. An obvious approach would be to aim for more data with a better resolution. Yet, we doubt that an extension of this study would really help to distinguish between the alternatives. In our opinion, controlled experiments targeted at unravelling the mechanism behind temperature dependence and the upscaling from lower to higher levels are required to really challenge the metabolic theory of ecology.

Acknowledgments

We thank J.J. van Beusekom at AWI-Sylt and J. Roggeveld for carrying out part of the nutrient analysis and Rijkswaterstaat, National Institute for Coastal and Marine Management/ RIKZ Middelburg for the analysis of organic carbon and organic nitrogen. We also thank and two anonymous referees for comments on the manuscript. VNdeJ acknowledges Rijkswaterstaat/ WD for its continuous financial support. VSB acknowledges T.W. Berngruber for discussions and comments on the manuscript. VSB was supported by an Ubbo-Emmius scholarship by the University of Groningen.

Chapter 6

Synthesis

The aim of this thesis is to better understand how temperature, nutrients and light control patterns and processes in microbial plankton communities. In this chapter I will first zoom in on the physiological mechanisms that dictate the strong temperature-dependency of unicellular N_2-fixing cyanobacteria, and whether these mechanisms may also apply to other diazotrophic cyanobacteria in the marine pelagic ecosystem. Subsequently, I will focus on the more general question of how the temperature sensitivity of community processes and species composition depends on the degree of nutrient and light limitation. Finally, I will propose ideas how the predictions of the nutrient-load hypothesis can be tested and applied to understand the dynamics and species composition of phytoplankton communities.

Is the distribution of marine N_2-fixing cyanobacteria related to temperature?

Unicellular N_2-fixing cyanobacteria photosynthesize during the day, and respire the obtained carbohydrates to drawdown oxygen and fuel N_2 fixation during the night. Chapter 2 demonstrates that, in the unicellular cyanobacterium *Cyanothece*, temperatures below 21 °C strongly increase the amount of oxygen that needs to be respired in order to fix one molecule of N_2. Basically, the reason is that the N_2-fixation rate decreases with temperature, while the cells still need to create an oxygen-free environment to enable functionality of the nitrogenase enzyme. Moreover, below 21 °C the onset of nitrogenase activity is strongly delayed to the end of the night, probably because at low temperature the time for the *de novo* synthesis of nitrogenase is increased. These physiological mechanisms explain why *Cyanothece* only grows well in warm habitats, and they may also offer a plausible explanation for why other unicellular N_2-fixing cyanobacteria (of groups B and C) are restricted to the (sub)tropics (Stal, 2009). However, do the physiological mechanisms underlying the temperature-sensitivity of *Cyanothece* also act in diazotrophic cyanobacteria that have different N_2-fixation strategies?

Among the most important marine N_2-fixing cyanobacteria are the filamentous, non-heterocystous *Trichodesmium* spp., which perform simultaneous oxygenic photosynthesis and N_2 fixation during the day. All cells of a trichome seem to be able to perform both oxygenic photosynthesis and N_2 fixation. Yet, nitrogenase is located only in a subset of cells in the trichome, in which the activity of the oxygen-evolving complex PSII is down regulated (Berman-Frank *et al.*, 2001). Oxygen diffusing into the cell is consumed by respiration and by light-enhanced oxygen-scavenging

mechanisms such as the Mehler-reaction of PSI (Bergman *et al.*, 1993; Milligan *et al.*, 2007). If respiration is important for the protection of nitrogenase against oxygen inactivation in this organism, low temperature (probably below 21 °C, see e.g. Capone *et al.*, 1997) might increase the respiratory cost of nitrogen fixation, similar to our observations for *Cyanothece*. Moreover, nitrogenase in *Trichodesmium* is inactivated during the night and has to be synthesized *de novo* every day (Capone *et al.*, 1990). Nitrogenase gene expression in *Trichodesmium* is controlled by a circadian clock (Chen *et al.*, 1998). The circadian clock is temperature-compensated, which means that nitrogenase synthesis should be initiated at the same time during the day irrespective of temperature. Low temperature might slow down the synthesis of nitrogenase and thereby delay the onset of N_2 fixation until late in the day, leaving little daytime to fix sufficient nitrogen. Hence, it is expected that, similar to our findings for *Cyanothece*, low temperature increases the respiratory cost and delays the timing of nitrogen fixation in *Trichodesmium* as well.

Although the unicellular diazotrophic cyanobacteria of group A (UCYN-A) have only been discovered about a decade ago, there is increasing evidence that these organisms are responsible for a substantial part of oceanic N_2 fixation (Zehr *et al.*, 2001; Zehr, 2011). UCYN-A fix N_2 during the day. These organisms lack the genes for the oxygen-evolving PSII and live as photoheterotrophic symbionts with a prymnesiophyte (Thompson *et al.*, 2012). In order to fix N_2, oxygen diffusing into the cell must be scavenged by respiration or by other oxygen-scavenging mechanisms. If respiration is important for nitrogenase protection in UCYN-A, low temperature is expected to increase the respiratory cost of N_2 fixation as is the case in *Cyanothece*. Because little is known about the regulation of nitrogenase in UCYN-A it is unclear whether temperature also delays the timing of N_2 fixation in these organisms. There are currently no cultured representatives of UCYN-A, and therefore a detailed investigation of the effect of temperature on its physiology is not yet possible. However, field observations indicate that UCYN-A differ from other marine diazotrophic cyanobacteria because they are active at temperatures below 20 °C (Needoba *et al.*, 2007; Langlois *et al.*, 2008).

Filamentous heterocystous symbionts of microalgae (mostly diatoms) form another important group of marine N_2-fixing cyanobacteria. Although these organisms have mainly been found in warm habitats (e.g. Foster *et al.*, 2007; Fong *et al.*, 2008), it is not clear whether they might be affected by temperature in the same way as free-living non-heterocystous diazotrophs. Filamentous heterocystous cyanobacteria protect nitrogenase from oxygen by confining N_2 fixation to differentiated cells, the

heterocysts. Heterocysts lack the oxygenic PS II and are surrounded by a thick glycolipid layer that serves as a gas-diffusion barrier. The limited diffusion of oxygen into the heterocyst, the absence of photosynthetic oxygen evolution, and respiration create a nearly anoxic environment within the heterocyst, in which nitrogenase can be active. Free-living heterocystous species adapt to a wide range of temperatures and occur in brackish and freshwater environments in all climate zones from the tropics to the polar regions. Nevertheless, the heterocystous symbionts of marine diatoms have only been found in the tropics.

Based on the above considerations, it is conceivable that temperature is indeed the key factor restricting free-living open ocean N_2-fixing cyanobacteria to warmer habitats. Although our findings need to be confirmed by experiments with a wider range of N_2-fixing cyanobacteria, Chapters 2 and 3 suggest that above approximately 18 °C free-living diazotrophic cyanobacteria in the marine pelagic increase in abundance with increasing temperature. This has recently been reported for the unicellular *Crocosphaera*, which thrives between 22 and 30 °C in the South Pacific Ocean (Moisander *et al*., 2010). The same study showed that the abundance of UCYN-A decreased with temperature between 24 and 30 °C (Moisander *et al*., 2010), providing additional evidence that these symbiotic diazotrophs are affected by temperature in a different way.

In nature, diazotrophic bacteria are embedded in complex communities that involve many species of phytoplankton, bacteria, grazers and viruses. The strong temperature response of diazotrophs might stimulate the pelagic food web in various ways, e.g. through the release of fixed carbon and nitrogen, by providing a larger food source for grazers, and as a larger host population for viruses (Fig. 1.1; see also LaRoche and Breitbarth, 2005; Mulholland, 2007). Chapter 3 suggests that higher temperature would indeed increase the abundance of chemotrophic bacteria to some extent, because they profit from higher amounts of nitrogen and organic carbon released by the diazotrophs. However, the data in Chapter 3 did not give evidence for strong facilitation of the chemotrophic bacteria by diazotrophs, although other studies have reported strong facilitation of the non-diazotrophic picocyanobacterium *Synechococcus* sp. by *Cyanothece* through the release of fixed N (Agawin *et al*., 2007). It remains an interesting open question to what extent grazing microzooplankton and viruses may profit from the strong temperature response of the diazotrophs. Furthermore, in natural waters a positive temperature response might not always be evident because other factors such as phosphorus and iron limitation, wind-induced mixing and water column stratification also affect the growth of N_2-fixing cyanobacteria and their

associated community (Capone *et al.*, 1997; Sañudo-Wilhelmy *et al.*, 2001; Karl *et al.*, 2002; Mills *et al.*, 2004). Nevertheless, many field studies report that temperature is a major factor explaining the abundance of diazotrophic cyanobacteria and *nifH*-gene sequences and the amount of N_2 fixation in the ocean (Lugomela *et al.*, 2002; Mazard *et al.*, 2004; Langlois *et al.*, 2005; Staal *et al.*, 2007; Langlois *et al.*, 2008).

Does the metabolic theory of ecology explain the temperature response of microbial plankton communities?

A major open question in microbial community ecology is whether there are general trends in the way communities respond to changes in temperature (Daufresne *et al.*, 2009). The metabolic theory of ecology (MTE) predicts that species and community processes, when corrected for the effect of individual size, increase with increasing temperature according to the Arrhenius equation (Gillooly *et al.*, 2001; Brown *et al.*, 2004). Depending on whether these processes are driven by autotrophic or by heterotrophic metabolism they should exhibit an activation energy of approximately 0.32 eV or 0.65 eV, respectively (Gillooly *et al.*, 2001; Allen *et al.*, 2005). It was shown in chapter 5 that the effect of temperature on the maximum specific growth rate of natural plankton communities was well described by the Arrhenius-equation with an activation energy of 0.33 eV, although there was no data to correct for the effect of cell size on growth rate. As these communities were supplied with ample light, inorganic N and P but not with organic carbon, they were dominated by photoautotrophs. These data thus fit the MTE-predictions well.

In chapter 2 the maximum specific growth rate of *Cyanothece* in the temperature range from 18 to 30 °C was fitted to the Arrhenius-function and exhibited an activation energy of 0.81 eV for diazotrophic growth and 0.90 eV for non-diazotrophic growth on nitrate. Hence, the activation energy of *Cyanothece* was much higher than the value of 0.32 eV predicted by MTE, illustrating once more that unicellular N_2-fixing cyanobacteria show an exceptionally strong temperature response. These data therefore demonstrate that the predictions of MTE do not apply to all planktonic organisms, especially if the details of their physiology evade the underlying mechanisms assumed by MTE.

Maximum specific growth rates are measured under idealized conditions, with an ample nutrient supply and optimal light conditions. Yet, low nutrient concentrations or light intensities can limit the specific growth rate of an organism and suppress its response to temperature. Rhee and Gotham (1981) demonstrated that at lower

temperatures the specific growth rates of phytoplankton species were controlled by temperature, whereas at higher temperatures they were controlled by nutrient limitation and were therefore temperature-independent. The temperature at which organisms switched from temperature-controlled to nutrient-controlled growth decreased with the degree of nutrient limitation (Rhee and Gotham, 1981). Comparable results are shown in Figure 6.1, which demonstrates the effect of temperature on the specific growth rate of *Cyanothece* at different light intensities, based on our data from Chapter 2. When grown on nitrate and at low light intensities (5.5 and 17.1 µmol photons m^{-2} s^{-1}) the specific growth rate of *Cyanothece* increased only in the range from 14 to 18 °C, and then remained at a constant low level until at least 30 °C. Beyond 30 °C the growth rates at the low light intensities even decreased again (Fig. 6.1A). At an intermediate light intensity (40 µmol photons m^{-2} s^{-1}) the switch from temperature-controlled to light-controlled growth occurred at approximately 30 °C. At a high light intensity (110 µmol photons m^{-2} s^{-1}) the specific growth rate was temperature-controlled almost throughout the entire experimental temperature range and thus increased from 14 up to 34 °C. Qualitatively similar results were observed when *Cyanothece* was grown on N_2 (Fig. 6.1B), although at high temperatures and light intensities the specific growth rate of *Cyanothece* did not increase any further because it was limited by the N_2 fixation rate.

Thus, in resource-limited environments, i.e. in oligotrophic systems or at low light intensities, biological rates are more likely to be temperature independent than in nutrient-rich systems and at high light intensities. In natural ecosystems, limitation of microbial processes by nutrients or light is widespread (Huisman *et al.*, 2004; Elser *et al.*, 2007). As a consequence, especially in oligotrophic environments many microbial processes show only a weak or no relationship with temperature (Lopéz-Urrutia and Morán, 2007; O'Connor *et al.*, 2009; Degerman *et al.*, 2013; Serna-Chavez *et al.*, 2013; Marañón *et al.*, 2014). In eutrophic ecosystems, however, microorganisms may show a strong response to rising temperature (Jöhnk *et al.*, 2008; Paerl and Huisman, 2009).

Chapter 3 investigated the relative importance of temperature and resource effects on the composition of a microbial plankton community consisting of the N_2-fixing cyanobacterium *Cyanothece* and several associated chemotrophic bacteria. The species composition of the chemotrophic bacteria was mainly determined by the availability of nitrate and dissolved organic carbon and little by temperature. This indicated a stronger role of resource control than of temperature control for the bacterial

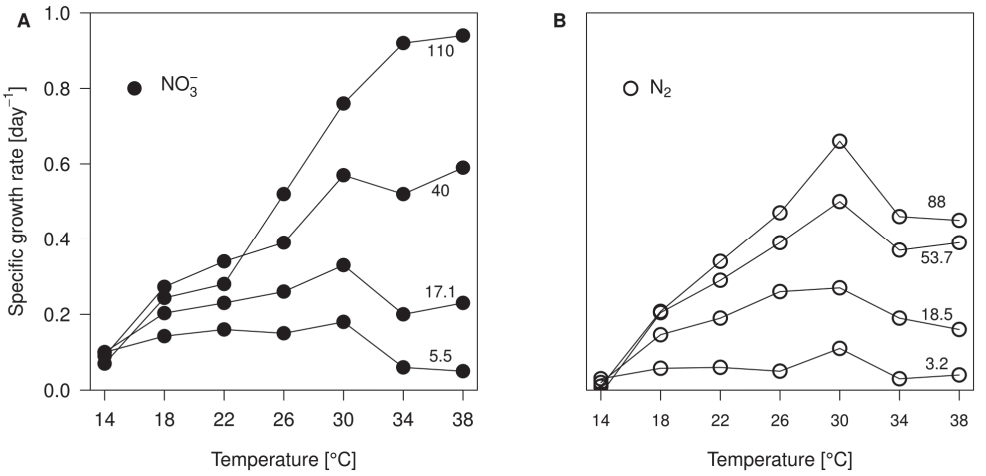

Figure 6.1: Effect of temperature on the specific growth rate of *Cyanothece* at different light intensities. A) Cultures grown on nitrate. B) N_2-fixing cultures. Numbers indicate light intensities in µmol photons m^{-2} s^{-1}. Growth rates are based on cell counts; data are from the experiments reported in Chapter 2.

community composition. However, temperature increased the abundance of the N_2-fixing cyanobacterium *Cyanothece* relative to the bulk of chemotrophic bacteria, consistent with the strong temperature response of its N_2 fixation activity (Chapter 2). This indicated that temperature control dominated over resource control in the N_2-fixing cyanobacterium *Cyanothece*. The dynamics and structure of the entire community was therefore determined by both resources and temperature.

In conclusion, these results suggest that in natural waters, where nutrient and light limitation is common, the composition of microbial plankton communities cannot be solely inferred from the fundamental temperature dependence of biological processes as advocated by the MTE, but that it is likely to be the result of the interplay between temperature and resource control. Moreover, the results also show that the relative importance of temperature versus resource control may vary strongly among different species.

Tests and applications of the nutrient-load hypothesis

In the previous paragraph I described that temperature is likely to control phytoplankton growth at low temperature, whereas at high temperatures other factors

are more likely to become growth limiting, such as nutrients and light. To predict how nutrient and light limitation control the assembly of autotrophic microbial communities along an enrichment gradient, Chapter 4 proposes the nutrient-load hypothesis. This hypothesis predicts that in nutrient-poor waters, the ratio at which nutrients are supplied determines the composition of autotrophic communities as a result of differences in elemental stoichiometry of the species (Tilman, 1985; Hillebrand *et al.*, 2014). In nutrient-rich waters, however, absolute nutrient concentrations are decisive because high biomass concentrations induce light limitation. Furthermore, the nutrient-load hypothesis predicts highest phytoplankton diversity at intermediate nutrient loads. An important future step would be to test these predictions in an experimental set-up, for instance by growing phytoplankton in flat-panel chemostats that allow a constant supply of nutrients and light. The main difficulty of this experiment is to select at least two suitable species that differ in their competitive abilities for two easy to handle nutrients such as nitrate and phosphate. According to the nutrient-load hypothesis the nutrient supply ratio should determine the outcome of competition at low nutrient load but the supply ratio should have no effect at high nutrient load, because the outcome will be determined by competition for light.

The nutrient-load hypothesis could also be tested in applied research fields, for instance in synthetic microbiology and the engineering of microbial consortia (Bernstein and Carlson, 2012). Microbial consortia are of interest for industry as diverse communities generally perform more complicated and varied tasks and endure more changeable environments than monocultures. Generally, evolutionary and ecological theory can help synthesizing microbial communities that are stable, productive and competitive. To be commercially viable, biotechnological industrial processes typically require microbial consortia exhibiting high cell densities. Yet, when phototrophic microorganisms are involved, high biomass concentrations would result in light limitation and the dominance of a single species. The nutrient-load hypothesis predicts that in a well-mixed system stable coexistence of several competing species would require intermediate biomass concentrations that allow simultaneous limitation by light and several nutrients. Thus, the nutrient-load hypothesis offers a useful theoretical framework for the application of engineered mixtures of phototrophic microbes, e.g., in biofuel industry or for the production of specialty chemicals.

The nutrient-load hypothesis might also be applied in the context of eutrophication management, where high biomass concentrations may lead to light limitation and the dominance of a single (and possibly harmful) species. The predictions of the nutrient-

load hypothesis as formulated in Chapter 4 should be of particular interest for systems that are well-mixed, such as shallow lakes or coastal lagoons. Yet, it has to be emphasized that the current model still neglects important factors that might influence the predictions. For instance, surface blooms in eutrophic waters are often affected by stratification and turbulence, and can therefore be suppressed not only by nutrient load reductions but also by altering the system's turbulence (Huisman *et al.*, 2004; Jöhnk *et al.*, 2008). Moreover, blooms might be dominated by species that are not grazed upon because they are toxic or colony-forming (Huisman *et al.*, 2005; Irigoien *et al.*, 2005; van Donk *et al.*, 2011). Accordingly, the predictions of the nutrient-load hypothesis might not hold if the species composition is the result of resistance to grazing rather than competition for limiting resources.

The nutrient-load hypothesis could be further developed in order to explain other ecological phenomena as well. A first step into this direction was recently accomplished by Verspagen *et al.* (2014). The authors extended the nutrient-load hypothesis by developing new theory to explain the contrasting effects of rising CO_2 on population density and carbon:nitrogen stoichiometry of phytoplankton at low and high nutrient load. They formulated a model for phytoplankton growth on one nutrient, light, and dissolved inorganic carbon, and predicted that rising CO_2 levels would lead to a shift from carbon to nutrient limitation at low nutrient load and to a shift from carbon to light limitation at high nutrient load (Fig. 6.2). As a consequence, rising CO_2 levels will increase phytoplankton biomass more at high nutrient loads than at low nutrient loads, but it will increase the carbon:nutrient stoichiometry of phytoplankton biomass more at low than at high nutrient loads. Verspagen *et al.* (2014) demonstrated that the model predictions were qualitatively and quantitatively in good agreement with data from chemostat experiments using the cyanobacterium *Microcystis* aeruginosa.

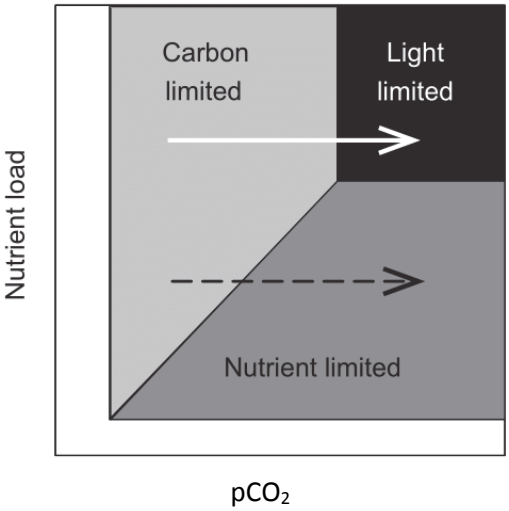

Figure 6.2: Extension of the nutrient-load hypothesis to the context of rising CO_2 and climate change. Shaded areas indicate that different resources become limiting at different pCO_2-levels and nutrient loads. Figure redrawn from Verspagen *et al.* (2014).

Conclusions

The work in this thesis shows that temperature, nutrients and light have interactive effects on microbial plankton communities. The effects can be grouped according to the nutrient status of the environment. In oligotrophic systems, temperature has a weak or no direct effect on species and community processes because their growth is limited by nutrients. Community structure is strongly determined by competition for nutrients between species, where the outcome depends on the supply ratio of the growth-limiting nutrients. In eutrophic systems rising temperatures can strongly increase biological processes because the growth rates of the organisms are not limited by nutrients. Yet, the growth of phototrophic species may become limited by light, because eutrophic systems often develop high biomass concentrations, which lead to self-shading. Under light-limited conditions, temperature has again a weak or no effect on the biological processes of phototrophic species and communities. The structure of phototrophic communities in eutrophic ecosystems is much less sensitive to the nutrient supply ratio but may respond strongly to changes in the absolute nutrient load.

The relative importance of temperature versus resource control does not only vary among habitats but also differs between species. In particular, our results indicate that

rising temperatures may strongly increase the abundance of unicellular N_2-fixing cyanobacteria and, hence, also to some extent the abundance of non-N_2-fixing microorganisms facilitated by the N_2-fixing cyanobacteria. The results of this thesis thus imply that global warming is likely to have major impacts on microbial plankton communities in eutrophic environments, but also in warm oligotrophic oceans harboring marine N_2-fixing cyanobacteria.

REFERENCES

Aerts R, Berendse F, de Caluwe H, Schmitz M. (1990). Competition in heathland along an experimental gradient of nutrient availability. *Oikos* 57: 310-318.

Agawin NSR, Rabouille S, Veldhuis MJW, Servatius L, Hol S, Van Overzee HMJ, Huisman J. (2007). Competition and facilitation between unicellular nitrogen-fixing cyanobacteria and non-nitrogen-fixing phytoplankton species. *Limnol Oceanogr* 52: 2233-2248.

Aguirre von Wobeser E, Ibelings BW, Bok J, Krasikov V, Huisman J, Matthijs HCP. (2011). Concerted changes in gene expression and cell physiology of the cyanobacterium *Synechocystis* sp. strain PCC 6803 during transitions between nitrogen and light-limited growth. *Plant Physiol* 155: 1445-1457.

Ahlgren G. (1987). Temperature functions in biology and their application to algal growth constants. *Oikos* 49: 177-190.

Allen AE, Booth MG, Verity PG, Frischer ME. (2005). Influence of nitrate availability on the distribution and abundance of heterotrophic bacterial nitrate assimilation genes in the Barents Sea during summer. *Aquat Microb Ecol* 39: 247-255.

Allen AP, Gillooly JF, Brown JH. (2005). Linking the global carbon cycle to individual metabolism. *Funct Ecol* 19: 202-213.

Andersen RA. (2005). *Algal Culturing Techniques*. Elsevier, Amsterdam, The Netherlands.

Angilletta Jr MJ, Wilson RS, Navas CA, James RS. (2003). Tradeoffs and the evolution of thermal reaction norms. *Trends Ecol Evol* 18: 234-240.

Apple JK, del Giorgio PA, Kemp WM. (2006). Temperature regulation of bacterial production, respiration, and growth efficiency in a temperate salt-marsh estuary. *Aquat Microb Ecol* 43: 243-254.

Armstrong RA, McGehee R. (1980). Competitive exclusion. *Am Nat* 115: 151-170.

Arrigo KR. (2005). Marine microorganisms and global nutrient cycles. *Nature* 437: 349-255.

Atkinson D, Ciotti BJ, Montagnes DJS. (2003). Protists decrease in size linearly with temperature: ca. 2.5 % degrees C^{-1}. *Proc R Soc Lond B* 270: 2605-2611.

Azam F. (1998). Microbial control of oceanic carbon flux: the plot thickens. *Science* 280: 694-696.

Benavides M, Agawin NSR, Arístegui J, Peene J, Stal LJ. (2013). Dissolved organic nitrogen and carbon release by a marine unicellular diazotrophic cyanobacterium. *Aquat Microb Ecol*. 69: 69-80.

Berger SA, Diehl S, Kunz TJ, Albrecht D, Oucible AM, Ritzer S. (2006). Light supply, plankton biomass, and seston stoichiometry in a gradient of lake mixing depths. *Limnol Oceanogr* 51:1898-1905.

Bergman B, Siddiqui PJA, Carpenter EJ, Peschek GA. (1993). Cytochrome oxidase: subcellular distribution and relationship to nitrogenase expression in the nonheterocystous marine cyanobacterium *Trichodesmium thiebautii*. *Appl Environ Microbiol* 59: 3239-3244.

Bergman B, Gallon JR, Rai AN, Stal LJ. (1997). N_2 fixation by non-heterocystous cyanobacteria. *FEMS Microbiol Rev* 19: 139-185.

Berman-Frank I, Lundgren P, Chen YB, Küpper H, Kolber Z, Bergman B, Falkowski P. (2001). Segregation of nitrogen fixation and oxygenic photosynthesis in the marine cyanobacterium *Trichodesmium*. *Science* 294: 1534-1537.

Bernstein HC, Carlson RP. (2012). Microbial consortia engineering for cellular factories: *in vitro* to *in silico* systems. *Comp Struct Biotechnol J* 3: e201210017.

Bouvy M, Bettarel Y, Bouvier C, Domaizon I, Jacquet S, Le Floc'h E, *et al*. (2011). Trophic interactions between viruses, bacteria and nanoflagellates under various nutrient conditions and simulated climate change. *Environ Microbiol* 13: 1842-1857.

Bratbak, G. (1985). Bacterial biovolume and biomass estimations. *Appl Environ Microbiol* 49: 1488 1493.

Bratbak G, Thingstad TF. (1985). Phytoplankton-bacteria interactions: an apparent paradox? Analysis of a model system with both competition and commensalism. *Mar Ecol Prog Ser* 25: 23-30.

Bratbak G, Thingstad F, Heldal M. (1994). Viruses and the microbial loop. *Microb Ecol* 28: 209-221.

Brauer VS, Stomp M, Huisman J. (2012). The nutrient-load hypothesis: patterns of resource limitation and community structure driven by competition for nutrients and light. *Am Nat* 179: 721-740.

Brauer VS, Stomp M, Rosso C, van Beusekom SAM, Emmerich B, Stal l_j, Huisman J. (2013). Low temperature delays timing and enhances the cost of nitrogen fixation in the unicellular cyanobacterium *Cyanothece*. *ISME J* 7: 2105-2115.

Breitbarth E, Oschlies A, La Roche J. (2007). Physiological constraints on the global distribution of *Trichodesmium*: effects of temperature on diazotrophy. *Biogeosciences* 4: 53-61.

Brown JH, Gillooly JF, Allen AP, Savage VM, West GB. (2004). Toward a metabolic theory of Ecology. *Ecology* 85: 1771-1789.

Bruns A, Rohde M, Berthe-Corthi L. (2001). *Muricauda restringensis* gen. nov., sp. nov., a facultatively anaerobic, appendaged bacterium from German North Sea intertidal sediment. *Int J Syst Evol Micr* 51: 1997-2006.

Cai H, Jiao N. (2008). Diversity and abundance of nitrate assimilation genes in the northern South China Sea. *Microb Ecol* 56: 751-764.

Canfield DE, Phlips E, Duarte CM. (1989). Factors influencing the abundance of blue-green algae in Florida lakes. *Can J Fish Aquat Sci* 46: 1132-1237.

Capone DG, O'Neil JM, Zehr J, Carpenter EJ. (1990). Basis for diel variation in nitrogenase activity in the marine planktonic cyanobacterium *Trichodesmium thiebautii*. *Appl Environ Microbiol* 56: 3532-3536.

Capone DG, Zehr JP, Paerl HW, Bergman B, Carpenter EJ. (1997). *Trichodesmium*, a globally significant marine cyanobacterium. *Science* 276: 1221-1229.

Carpenter SR, Caraco NF, Correll DL, Howarth RW, Sharpley AN, Smith VH. (1998). Nonpoint pollution of surface waters with phosphorus and nitrogen. *Ecol App* 8:559-568.

Cervený J, Nedbal L. (2009). Metabolic rhythms of the cyanobacterium *Cyanothece* sp. ATCC 51142 correlate with modeled dynamics of circadian clock. *J Biol Rhythms* 24: 295-303.

Chen YB, Dominic B, Mellon MT, Zehr JP. (1998). Circadian rhythm of nitrogenase gene expression in the diazotrophic filamentous nonheterocystous cyanobacterium *Trichodesmium* sp. strain IMA101. *J Bacteriol* 180: 3598-3605.

Chen YLL, Chen HY, Lin YH. (2003). Distribution and downward flux of *Trichodesmium* in the South China Sea as influenced by the transport from the Kuroshio Current. *Mar Ecol Prog Ser* 259: 47-57.

Church MJ, Björkman KM, Karl DM, Saito MA, Zehr JP. (2008). Regional distributions of nitrogen-fixing bacteria in the Pacific Ocean. *Limnol Oceanogr* 53: 63-77.

Ciros-Pérez J, Carmona MJ, Serra M. (2001). Resource competition between sympatric sibling rotifer species. *Limnol Oceanogr* 46: 1511-1523.

Clarke A. (2004). Is there a universal temperature dependence of metabolism? *Funct Ecol* 18: 252-256.

Clarke A. (2006). Temperature and the metabolic theory of Ecology. *Funct Ecol* 20: 405-412.

Clarke A, Fraser KPP. (2004). Why does metabolism scale with temperature? *Funct Ecol* 18: 243-251.

Colón-López MS, Sherman DM, Sherman LA. (1997). Transcriptional and translational regulation of nitrogenase in light-dark- and continuous-light-grown cultures of the unicellular cyanobacterium *Cyanothece* sp. strain ATCC 51142. *J Bacteriol* 179: 4319-4327.

Cottingham KL, Zens MS. (2004). Metabolic rate opens a grand vista on Ecology? *Ecology* 85: 1805-1807.

Currie DJ, Kalff J. (1984). Can bacteria outcompete phytoplankton for phosphorus? A chemostat test. *Microb Ecol* 10: 205-216.

Cyr H, Walker SC. (2004). An illusion of mechanistic understanding. *Ecology* 85: 1802-1804.

Daufresne M, Lengfellner K, Sommer U. (2009). Global warming benefits the small in aquatic ecosystems. *Proc Natl Acad Sci USA* 106: 12788-12793.

De Castro F, Gaedke U. (2008). The metabolism of lake plankton does not support the metabolic theory of Ecology. *Oikos* 117: 1218-1226.

De Jonge VN. (1980). Fluctuations in the organic carbon to chlorophyll-a ratios for estuarine benthic diatom populations. *Mar Ecol* 2: 345-353.

De Tezanos Pinto P, Litchman E. (2010). Interactive effects of N:P ratios and light on nitrogen-fixer abundance. *Oikos* 119:567-575.

Degerman R, Dinasquet J, Riemann L, Sjöstedt de Luna S, Andersson A. (2013). Effect of resource availability on bacterial community responses to increased temperature. *Aquat Microb Ecol* 68: 131-142.

Dell AI, Pawar S, Savage VM. (2011). Systematic variation in the temperature dependence of physiological and ecological traits. *Proc Natl Acad Sci USA* 108: 10591-10596.

Diehl S, Berger S, Ptacnik R, Wild A. (2002). Phytoplankton, light, and nutrients in a gradient of mixing depths: field experiments. *Ecology* 83: 399-411.

Donald CM. (1958). The interaction of competition for light and for nutrients. *Austr J Agr Res* 9: 421-435.

Dhooge A, Govaerts W, Kuznetsov YA. (2003). MATCONT: a MATLAB package for numerical bifurcation analysis of ODEs. ACM *Trans Math Software* 29:141-164.

Dore JE, Letelier RM, Church MJ, Lukas R, Karl DM. (2008). Summer phytoplankton blooms in the oligotrophic North Pacific Subtropical Gyre: historical perspective and recent observations. *Progr Oceanogr* 76: 2-38.

Downing JA, Watson SB, McCauley E. (2001). Predicting cyanobacteria dominance in lakes. *Can J Fish Aquat Sci* 58: 1905-1908.

Dron A, Rabouille S, Claquin P, Le Roy B, Talec A, Sciandra A. (2012a). Light–dark (12:12) cycle of carbon and nitrogen metabolism in *Crocosphaera watsonii* WH8501: relation to the cell cycle. *Environ Microbiol* 14: 967-981.

Dron A, Rabouille S, Claquin P, Chang P, Raimbault V, Talec A, Sciandra A. (2012b). Light:dark (12:12 h) quantification of carbohydrate fluxes in *Crocosphaera watsonii*. *Aquat Microb Ecol* 68: 43-55.

Dybzinski R, Tilman D. (2007). Resource use patterns predict long-term outcomes of plant competition for nutrients and light. *Am Nat* 170: 305-318.

Edwards KF, Klausmeier CA, Litchman E. (2011). Evidence for a three-way trade-off between nitrogen and phosphorus competitive abilities and cell size in phytoplankton. *Ecology* 92: 2085-2095.

Eiler A. (2006). Evidence for the ubiquity of mixotrophic bacteria in the upper ocean: implications and consequences. *Appl Environ Microbiol* 72: 7431-7437.

Elser JJ, Bracken MES, Cleland EE, Gruner DS, Harpole WS, Hillebrand H *et al.* (2007). Global analysis of nitrogen and phosphorus limitation of primary producers in freshwater, marine and terrestrial ecosystems. *Ecol Lett* 10: 1135-1142.

Enquist BJ, Economo EP, Huxman TE, Allen AP, Ignace DD, Gillooly JF. (2003). Scaling metabolism from organisms to ecosystems. *Nature* 423: 639-642.

Evans, J. R. 1989. Photosynthesis and nitrogen relationships in leaves of C3 plants. *Oecologia* 78:9-19.

Falcón LI, Pluvinage S, Carpenter EJ. (2005). Growth kinetics of marine unicellular N_2-fixing cyanobacterial isolates in continuous culture in relation to phosphorus and temperature. *Mar Ecol Prog Ser* 285: 3-9.

Falkowski PG, Fenchel T, DeLong EF. (2008). The microbial engines that drive earth's biogeochemical cycles. *Science* 320: 1034-1039.

Fay P. (1992). Oxygen relations of nitrogen fixation in cyanobacteria. *Microbiol Rev* 56: 340-373.

Field CB, Behrenfeld MJ, Randerson JT, Falkowski P. (2010). Primary production of the biosphere: integrating terrestrial and oceanic components. *Science* 281: 237-240.

Fong AA, Karl DM, Lukas R, Letelier RM, Zehr JP, Church MJ. (2008). Nitrogen fixation in an anticyclonic eddy in the oligotrophic North Pacific Ocean. *ISME J* 2: 663-676.

Foster RA, Subramaniam A, Mahaffey C, Carpenter EJ, Capone DG, Zehr JP. (2007). Influence of the Amazon River plume on distributions of free-living and symbiotic cyanobacteria in the western tropical North Atlantic Ocean. *Limnol Oceanogr* 52: 517-532.

Fu FX, Bell PRF. (2003). Factors affecting N_2 fixation by the cyanobacterium *Trichodesmium* sp. GBRTRLI101. *FEMS Microbiol Ecol* 45: 203-209.

Fuhrman JA. (1999). Marine viruses and their biogeochemical and ecological effects. *Nature* 399: 541-548.

Fuhrman JA. (2009). Microbial community structure and its functional implications. *Nature* 459, 193-199.

Gallon JR. (1992). Reconciling the incompatible: N_2 fixation and O_2. *New Phytol* 122: 571-609.

Gallon JR, Pederson DM, Smith GD. (1993). The effect of temperature on the sensitivity of nitrogenase to oxygen in the cyanobacteria *Anabaena cylindrica* (Lemmermann) and *Gloeothece* (Nägeli). *New Phytol* 124: 251-257.

Garcia N, Raimbault P, Sandroni V. (2007). Seasonal nitrogen fixation and primary production in the Southwest Pacific: nanoplankton diazotrophy and transfer of nitrogen to picoplankton organisms. *Mar Ecol Prog Ser* 343: 25-33.

Gaumont-Guay D, Black TA, Griffis TJ, Barr AG, Jassal RD, Nesic Z. (2006). Interpreting the dependence of soil respiration on soil temperature and water content in a boreal aspen stand. *Agr Forest Meteorol* 140: 220-235.

Gerla DJ, Wolf WM, Huisman J. (2011). Photoinhibition and the assembly of light-limited phytoplankton communities. *Oikos* 120: 359-368.

Gillooly JF, Brown JH, West GB, Savage VM, Charnov EL. (2001). Effects of size and temperature on metabolic rate. *Science* 293: 2248-2251.

Glibert PM, Bronk DA. (1994). Release of dissolved organic nitrogen by marine diazotrophic cyanobacteria, *Trichodesmium* spp. *Appl Environ Microbiol* 60: 3996-4000.

Goldman JC, Dennett MR. (2000). Growth of marine bacteria in batch and continuous culture under carbon and nitrogen limitation. *Limnol Oceanogr* 45: 789-800.

Grime JP. (1973). Competitive exclusion in herbaceous vegetation. *Nature* 242: 344-347.

Grossart HP, Levold F, Allgaier M, Simon M, Brinkhoff T. (2005). Marine diatom species harbor distinct bacterial communities. *Environ Microbiol* 7: 860-873.

Großkopf T, LaRoche J. (2012). Direct and indirect costs of dinitrogen fixation in *Crocosphaera watsonii* WH8501 and possible implications for the nitrogen cycle. *Front Microbiol* 3: 236. doi: 10.3389/fmicb.2012.00236.

Großkopf T, Mohr W, Baustian T, Schunck H, Gill D, Kuypers MMM *et al*. (2012). Doubling of marine dinitrogen-fixation rates based on direct measurements. *Nature* 488: 361-364.

Grover JP. (1997). *Resource Competition*. Chapman & Hall, London, UK.

Grover JP, Chrzanowski TH. (2004). Limiting resources, disturbance, and diversity in phytoplankton communities. *Ecol Mon* 74: 533-551.

Gruber N, Sarmiento JL. (1997). Global patterns of marine nitrogen fixation and denitrification. *Global Biogeochem Cycles* 11: 235-266.

Hancke K, Glud RN. (2004). Temperature effects on respiration and photosynthesis in three diatom-dominated benthic communities. *Aquat Microb Ecol* 37: 265-281.

Hardy RWF, Holsten RD, Jackson EK, Burns RC. (1968). Acetylene-ethylene assay for N_2 fixation: laboratory and field evaluation. *Plant Physiol* 43: 1185-1207.

Harpole WS, Tilman D. (2007). Grassland species loss resulting from reduced niche dimension. *Nature* 446: 791-793.

Harpole WS, Suding KN. (2011). A test of the niche dimension hypothesis in an arid annual grassland. *Oecologia* 166: 197-205.

Hauruseu D, Koblížek M. (2012). Influence of light on carbon utilization in aerobic anoxygenic phototrophs. *Appl Environ Microbiol* 78: 7414-7419.

Hautier Y, Niklaus PA, Hector A. (2009). Competition for light causes plant diversity loss after eutrophication. *Science* 324: 636-638.

Havens KE, James RT, East TL, Smith VH. (2003). N:P ratios, light limitation, and cyanobacterial dominance in a subtropical lake impacted by non-point source nutrient pollution. *Environ Poll* 122: 379-390.

Hays GC, Richardson AJ, Robinson C. (2005). Climate change and marine plankton. *Trends Ecol Evol* 20: 337-344.

Healey FP. (1985). Interacting effects of light and nutrient limitation on the growth rate of *Synechococcus linearis* (Cyanophyceae). *J Phycol* 21: 134-146.

Hillebrand H, Dürselen CD, Kirschel D, Pollingher U, Zohary T. (1999). Biovolume calculation for pelagic and benthic microalgae. *J Phycol* 35: 403-424.

Hillebrand H, Cowles JM, Lewandowska A, Van de Waal DB, Plum C. (2014). Think ratio! A stoichiometric view on biodiversity–ecosystem functioning research. Basic Appl Ecol 15: 465-474.

Hmelo LR, van Mooy BAS, Mincer RJ. (2012). Characterization of bacterial epibionts on the cyanobacterium *Trichodesmium*. *Aquat Microb Ecol* 67: 1-14.

Huang TC, Chow TJ, Hwang IS. (1988). The cyclic synthesis of the nitrogenase of *Synechococcus* RF-1 and its control at the transcription level. FEMS Microbiol Lett 50: 127-130.

Hubbell SP. (2001). *The Unified Neutral Theory of Biodiversity and Biogeography*. Princeton University Press, Princeton, NJ.

Hügler M, Sievert SM. (2011). Beyond the Calvin Cycle: autotrophic carbon fixation in the ocean. *Annu Rev Mar Sci* 3: 261-289.

Huisman J. (1999). Population dynamics of light-limited phytoplankton: microcosm experiments. *Ecology* 80: 202-210.

Huisman J, Weissing FJ. (1994). Light-limited growth and competition for light in well-mixed aquatic environments: an elementary model. *Ecology* 75: 507-520.

Huisman J, Weissing FJ. (1995). Competition for nutrients and light in a mixed water column: a theoretical analysis. *Am Nat* 146: 536-564.

Huisman J, Weissing FJ. (1999). Biodiversity of plankton by species oscillations and chaos. *Nature* 402: 407-410.

Huisman J, Weissing FJ. (2001). Biological conditions for oscillations and chaos generated by multispecies competition. *Ecology* 82: 2682-2695.

Huisman J, Jonker RR, Zonneveld C, Weissing FJ. (1999). Competition for light between phytoplankton species: experimental tests of mechanistic theory. *Ecology* 80: 211-222.

Huisman J, Sharples J, Stroom JM, Visser PM, Kardinaal WEA, Verspagen JMH, Sommeijer B. (2004). Changes in turbulent mixing shift competition for light between phytoplankton species. *Ecology* 85: 2960-2970.

Huisman J, Matthijs HCP, Visser PM, eds. (2005). *Harmful Cyanobacteria*. Springer Aquatic *Ecology* Series 3. Springer, Dordrecht, The Netherlands.

Huisman J, Pham Thi NN, Karl DM, Sommeijer B. (2006). Reduced mixing generates oscillations and chaos in the oceanic deep chlorophyll maximum. *Nature* 439: 322-325.

Hunt DE, David LA, Gevers D, Preheim SP, Alm EJ, Polz MF. (2008). Resource partitioning and sympatric differentiation among closely related bacterioplankton. *Science* 320: 1081-1085.

Huston MA, DeAngelis DL. (1994). Competition and coexistence: the effects of resource transport and supply rates. *Am Nat* 144: 954-977.

Hutchinson GE. (1961). The paradox of the plankton. *Am Nat* 95: 137-145.

Hwang CY, Kim MH, Bae GD, Zhang GI, Kim YH, Cho BC. (2009). *Muricauda olearia* sp. nov., isolated from crude-oil-contaminated seawater, and emended description of the genus *Muricauda*. *Int J Syst Evol Micr* 59: 1856-1861.

Inouye RS, Huntley NJ, Tilman D, Tester J, Stillwell M, Zinnel K. (1987). Old-field succession on a Minnesota sand plain. *Ecology* 68: 12-26.

Interlandi SJ, Kilham SS. (2001). Limiting resources and the regulation of diversity in phytoplankton communities. *Ecology* 82: 1270-1282.

Irigoien X, Huisman J, Harris RP. (2004). Global biodiversity patterns of marine phytoplankton and zooplankton. *Nature* 429: 863-867.

Irigoien X, Flynn KJ, Harris RP. (2005). Phytoplankton blooms: a 'loophole' in microzooplankton grazing impact? *J Plank Res* 27: 313-321.

Jäger CG, Diehl S, Schmidt GM. (2008). Influence of water-column depth and mixing on phytoplankton biomass, community composition, and nutrients. *Limnol Oceanogr* 53: 2361-2373.

Jensen JP, Jeppesen E, Olrik K, Kristensen P. (1994). Impact of nutrients and physical factors on the shift from cyanobacterial to chlorophyte dominance in shallow Danish lakes. *Can J Fish Aquat Sci* 51: 1692-1699.

Jöhnk KD, Huisman J, Sharples J, Sommeijer B, Visser PM, Stroom JM. (2008). Summer heatwaves promote blooms of harmful cyanobacteria. *Glob Change Biol* 14: 495-512.

Karl DM, Bidigare RR, Letelier RM. (2001). Long-term changes in plankton community structure and productivity in the North Pacific subtropical gyre: the domain shift hypothesis. *Deep-Sea Res II* 48: 1449-1470.

Karl DM, Michaels A, Bergman B, Capone D, Carpenter E, Letelier R, *et al*. (2002). Dinitrogen fixation in the world's oceans. *Biogeochem* 57/58: 47-98.

Kazamia E, Czesnick H, Nguyen TTV, Croft MT, Sherwood E, Sasso S, *et al*. (2012). Mutualistic interactions between vitamin B12-dependent algae and heterotrophic bacteria exhibit regulation. *Environ Microbiol* 14: 1466-1476.

Kerr B, Riley MA, Feldman MW, Bohannan BJM. (2002). Local dispersal promotes biodiversity in a real-life game of rock-paper-scissors. *Nature* 418: 171-174.

Kirchman DL, Malmstrom RR, Cottrell MT. (2005). Control of bacterial growth by temperature and organic matter in the Western Arctic. *Deep-Sea Res II* 52: 3386-3395.

Koblížek M, Béjà O, Bidigare RR, Christensen S, Benitez-Nelson B, Vetriani C, *et al*. (2003). Isolation and characterization of *Erythrobacter* sp. strains from the upper ocean. *Arch Microbiol* 180: 327-338.

Kolber ZS, Plumley FG, Lang AS, Beatty JT, Blankenship RE, VanDover CL, *et al*. (2001). Contribution of aerobic photoheterotrophic bacteria to the carbon cycle in the ocean. *Science* 292: 2492-2495.

Laird RA, Schamp BS. (2006). Competitive intransitivity promotes species coexistence. *Am Nat* 168: 182-193.

Langlois RJ, LaRoche J, Raab PA. (2005). Diazotrophic diversity and distribution in the tropical and subtropical Atlantic Ocean. *Appl Environ Microbiol* 71: 7910-7919.

Langlois RJ, Hümmer D, LaRoche J. (2008). Abundances and distributions of the dominant *nifH* phylotypes in the Northern Atlantic Ocean. *Appl Environ Microbiol* 74: 1922-1931.

LaRoche J, Breitbarth E. (2005). Importance of diazotrophs as a source of new nitrogen in the ocean. *J Sea Res* 53: 67-91.

Le Chevanton M, Garnier M, Bougaran G, Schreiber N, Lukomska E, Bérard JB, *et al*. (2013). Screening and selection of growth-promoting bacteria for *Dunaliella* cultures. *Algal Research* 2: 212-222.

Lenes JM, Darrow BP, Cattrall C, Heil CA, Callahan M, Vargo GA, *et al*. (2001). Iron fertilization and the *Trichodesmium* response on the West Florida shelf. *Limnol Oceanogr* 46: 1261-1277.

León JA, Tumpson DB. (1975). Competition between two species for two complementary or substitutable resources. *J Theor Biol* 50: 185-201.

Litchman E, Klausmeier CA. (2001). Competition of phytoplankton under fluctuating light. *Am Nat* 157: 170-187.

Litchman E, Klausmeier CA, Bossard P. (2004). Phytoplankton nutrient competition under dynamic light regimes. *Limnol Oceanogr* 49:1457-1462.

Litchman E, Klausmeier CA, Schofield OM, Falkowski PG. (2007). The role of functional traits and trade-offs in structuring phytoplankton communities: scaling from cellular to ecosystem level. *Ecol Lett* 10: 1170-1181.

López-Urrutia A, San Martin E, Harris RP, Irigoien X. (2006). Scaling the metabolic balance of the oceans. *Proc Natl Acad Sci USA* 103: 8739-8744.

López-Urrutia Á, Morán XA. (2007). Resource limitation of bacterial production distorts the temperature dependence of oceanic carbon cycling. *Ecology* 88: 817-822.

Lorenzen CJ. (1967). Determination of chlorophyll and phaeopigments: spectrophotometric equations. *Limnol Oceanogr* 12: 343-346.

Lugomela C, Lyimo TJ, Bryceson I, Semesi AK, Bergman B. (2002). *Trichodesmium* in coastal waters of Tanzania: diversity, seasonality, nitrogen and carbon fixation. *Hydrobiologia* 477: 1-13.

Marañón E, Cermeño P, Huete-Ortega M, López-Sandoval DC, Mouriño-Carballido B, Rodríguez-Ramos T. (2014). Resource supply overrides temperature as a controlling factor of marine phytoplankton growth. *PLoS ONE* 9: e99312.

Marquet PA, *et al*. (2004). Metabolic *Ecology*: linking individuals to ecosystems? *Ecology* 85: 1794-1796.

Maryan PS, Eady RR, Chaplin AE, Gallon JR. (1986). Nitrogen fixation by *Gloeothece* sp. PCC 6909: respiration and not photosynthesis supports nitrogenase activity in the light. *J Gen Microbiol* 132: 789-796.

Mazard SL, Fuller NJ, Orcutt KM, Bridle O, Scanlan DJ. (2004). PCR analysis of the distribution of unicellular cyanobacterial diazotrophs in the Arabian Sea. *Appl Environ Microbiol* 70: 7355-7364.

McCarthy MJ, James RT, Chen Y, East TL, Gardner WS. (2009). Nutrient ratios and phytoplankton community structure in the large, shallow, eutrophic, subtropical Lakes Okeechobee (Florida, USA) and Taihu (China). *Limnology* 10:215-227.

McDonald JH. (2009). *Handbook of Biological Statistics*. 2nd ed. Sparky House Publishing, Baltimore, MD.

Miller TE, Burns JH, Munguia P, Walters EL, Kneitel JM, Richards PM, Mouquet N, Buckley HL. (2005). A critical review of twenty years' use of the resource-ratio theory. *Am Nat* 165: 439-448.

Milligan AJ, Berman-Frank I, Gerchman Y, Dismukes GC, Falkowski PG. (2007). Light-dependent oxygen consumption in nitrogen-fixing cyanobacteria plays a key role in nitrogenase protection. *J Phycol* 43: 845-852.

Mills MM, Ridame C, Davey M, LaRoche J, Geider RJ. (2004). Iron and phosphorus co-limit nitrogen fixation in the eastern tropical North Atlantic. *Nature* 429: 292-294.

Mitsui A, Cao S. (1988). Isolation and culture of marine nitrogen-fixing unicellular cyanobacteria *Synechococcus*. Pages 105-113 in: Packer L, Glazer AN (eds).

Methods in Enzymology, Cyanobacteria, vol 167. Academic Press, San Diego, CA.

Mittelbach GG, Steiner CF, Scheiner SM, Gross KL, Reynolds HL, Waide RB, *et al.* (2001). What is the observed relationship between species richness and productivity? *Ecology* 82: 2381-2396.

Moisander PH, Beinart RA, Hewson I, White AE, Johnson KS, Carlson CA, *et al.* (2010). Unicellular cyanobacterial distributions broaden the oceanic N_2 fixation domain. *Science* 327: 1512-1514.

Mojica KDA, Brussaard CPD. (2014). Factors affecting virus dynamics and microbial host-virus interactions in marine environments. *FEMS Microbiol Ecol* doi: 10.1111/1574-6941.12343.

Monod J. (1950). La technique de culture continue, théorie et applications. *Annales de l'Institut Pasteur (Paris)* 79: 390-410.

Monteiro FM, Dutkiewicz S, Follows MJ. (2011). Biogeographical controls on the marine nitrogen fixers. *Global Biogeochem Cycles* 25: GB2003, doi: 10.1029/2010GB003902.

Moore CM, Mills MM, Arrigo KR, Berman-Frank I, Bopp L, Boyd PW, *et al.* (2013). Processes and patterns of oceanic nutrient limitation. *Nat Geosci* 6: 701-710.

Mota R, Guimarães R, Büttel Z, Rossi F, Colica G, Silva CJ, *et al.* (2013). Production and characterization of extracellular carbohydrate polymer from *Cyanothece* sp. CCY 0110. *Carbohyd Polym* 92: 1408-1415.

Mulholland MR. (2007). The fate of nitrogen fixed by diazotrophs in the ocean. *Biogeosci* 4: 37-51.

Mulholland MR, Bernhardt PW. (2005). The effect of growth rate, phosphorus concentration, and temperature on N_2 fixation, carbon fixation, and nitrogen release in continuous cultures of *Trichodesmium* IMS101. *Limnol Oceanogr* 50: 839-849.

Mulholland MR, Bronk DA, Capone DG. (2004). Dinitrogen fixation and release of ammonium and dissolved organic nitrogen by *Trichodesmium* IMS101. *Aquat Microb Ecol* 37: 85-94.

Mulholland MR, Bernhardt PW, Heil CA, Bronk DA, O'Neil JM. (2006). Nitrogen fixation and release of fixed nitrogen by *Trichodesmium* spp. in the Gulf of Mexico. *Limnol Oceanogr* 51: 1762-1776.

Mullineaux PM, Gallon JR, Chaplin AE. (1981). Nitrogen fixation in cultures of the cyanobacterium *Gloeocapsa* (*Gloeothece*) sp. 1430/3 incubated in the dark. *J Gen Microbiol* 124: 141-146.

Mur LR, Gons H_j, van Liere L. (1977). Some experiments on competition between green algae and blue-green bacteria in light-limited environments. *FEMS Microbiol Let* 1:335-338.

Nakajima M, Imai K, Ito H, Nishiwaki T, Murayama Y, Iwasaki O, *et al*. (2005). Reconstitution of circadian oscillation of cyanobacterial KaiC phosphorylation in vitro. *Science* 308: 414-415.

Nausch M. (1996). Microbial activities on *Trichodesmium* colonies. *Mar Ecol Prog Ser* 141: 173-181.

Needoba JA, Foster RA, Sakamoto C, Zehr JP, Johnson KS. (2007). Nitrogen fixation by unicellular diazotrophic cyanobacteria in the temperate oligotrophic North Pacific Ocean. *Limnol Oceanogr* 52: 1317-1327.

Niklinska M, Klimek B. (2007). Effect of temperature on the respiration rate of forest soil organic layer along an elevation gradient in the Polish Carpathians. *Biol Fert Soils* 43: 511-518.

Nõges T, Laugaste R, Nõges P, Tõnno I. (2008). Critical N:P ratio for cyanobacteria and N_2-fixing species in the large shallow temperate lakes Peipsi and Võrtsjärv, North-East Europe. *Hydrobiologia* 599: 77-86.

O'Connor MI, Piehler MF, Leech DM, Anton A, Bruno JF. (2009). Warming and resource availability shift food web structure and metabolism. *PLoS Biol* 7: e10000178.

O'Connor MP, Kemp SJ, Agosta SJ, Hansen F, Sieg AE, Wallace BP, *et al*. (2007). Reconsidering the mechanistic basis of the metabolic theory of ecology. *Oikos* 116: 1058-1072.

Oh HM, Giovannoni SJ, Ferriera S, Johnson J, Cho JC. (2009). Complete genome sequence of *Erythrobacter litoralis* HTCC2594. *J Bacteriol* 191: 2419-2420.

Ohlendieck U, Stuhr A, Siegmund H. (2000). Nitrogen fixation by diazotrophic cyanobacteria in the Baltic Sea and transfer of the newly fixed nitrogen to picoplankton organisms. *J Mar Syst* 25: 213-219.

Olff H, Huisman J, van Tooren BF. (1993). Species dynamics and nutrient accumulation during early primary succession in coastal sand dunes. *J Ecol* 81: 693-706.

Paerl HW. (1984). Transfer of N_2 and CO_2 fixation products from *Anabaena oscillarioides* to associated bacteria during inorganic carbon sufficiency and deficiency. *J Phycol* 20: 600-608.

Paerl HW, Huisman J. (2009). Climate change: a catalyst for global expansion of harmful cyanobacterial blooms. *Environ Microbiol* Rep 1: 27-37.

Paerl HW, Bebout BM, Prufert LE. (1989). Bacterial associations with marine *Oscillatoria* sp. (*Trichodesmium* sp.) populations: ecophysiological implications. *J Phycol* 25: 773-784.

Passarge J, Hol S, Escher M, Huisman J. (2006). Competition for nutrients and light: stable coexistence, alternative stable states, or competitive exclusion? *Ecol Mon* 76: 57-72.

Pedrós-Alió C. (2006). Marine microbial diversity: can it be determined? *Trends Microbiol* 14: 257-263.

Perry LG, Neuhauser C, Galatowitsch SM. (2003). Founder control and coexistence in a simple model of asymmetric competition for light. *J Theor Biol* 222:425-436.

Peschek GA, Villgrater K, Wastyn M. (1991). 'Respiratory protection' of the nitrogenase in dinitrogen-fixing cyanobacteria. *Plant Soil* 137: 17-24.

Pietikäinen, J, Pettersson M, Baath E. (2005). Comparison of temperature effects on soil respiration and bacterial and fungal growth rates. *FEMS Microbiol Ecol* 52: 49-58.

Ploug H, Musat N, Adam B, Moraru CL, Lavik G, Vagner T, *et al*. (2010). Carbon and nitrogen fluxes associated with the cyanobacterium *Aphanizomenon* sp. in the Baltic Sea. *ISME J*. 4: 1215-1223.

Ploug H, Adam B, Musat N, Kalvelage T, Lavik G, Wolf-Gladrow D, *et al*. (2011). Carbon, nitrogen and O_2 fluxes associated with the cyanobacterium *Nodularia spumigena* in the Baltic Sea. *ISME J* 5: 1549-1558.

Precht H. (1973). *Temperature and life*. Springer-Verlag, New York, NY.

Price PB, Sowers T. (2004). Temperature dependence of metabolic rates for microbial growth, maintenance, and survival. *Proc Natl Acad Sci USA* 101: 4631-4636.

Prosser JI, Bohannan BJM, Curtis TP, Ellis RJ, Firestone MK, Freckleton RP, *et al*. (2007). The role of ecological theory in microbial *Ecology*. *Nature Rev Microbiol* 5: 384-392.

Ptacnik R, Diehl S, Berger S. (2003). Performance of sinking and nonsinking phytoplankton taxa in a gradient of mixing depths. *Limnol Oceanogr* 48: 1903-1912.

Raven JA, Geider RJ. (1988). Temperature and algal growth. *New Phytol* 110: 441–461.

Rees M, Bergelson J. (1997). Asymmetric light competition and founder control in plant communities. *J Theor Biol* 184: 353-358.

Renaud F, Pringault O, Rochelle-Newall E. (2005). Effects of the colonial cyanobacterium *Trichodesmium* spp. on bacterial activity. *Aquat Microb Ecol* 41: 261-270.

Revilla TA, Weissing FJ. (2008). Nonequilibrium coexistence in a competition model with nutrient storage. *Ecology* 89: 865-877.

Reynolds CS. (1997). Vegetation processes in the pelagic: a model for ecosystem theory. *Ecology* Institute, Oldendorf.

Reynolds CS. (1998). What factors influence the species composition of phytoplankton in lakes of different trophic status? *Hydrobiologia* 369/370:11-26.

Rhee GY, Gotham IJ. (1981). The effect of environmental factors on phytoplankton growth: temperature and the interactions of temperature with nutrient limitation. *Limnol Oceanogr* 26: 635-648.

Rooney-Varga JN, Giewat MW, Savin MC, Sood S, LeGresley M, Martin JL. (2005). Links between phytoplankton and bacterial community dynamics in a coastal marine environment. *Microb Ecol* 49: 163-175.

Rothhaupt KO. (1988). Mechanistic resource competition theory applied to laboratory experiments with zooplankton. *Nature* 333: 660-662.

Ryabov AB, Blasius B. (2011). A graphical theory of competition on spatial resource gradients. *Ecol Let* 14: 220-228.

Ryabov AB, Rudolf L, Blasius B. (2010). Vertical distribution and composition of phytoplankton under the influence of an upper mixed layer. *J Theor Biol* 263: 120-133.

Salomon PS, Janson S, Granéli E. (2003). Molecular identification of bacteria associated with filaments of *Nodularia spumigena* and their effect on the cyanobacterial growth. *Harm Alg* 2: 261-272.

Sañudo-Wilhelmy SA, Kustka AB, Gobler CJ, Hutchins DA, Yang M, Lwiza K, *et al.* (2001). Phosphorus limitation of nitrogen fixation by *Trichodesmium* in the central Atlantic Ocean. *Nature* 411: 66-69.

Sarmento H, Montoya JM, Vázquez-Domínguez E, Vaqué D, Gasol JM. (2010). Warming effects on marine microbial food web processes: how far can we go when it comes to predictions? *Phil Trans Roy Soc B* 365: 2137-2149.

Savage VM, Gillooly JF, Brown JH, West GB, Charnov EL. (2004). Effects of body size and temperature on population growth. *Am Nat* 163: 429-441.

Schäfer H, Abbas B, Witte H, Muyzer G. (2002). Genetic diversity of 'satellite' bacteria present in cultures of marine diatoms. *FEMS Microbiol Ecol* 42: 25-35.

Schneegurt MA, Sherman DM, Nayar S, Sherman LA. (1994a). Oscillating behavior of carbohydrate granule formation and dinitrogen fixation in the cyanobacterium *Cyanothece* sp. strain ATCC 51142. *J Bacteriol* 176: 1586-1597.

Schneegurt MA, Tucker DL, Ondr JK, Sherman DM, Sherman LA. (1994b). Metabolic rhythms of a diazotrophic cyanobacterium, *Cyanothece* sp. strain ATCC 51142, heterotrophically grown in continuous dark. *J Phycol* 36: 107-117.

Schwaderer AS, Yoshiyama K, Tezanos Pinto P, Swenson NG, Klausmeier CA, Litchman E. (2011). Eco-evolutionary differences in light utilization traits and distributions of freshwater phytoplankton. *Limnol Oceanogr* 56:589-598.

Serna-Chavez HM, Fierer N, van Bodegom PM. (2013). Global drivers and patterns of microbial abundance in soil. *Glob Ecol Biogeogr* 22: 1162-1172.

Sheridan CC, Steinberg DK, Kling GW. (2002). The microbial and metazoan community associated with colonies of *Trichodesmium* spp.: a quantitative survey. *J Plankton Res* 24: 913-922.

Simó R. (2001). Production of atmospheric sulfur by oceanic plankton: biogeochemical, ecological and evolutionary links. *Trends Ecol Evol* 16: 287-294.

Sison-Mangus MP, Jiang S, Tran KN, Kudela RM. (2014). Host-specific adaptation governs the interaction of the marine diatom, *Pseudo-nitzschia* and their microbiota. *ISME J.* 8: 63-76.

Smith VH. (1983). Low nitrogen to phosphorus ratios favor dominance by blue-green algae in lake phytoplankton. *Science* 221: 669-670.

Smith VH. (1986). Light and nutrient effects on the relative biomass of blue-green algae in lake phytoplankton. *Can J Fish Aquat Sci* 43: 148-153.

Smith VH. (1993). Applicability of resource-ratio theory to microbial *Ecology*. *Limnol Oceanogr* 38:239-249.

Smith VH. (2003). Eutrophication of freshwater and coastal marine ecosystems: a global problem. *Env Sci Poll Res* 10: 126-139.

Smith VH, Bennett SJ. (1999). Nitrogen:phosphorus supply ratios and phytoplankton community structure in lakes. *Arch Hydrobiol* 146: 37-53.

Sommer U. (1985). Comparison between steady-state and non-steady state competition: experiments with natural phytoplankton. *Limnol Oceanogr* 30:335-346.

Sommer U. (1989). Nutrient status and nutrient competition of phytoplankton in a shallow, hypertrophic lake. *Limnol Oceanogr* 34: 1162-1173.

Sommer U. (1993). Phytoplankton competition in Plußsee: a field test of the resource-ratio hypothesis. *Limnol Oceanogr* 38: 838-845.

Sonntag S, Hense I. (2011). Phytoplankton behavior affects ocean mixed layer dynamics through biological-physical feedback mechanisms. *Geophys Res Let* 38: L15610.

Staal M, Meysman FJR, Stal LJ. (2003). Temperature excludes N_2-fixing heterocystous cyanobacteria in the tropical oceans. *Nature* 425: 504-507.

Staal M, te Lintel Hekkert S, Brummer GJ, Veldhuis M, Sikkens C, Persijn S, *et al*. (2007). Nitrogen fixation along a north-south transect in the eastern Atlantic Ocean. *Limnol Oceanogr* 52: 1305-1316.

Stal LJ. (1988). Nitrogen fixation in cyanobacterial mats. Pages 474-484 in: Packer L, Glazer AN (eds). *Methods in Enzymology, Cyanobacteria*, vol 167. Academic Press, San Diego, CA.

Stal LJ. (2009). Is the distribution of nitrogen-fixing cyanobacteria in the ocean related to temperature? *Environ Microbiol* 11: 1632-1645.

Sterner RW, Elser JJ, Fee EJ, Guildford SJ, Chrzanowski TH. (1997). The light:nutrient ratio in lakes: the balance of energy and materials affects ecosystem structure and process. *Am Nat* 150: 663-684.

Stevens CJ, Dise NB, Mountford JO, Gowing DJ. (2004). Impact of nitrogen deposition on the species richness of grasslands. *Science* 303: 1876-1879.

Stomp M, Huisman J, de Jongh F, Veraart AJ, Gerla D, Rijkeboer M, *et al*. (2004). Adaptive divergence in pigment composition promotes phytoplankton biodiversity. *Nature* 432: 104–107.

Stomp M, Huisman J, Vörös L, Pick FR, Laamanen M, Haverkamp T, Stal l_j. (2007). Colourful coexistence of red and green picocyanobacteria in lakes and seas. *Ecol Lett* 10: 290-298.

Stomp M, Huisman J, Mittelbach GG, Litchman E, Klausmeier CA. (2011). Large-scale biodiversity patterns in freshwater phytoplankton. *Ecology* 92: 2096-2107.

Striebel M, Behl S, Diehl S, Stibor H. (2009). Spectral niche complementarity and carbon dynamics in pelagic ecosystems. *Am Nat* 174: 141-147.

Tambi H, Flaten GAF, Egge JK, Bodtker G, Jacobsen A, Thingstad TF. (2009). Relationship between phosphate affinities and cell size and shape in various bacteria and phytoplankton. *Aquat Microb Ecol* 57: 311-320.

Taylor PA, Williams PJleB. (1975). Theoretical studies on the coexistence of competing species under continuous-flow conditions. *Can J Microbiol* 21: 90-98.

Teeling H, Fuchs BM, Becher D, Klockow C, Gardebrecht A, Bennke CM, *et al*. (2012). Substrate-controlled succession of marine bacterioplankton populations induced by a phytoplankton bloom. *Science* 336: 608-611.

Terblanche JS, Janion C, Chown SL. (2007). Variation in scorpion metabolic rate and rate-temperature relationships: implication for the fundamental equation of the metabolic theory of ecology. *J Evol Biol* 20: 1602-1612.

Thompson AW, Foster RA, Krupke A, Cartner BJ, Musat N, Vaulot S, *et al*. (2012). Unicellular cyanobacterium symbiotic with a single-celled eukaryotic alga. *Science* 337: 1546-1550.

Tilman D. (1977). Resource competition between planktonic algae: an experimental and theoretical approach. *Ecology* 58: 338-348.

Tilman D. (1980). Resources: a graphical-mechanistic approach to competition and predation. *Am Nat* 116: 362-393.

Tilman D. (1982). Resource Competition and Community Structure. Princeton University Press, Princeton, NJ.

Tilman D. (1985). The resource-ratio hypothesis of plant succession. *Am Nat* 125: 827-852.

Tilman D, Pacala S. (1993). The maintenance of species richness in plant communities. Pages 13-25 in R. E. Ricklefs and D. Schluter, eds. *Species Diversity in Ecological Communities: Historical and Geographical Perspectives*. University of Chicago Press, Chicago, IL.

Toepel J, Welsh E, Summerfield TC, Pakrasi HB, Sherman LA. (2008). Differential transcriptional analysis of the cyanobacterium *Cyanothece* sp. strain ATCC 51142 during light-dark and continuous-light growth. *J Bacteriol* 190: 3904-3913.

Toepel J, McDermott JE, Summerfield TC, Sherman LA. (2009). Transcriptional analysis of the unicellular, diazotrophic cyanobacterium *Cyanothece* sp. ATCC 51142 grown under short day/night cycles. *J Phycol* 45: 610-620.

Tomita J, Nakajima M, Kondo T, Iwasaki H. (2005). No transcription-translation feedback in circadian rhythm of KaiC phosphorylation. *Science* 307: 251-254.

Trimbee AM, Prepas EE. (1987). Evaluation of total phosphorus as a predictor of the relative biomass of blue-green algae with emphasis on Alberta Lakes. *Can J Fish Aquat Sci* 44: 1337-1342.

Tseng YF, Lin FJ, Chiang KP, Kao SJ, Shiah FK. (2005). Potential impacts of N_2-fixing *Trichodesmium* on heterotrophic bacterioplankton turnover rates and organic carbon transfer efficiency in the subtropical oligotrophic ocean system. *Terr Atmos Ocean Sci* 16: 361-376.

Tuomainen J, Hietanen S, Kuparinen J, Martikainen PJ, Servomaa S. (2006). Community structure of the bacteria associated with *Nodularia* sp. (*Cyanobacteria*) aggregates in the Baltic Sea. *Microb Ecol* 52: 513-522.

Tyrrell T. (1999). The relative influences of nitrogen and phosphorus on oceanic primary production. *Nature* 400: 525-531.

Van de Waal DB, Verspagen JMH, Finke JF, Vournazou V, Immers AK, Kardinaal WEA, *et al*. (2011). Reversal in competitive dominance of a toxic versus non-toxic cyanobacterium in response to rising CO_2. *ISME J* 5: 1438-1450.

Van der Meer J. (2006). Metabolic theories in *Ecology*. *Trends Ecol Evol* 21: 136-140.

Van Donk E, Kilham SS. (1990). Temperature effects on silicon- and phosphorus-limited growth and competitive interactions among three diatoms. *J Phycol* 26: 40-50.

Van Donk E, Ianora A, Vos M. (2011). Induced defences in marine and freshwater phytoplankton: a review. *Hydrobiologia* 668: 3-19.

Vasseur DA, McCann KS. (2005). A mechanistic approach for modeling temperature-dependent consumer-resource dynamics. *Am Nat* 166: 184-198.

Verspagen JMH, van de Waal DB, Finke JF, Visser PM, Huisman J. (2014). Contrasting effects of rising CO_2 on primary production and ecological stoichiometry at different nutrient levels. *Ecol Lett* 17: 951-960.

Vitousek PM, Howarth RW. (1991). Nitrogen limitation on land and in the sea: how can it occur? *Biogeochem* 13: 87-115.

Vojtech E, Turnbull LA, Hector A. (2007). Differences in light interception in grass monocultures predict short-term competitive outcomes under productive conditions. *PLoS ONE* 2:e449.

Von Liebig J. (1840). *Die organische Chemie in ihrer Anwendung auf Agrikultur und Physiologie*. Friedrich Vieweg Verlag, Braunschweig, Germany

Vrede T, Ballantyne A, Mille-Lindblom C, Algesten G, Gudasz C, Lindahl S, Brunberg AK. (2009). Effects of N:P loading ratios on phytoplankton community composition, primary production and N fixation in a eutrophic lake. Freshw Biol 54: 331-344.

Walsh JJ, Steidinger KA. (2001). Saharan dust and red tides: the cyanophyte connection. *J Geophys Res* 106: 11597-11612.

Wannicke N, Koch BP, Voss M. (2009). Release of fixed N_2 and C as dissolved compounds by *Trichodesmium erythreum* and *Nodularia spumigena* under the influence of high light and high nutrient (P). *Aquat Microb Ecol* 57: 175-189.

Wastyn M, Achaty A, Molitor V, Peschek GA. (1988). Respiratory activities and aa3-type cytochrome oxidase in plasma and thylakoid membranes from vegetative cells and heterocysts of the cyanobacterium *Anabaena* ATCC 29413. *Biochim Biophys Acta* 935: 217-224.

Webb EA, Ehrenreich IM, Brown SL, Valois FW, Waterbury JB. (2009). Phenotypic and genotypic characterization of multiple strains of the diazotrophic cyanobacterium, *Crocosphaera watsonii*, isolated from the open ocean. *Environ Microbiol* 11: 338-348.

Weiner J. (1990). Asymmetric competition in plant populations. *Trends Ecol Evol* 5: 360-364.

Weisburg WG, Barns SM, Pelletier DA, Lane DJ. (1991). 16S ribosomal DNA amplification for phylogenetic study. *J Bacteriol* 173: 697-703.

Whitman WB, Coleman DC, Wiebe WJ. (1998). Prokaryotes: the unseen majority. *Proc Natl Acad Sci USA* 95: 6578-6583.

Wilken S, Huisman J, Naus-Wiezer S, van Donk E. (2013). Mixotrophic organisms become more heterotrophic with rising temperature. *Ecol Lett* 16: 225-233.

Winship LJ, Tjepkema JD. (1985). Nitrogen fixation and respiration by root nodules of *Alnus rubra* Bong.: effects of temperature and oxygen concentration. *Plant Soil* 87: 91-107.

Yan JH, Wang YP, Zhou GY, Zhang DQ. (2006). Estimates of soil respiration and net primary production of three forests at different succession stages in South China. *Global Change Biol* 12: 810-821.

Yang S, Jin X. (2008). Critical light intensities for *Microcystis aeruginosa*, *Scenedesmus quadricauda* and *Cyclotella* sp. and competitive growth patterns under different light:N:P ratios. *J Freshw Ecol* 23: 387-396.

Yoshiyama K, Mellard JP, Litchman E, Klausmeier CA. (2009). Phytoplankton competition for nutrients and light in a stratified water column. *Am Nat* 174: 190-203.

Yuste JC, *et al*. (2007). Microbial soil respiration and its dependency on carbon inputs, soil temperature and moisture. *Global Change Biol* 13: 2018-2035.

Zar JH. (2010). *Biostatistical Analysis*, 5th edn. Pearson Prentice Hall, Upper Saddle River, NJ.

Zehr JP. (2011). Nitrogen fixation by marine cyanobacteria. *Trends Microbiol* 19: 162-173.

Zehr JP, Waterbury JB, Turner PJ, Montoya JP, Omoregie E, Steward GF, *et al*. (2001). Unicellular cyanobacteria fix N_2 in the subtropical North Pacific Ocean. *Nature* 412: 635-638.

Zehr JP, Bench SR, Carter BJ, Hewson I, Niazi F, Shi T, *et al*. (2008). Globally distributed uncultivated oceanic N_2-fixing cyanobacteria lack oxygenic photosystem II. *Science* 322: 1110-1112.

AFFILIATIONS OF AUTHORS

Thierry Bouvier
Eric Fouilland
Christophe Leboulanger
Laboratoire Ecologie des Systèmes Marins Côtiers ECOSYM, UMR 5119, CNRS, IRD, Ifremer, Université Montpellier 2, Place E. Bataillon, 34095 Montpellier cedex 05, France

Verena S. Brauer
brauervs@gmail.com

Anita G. J. Buma
Ocean Ecosystems, Energy and Sustainability Research Institute, University of Groningen, Nijenborgh 7, 9747 AG Groningen, The Netherlands

Veronique Confurius-Guns
Lucas J. Stal
Department of Marine Microbiology, Royal Netherlands Institute for Sea Research (NIOZ), Korringaweg 7, 4401 NT Yerseke, The Netherlands

Victor N. de Jonge
Institute of Estuarine & Coastal Studies, University of Hull, Hull HU6 7RX, UK

Barbara Emmerich
barbara.emmerich@mail.be

Jef Huisman
Maayke Stomp
Sebastiaan A. M. van Beusekom
Department of Aquatic Microbiology, Institute for Biodiversity and Ecosystem Dynamics, University of Amsterdam, Science Park 904, 1098 XH Amsterdam, The Netherlands

Camillo Rosso
c_rosso@hotmail.it

Franz J. Weissing
Department of Theoretical Biology, Center for Ecological and Evolutionary Studies, University of Groningen, Nijenborgh 7, 9747 AG Groningen, The Netherlands

LIST OF PUBLICATIONS

Biology:

Brauer VS, Stomp M, Bouvier T, Fouilland E, Leboulanger C, Confurius-Guns V, *et al*. (2015). Competition and facilitation between the marine nitrogen-fixing cyanobacterium *Cyanothece* sp. and its associated bacterial community. *Front Microbiol* 5: 795.

Brauer VS, Stomp M, Rosso C, van Beusekom SAM, Emmerich B, Stal LJ, Huisman J. (2013). Low temperature delays timing and enhances the cost of nitrogen fixation in the unicellular *Cyanothece*. *ISME J* 7: 2105-2115.

De Jonge VN, de Boer WF, de Jong DJ, **Brauer VS.** (2012). Long-term observations of microphytobenthos chlorophyll-a reveal a major role of air temperature. *Mar Ecol Prog Ser* 468: 43-56.

Brauer VS, Stomp M, Huisman J. (2012). The nutrient-load hypothesis: patterns of resource limitation and community structure driven by competition for nutrients and light. *Am Nat* 179: 721-740.

Brauer VS, de Jonge VN, Buma AGJ, Weissing FJ. (2009). Does universal temperature dependence apply to communities? - An experimental test using natural marine plankton assemblages. *Oikos* 118: 1102-1108.

Brauer VS, Schärer L, Michiels NK. (2007). Phenotypically flexible sex allocation in a simultaneous hermaphrodite. *Evolution* 61: 216-222.

De Jonge VN, **Brauer** VS, Elliot M. (2006). Marine monitoring: Its shortcomings and mismatch with the EU Water Framework Directive's objectives. *Mar Poll Bull* 53: 5-19.

Spoelstra K, Albrecht U, van der Horst GTJ, **Brauer V**, Daan S. (2004). Phase responses to light pulses in mice lacking functional *per* and *cry* genes. *J Biol Rhythms* 19: 518-529.

Lymphology:

Brauer WJ, **Brauer VS**. (2008). Lassen sich mit der Funktionslymphszintigraphie Aussagen zur Transportkapazität machen? *Lymph Forsch* 12: 71-75.

Brauer WJ, **Brauer VS**. (2008). Comparison of standardized lymphoscintigraphic function test and high resolution sonography of the lymphoedema of legs. *Phlebologie* 37: 247-252.

Brauer WJ, **Brauer VS**. (2005). Altersabhängigkeit des Lymphtransports beim Lipödem und Lipolymphödem. *Lymph Forsch* 9: 6-9.

Brauer VS, Brauer WJ. (2004). Vereinfachtes Schwächungskorrekturverfahren bei der Funktionslymphszintigraphie des Beines. *Lymph Forsch* 8: 66–71.

Brauer WJ, **Brauer VS**. (2003). Funktionslymphszintigraphie-Abflussszintigraphie: Ergebnisvergleich. *Lymph Forsch* 7: 69-71.